Master's thesis

NTNU
Norwegian University of Science and Technology
Faculty of Engineering
Department of Structural Engineering

Nikolai Øwre Ryvoll

Probability-based assessment of the Stavå bridge

Master's thesis in Civil and Environmental Engineering

Supervisor: Prof. Dr.-Ing. Jochen Köhler, Ph.D. Jorge Mendoza Espinosa

January 2020

NTNU
Norwegian University of Science and Technology

Nikolai Øwre Ryvoll

Probability-based assessment of the Stavå bridge

Master's thesis in Civil and Environmental Engineering
Supervisor: Prof. Dr.-Ing. Jochen Köhler, Ph.D. Jorge Mendoza Espinosa
January 2020

Norwegian University of Science and Technology
Faculty of Engineering
Department of Structural Engineering

NTNU
Norwegian University of Science and Technology

NTNU
Norwegian University of
Science and Technology

Probability-based assessment of the Stavå bridge

Nikolai Øwre Ryvoll

Master thesis
Submission date: 31. January 2020
Supervisor: Prof. Dr.-Ing. Jochen Köhler
Co-Supervisor: Ph.D. Jorge Mendoza Espinosa

Norwegian University of Science and Technology
Department of Structural Engineering

Preface

This master thesis has been written to finish the Master of Science degree in Civil and Environmental Engineering at the Norwegian University of Science and Technology (NTNU). The research was conducted for the Department of Structural Engineering from September 2019 to February 2020.

The master thesis has been a collaboration between the Norwegian Public Roads Administration and me. I want to thank Arild Christiansen, Igor Praskac, and Knut Ove Dahle in the Norwegian Public Road Administration for showing great interest to the master thesis. They have been of great help, participated with great insight on bridge reassessment, and shared essential details and documents about the bridge.

The field of structural reliability was new to me when I started the work on the project work, which was the introduction to the master thesis. I want to thank Prof.Dr.-Ing. Jochen Köhler and Ph.D. Jorge M. Espinosa for your guidance and support throughout the entire process.

Trondheim, January 31, 2020
Nikolai Øwre Ryvoll

Summary

This master thesis is about the decision-making process regarding the Stavå bridge. The main aim of the thesis is to find out what to do with the Stavå bridge. Different aspects of the decision-making process are considered. Namely, the organizational process of reassessing old structures, the socio-economics, and the structural capacity. Various decision alternatives have been established. A cost-benefit analysis has been carried out to find the cost of the alternatives. Several of the decision alternatives could already at an early stadium be dismissed because of the high costs.

Probabilistic methods were used to calculate the load-bearing capacity. In the project work, it was found that the traffic loads are of great importance for the safety of the bridge. The Norwegian rules on motor vehicles are used as a basis for the development of a site-specific load model. The load model takes the number of vehicles into account. The capacity of two different cross-sections has been assessed.

The calculations indicate that the probability of failure is too high. Based on the findings, it is recommended to implement measures to reduce the probability of failure. The socio-economic considerations indicate that to strengthen the bridge is the cheapest alternative.

Sammendrag

Denne masteroppgaven handler om beslutningsprosessen angående hva man skal gjøre med Stavåbrua. Hovedmålet med oppgaven er å finne ut hva man skal gjøre med Stavåbrua. Oppgaven tar ikke bare for seg på de rene konstrukjonstekniske vurderingene. Den inneholder også en samfunnsøkonomisk vurdering og det organisatoriske aspektet knyttet til beslutningsprosessen er berørt. Ulike besluttningslaternativer ble etablert. En samfunnøkonomisk kostnadsnytte analyse ble gjennomført for å finne kostnadene av implementering av de ulike alternativene. Mange av alternative kunne allerede på et tidlig stadium bli forkastet grunnet høye kostnader.

Lastkapasitietsberegningene er gjennomført med probabilistiske regnemetoder. I den innledende prosjektoppgaven ble det funnet at trafikklasten er av stor betydning for bruas sikkerhet. En egenutviklet lastmodell som er basert på forskrift om bruk av kjøretøy er brukt. Lastmodellen tar hensyn til antall kjøretøy som kjører over brua. Kapasiteten til to ulike tverrsnitt har blitt vurdert.

Beregningene antyder at sannsynligheten for brudd er for høy. Det burde derfor iverksettes tiltak for å redusere bruddsannsynligheten. De samfunnsøkonomiske beregningene antyder at å forsterke brua er den mest kostnadseffektive måten å redusere bruddsannsynligheten.

Contents

Chapter 1

Introduction

1.1 Background

The Stavå bridge is located between Ulsberg and Berkårk. It is a part of the main road, the E6, between the two major cities Oslo and Trondheim. The bridge is located inside the green circle on the map in figure 1.1. It was built in 1942 during wartime. The part of the E6, which the Stavå bridge is a part of, is planned to be replaced by a new, better highway. The contract has already been made with the contractor. The construction is planned to start in 2020, and it is planned to be finished by the end of 2023 [10]. Afterward, the bridge is intended to be kept in service, serving no longer the national, but the regional road network. The old road is meant to act as a backup road. When the new road is completed, the traffic on the old road will most likely be massively reduced.

Figure 1.1: [59] The loacation of the bridge.

1.2 The Stavå bridge

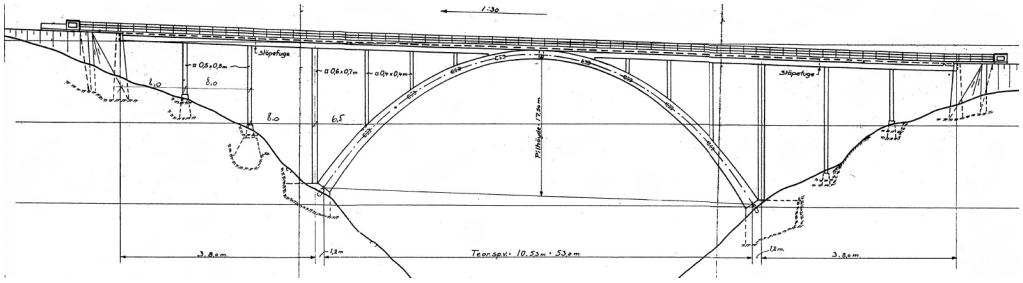

Figure 1.2: The bridge.

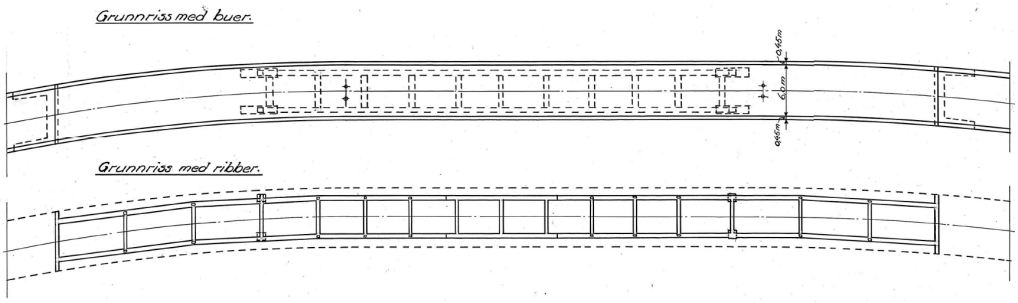

Figure 1.3: Horizontal projection of the bridge.

The Stavå bridge is a reinforced concrete beam arch bridge with three side spans. The main span is 53 meters, and each of the side spans is 8 meters. The arch is fixed at both support. The arch is made up by two arches connected together by cross-members. The cross-section of the arch is largest by the supports and becomes gradually smaller towards the crown. The bridge beam is a continues double T-beam, which is supported on roller supports at both the abutments. The bridge beam is connected directly to the top point of the arch. The rest of the bridge beam rests on columns. In the transverse direction, the web of the T-beam rest on one column each. There is a cross member between the two webs at each point where the bridge beam is connected to columns. All the columns are pinned in both ends.

The original construction drawings and the bending lists have been stored. The bridge has been inspected on several occasions during the last two decades in order to monitor the deterioration processes. There are serious concerns about the integrity of the bridge. Signs that admonish heavy vehicles to keep at least 50 meters distance are installed in front of the bridge. Concrete cores have been extracted from the T-beams in order to test the concrete compression strength. The carbonatization depth has been measured on all the major parts of the structure. The carbonatization front has reached the reinforcement in the bridge beam and in the columns. The deepest carbonatization depth was measured to 45 mm.

The arch reinforcement is not reached by the carbonatization. Accelerometers are installed. The load bearing capacity of the bridge has been assessed by independent external consulting firms. Several critical cross-sections were identified. One report states that the bridge beam in the middle of the side spans are most utilized (cross-section A-A in fig 1.4)[6]. Another states that the bottom of the arch right above one of the supports is most utilized [7]. A third report states that the arch is most critical and that it is most utilized between the crown and the column closest to the crown [48] (cross-section B-B in figure 1.4). This master thesis is going to use cross-section A-A and B-B as the basis for the analysis of the bridge.

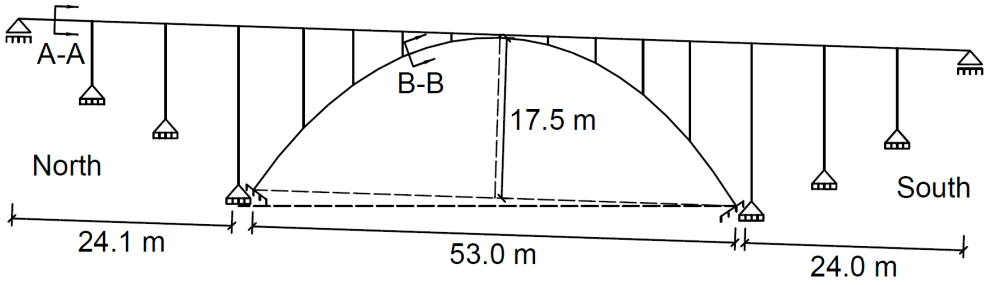

Figure 1.4: Sketch of the Stavå bridge indicating the critical cross-sections identified in previous studies.

The reports provide information about the condition of the bridge. The expansion joint of the southern abutment is filled with bitumen and sand. The bridge beam beams have vertical cracks in every single span. The cracks are between 0.2-0.3 mm. There is also one crack close to the transition between the bridge beam and the arch. The crack is located on the south side. The crack is 0.8 mm wide. The arch has areas where the concrete is poorly compacted. An alkali-silica reaction crack pattern is observed in some places at the side surfaces of the arch.

1.3 Traffic situation

The annual average daily traffic (AADT) over the bridge for both passenger vehicles and trucks is given in table 1.1 [59]. The road is one of the busiest two-lane roads in Norway. It is also one of the main roads with the highest percentage of heavy vehicles. The new road is planned to be finished in 2023. The Stavå bridge is not going to serve as part of the main road anymore. The traffic situation is going to change. The traffic situation after the completion of the new road is associated with uncertainty. Both the traffic amount and the percentage of heavy traffic is expected to be reduced. It is assumed that the AADT is not going to exceed 500 vehicles and that heavy vehicles are going to constitute 15% of the total traffic. The projected 2023 traffic is summarized in the last row of table 1.1.

Table 1.1: Annual average daily traffic 2020.

Time	AADT	% AADT heavy vehicles	AADT heavy vehicles	AADT passenger cars
2020	5140	26	1336.4	3803.6
2023	500	15	75	425

1.4 Scope and objectives

The scope of this master thesis is to provide the decision-maker with a solid foundation to support the decision making process for the Stavå bridge. The main question is, what to do with the Stavå bridge? Different aspects of the decision-making process are going to be visited to answer this question. The organizational process of reassessing old structures is regarded. Several decision alternatives are studied, such as doing nothing, reducing the allowed maximum weight, and building a temporary bridge. The alternatives are are assessed under

both socio-economic and structural considerations. The alternatives are ranked based on risk-based decision analysis. A probabilistic model is developed to assess the probability of failure. Special emphasis is placed on the load model, due to the importance of the load on the reliability of the bridge.

1.5 Outline of the Thesis

Chapter 1 presents the background information about the Stavå bridge and the traffic situation. The master thesis is a continuation of the project work. In *Chapter 2*, the most important findings from the project work are presented. The findings are essential for an essential starting point for this thesis. The traffic load was found to be of great importance for structural safety. *Chapter 3* presents the basic methods of structural reliability, different risk acceptance criteria, and assessment methods for existing structures. *Chapter 4* gives a summary of the preliminary documents. *Chapter 5* establishes different decision alternatives, which are used for further analysis. The framework for the socio-economic analysis is developed. An assessment of the socio-economic costs of the various decision alternatives is carried out. *Chapter 6* is a direct consequence of the previous findings. The Norwegian regulations on motor vehicles are used as a basis for establishing a site-specific load model that takes into consideration the traffic volume. *Chapter 7* presents the probabilistic assessment of the load-bearing capacity of the Stavå bridge. Two different cross-sections are considered. The result of the analyses is shown in *Chapter 8*. The socio-economic considerations are revisited. *Chapter 9* presents a discussion of the most important assumptions of the analysis. The assumptions are put in a critical light. *Chapter 10* presents the conclusion and alternatives for further assessment of the bridge.

Chapter 2

Previous findings

The master thesis is a continuation of the project work [32]. The aim of this chapter is to give the reader a summary of the most important findings from the project work.
The most important findings of the project work with relevance for the master thesis are summarized in this chapter. The concrete core compression test results were used to assess the probability distribution of the concrete compression strength. Different load models were compared to each other. The design philosophy and the empirical background behind the different load models were studied. An assessment of the capacity of three different cross-sections where carried out and a sensitivity analysis where performed. The aim of this chapter is to give the reader a summary of the most important findings from the project work.

2.1 Concrete compression strength

Concrete samples from the bridge and tested the concrete compression strength [4]. The concrete compression strength is assumed to be log-normal distributed. The maximum likelihood method was used to estimate the distribution param-

eters. Since the number of samples is small, one has to consider the statistical uncertainty carefully. The predictive distribution is obtained by integrating the statistical uncertainty to the conditional distribution. This distribution is approximately log-normal with a mean of 17.37 MPa and a coefficient of variation equal to 0.3. The characteristic concrete compression strength (f_{ck}) is 10.37 MPa. f_{ck} is defined as the 5%-fractile of the distribution. The result from the concrete compression tests, a detailed description of the calculation method, and plots of the concrete compression strength distribution are given in Appendix B.

2.2 Load models

Three different load models have been studied. Namely, the original load model that was used for the design of the bridge (i) , the Norwegian Public Road Administration's load model (ii), and the Eurocode 1 load model (iii). The traffic load has increased over the years.

(i) The bridge was designed according to load model 1 in the load standard that was valid between 1930 and 1947 [2]. The design vehicle was a three axle 15 ton truck with a two axle 20 ton trailer. The axle load is 5 tons for the truck and 10 tons for the trailer. The distance between the axles is 4.5 meters. Additionally, a dynamic amplification factor (DAF) dependent on the length of the bridge span was to be multiplied to the vehicle load. The safety format that was used is different than today's safety format. The permissible stress design method was used instead of the partial safety factor format. [52].

(ii) The Norwegian Public Roads Administration has its own load model, which is used to reassess old bridges. The standard is base on old Norwegian standards. The Stavå bridge is classified as Bk10/60, which means that the maximum permitted axle load is 10 tons, and the maximum permitted total weight is 60 tons.

The characteristic load is according to the Norwegian Public Road Administration's load model decided either by an axle, double axle, triple axle, vehicle, or truckload. The axle loads are treated as point loads. The vehicle and the truckload is a distributed load. The dynamic load is a point load with a magnitude of 40 kN and is a part of the characteristic load. The characteristic triple axle load is included in the dynamic load of 28 kN. The characteristic truckload is a 600 kN load that is distributed over 18 meters and a 40 kN point load. It is not known if the load model is based on any probabilistic considerations. The safety factor for the traffic load is 1.4 for traffic in one lane only, and 1.3 for traffic in two lanes.[53, 56]

(iii) The Eurocode 1 traffic load model is a semi-probabilistic load model. Weight in motion (WIM) traffic data from several European countries, among other data from the French A6 motorway near Auxerre, are used as a basis for the calibration of the Eurocode traffic load model. The characteristic load and the safety factors are calibrated to ensure adequate safety for a great variety of different load situations and structure types. Structural safety shall be ensured. At the same time, the model shall be easy to use for practical applications. According to Eurocode 1 - Part 2 [13], the characteristic traffic load is a combination of a distributed load and a double axle group. The load model divides the bridge into notional lanes. The load magnitude is different in each lane. In the first lane, the load on each axle in the double axle group is 300 kN, which is more than the complete triple axle grope of the Norwegian Public Road Administration load model. The characteristic load is according to the Eurocode defined as the 99.9%-fractile of the yearly probability distribution or the load with a 1000 year return period. The safety factor for traffic loads are 1.35 [14, 30].

2.3 Assessment of the load bearing capacity

An assessment of the load bearing capacity for the part of the bridge over land was carried out, i.e., the part of the bridge beam that is not directly over the arch. Three failure modes were considered. The first was an assessment of the moment capacity of cross-section A-A. The second was an assessment of the moment capacity over the first column. The third was an assessment of the shear capacity. The Norwegian Public Road Administration's load model was used as the basis for the calculations. Cross-section A-A was found to be the most critical cross-section.

2.4 Sensitivity analysis

A FORM analysis was carried out in order to study the sensitivity of the different variables. The cross-section that was examined is the one located at mid-span between the first column and the abutment. The cross-section is a T-beam, and the flange is in compression. The Norwegian Public Roads Administration load model was used as a basis for the analysis. This is not a probabilistic load model. So it was assumed that the traffic load is Gumbel distributed with a CoV of 0.4, and that the load obtained from the standard represents the 98%-fractile. The calculations are found in appendix B. The results of the sensitivity analysis are presented in table 2.1.

Table 2.1: α-factors.

α-factors				
Model uncertainty	**Steel strength**	**Concrete strength**	**Traffic load**	**Self-weight load**
-0.3536	-0.1734	-0.0217	0.9154	0.0811

The α-factors measure the relative importance of the different random variables

for the location of the design point, i.e., the structural reliability. The sign in front of the number is telling whether it is a resistance or load variable. The closer the value is to 1 or -1, the more do a change to the variable affect the probability of failure. Resistance variables are negative. Load variables are positive. As one can see from table 2.1, the traffic load is of extreme importance. It is far more important than the concrete resistance.

One has a situation where the load variable is by far the most important variable for the assessment of the probability of failure and two load models that are operating with two complete different characteristic loads. The Eurocode traffic model is developed using probabilistic model and is formulated to cover various design situations. It can, in many situations, be conservative. The Norwegian Public Roads Administration load model is based on some old Norwegian standards. The characteristic load is not clearly defined in the same way as the Eurocode load model. In the case of the Stavå bridge, it is worth to invest time in describing the traffic load more accurately.

Chapter 3

Theory

This chapter introduces the methods of structural reliability. It presents an introduction to risk-based decision making and how to assess old structures.

3.1 The probability format

3.1.1 Basic concept and solution methods

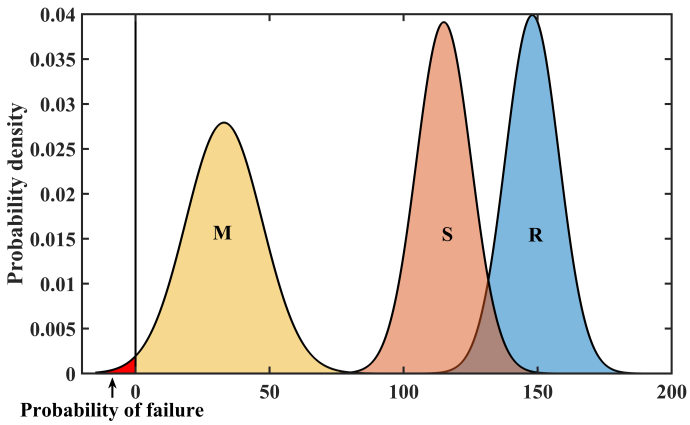

Figure 3.1: [24] Graphical representation of the limit state function.

The basis for structural reliability analysis is to use probability theory for the representation of the structural safety and serviceability problem. It has since long been known that absolute safety cannot be achieved. The loads that act on a structure are uncertain. The material properties, such as concrete compression capacity and reinforcement yield strain, are uncertain. And structural models are in itself uncertain. Probability methods can quantify and threat uncertainties consistently. The notion of structural reliability can be conveniently introduced by considering the so-called fundamental case. correspondingly, equation that must be solved is equation (3.2), which hereafter is denoted as the limit state function. The limit state function is a function of the resistance and load effect. As shown by equation (3.2), the probability of failure is equal to the probability that the safety margin is less than or equal to zero. The limit state function is represented graphically in figure 3.1.

The elementary equation:

$$g(r, s) = r - s \tag{3.1}$$

Where, g is the limit state function. r is the resistance. s is the stress or load effect.

$$p_f = P(g(r, s) \leq 0) \tag{3.2}$$

Where, p_f is the probability of failure.

The probability of failure can be calculated explicitly if the resistance and the load effect in equation (3.1) are normally distributed [16, 1] and the two variables are uncorrelated. Equation (3.3) and 3.4 shows the calculation procedure. Note that β is the reliability index.

$$\beta = \frac{\mu_r - \mu_s}{\sqrt{\sigma_r^2 + \sigma_s^2}} \tag{3.3}$$

Where, μ_r and μ_s are the mean value of the resistance and load effect distribution respectively. σ_r and σ_s are the standard deviation of the two distributions.

$$p_f = \Phi(-\beta) \tag{3.4}$$

Where, $\Phi(\cdot)$ denotes the cumulative distribution function of the standard normal distribution, i.e., a normal distribution with a mean value of zero and a standard deviation of one.

The ratio between the standard deviation and the mean value is denoted coefficient of variation (CoV).

$$CoV = \frac{\sigma}{\mu} \tag{3.5}$$

For real engineering problems, the variables in the limit state function are rarely normally distributed and the limit state function is often much more complicated. Other methods must be used either to find an approximate or exact solution. The Monte Carlo method is perhaps the most intuitive solution method. A large number of random samples are generated for each of the underlying distributions. The limit state function is solved with one set of random samples at the time. The evaluation of the limit state function is counted as a failure if it smaller or equal to zero. As shown by equation (3.6), the probability of failure is calculated by dividing the number of failures on the total number of trails. The solution converges towards the real solution as the number of trails grows big. The probability of failure is usually rather small for civil engineering structures. It is necessary to generate several million samples to find an accurate solution.

$$p_f = \lim_{n \to \infty} \frac{n_f}{n} \tag{3.6}$$

Where, n_f is the number of failures. n is the number of trails.

3.1.2 Accounted risks and consistency of the probability model

The result of probabilistic assessments is only as good as the assumptions of the analysis. The type of distribution of the probabilistic variables must be assumed. The small probability of failure makes the final result particularly sensitive to the tail properties of the distributions. There are, for instance, no practical way to verify that a given level of seismic activity has a return period of 500 years [18, 40]. The tail sensitivity problem is partly controlled by using a standardized type of distribution to describe certain phenomena. The log-normal distribution is for instance, frequently used to describe material strength. The Gumbel distribution is used to describe extreme natural events. And the normal distribution may be used for geometrical dimensions. The Joint Committee on Structural Safety (JCSS) has developed a probabilistic model code that provides recommendations on which distributions to use [23]. The International standard ISO 2394 [50] provides the general principles on reliability for structures. The background documents for the Eurocodes provides information on the general assumptions [29, 30, 22]. The Danish Road Directorate has a probabilistic model for reassessing existing bridges [63]. The probability of failure is seen as a nominal value that does not necessarily represent the actual failure rates but is used as operational values for code calibration purposes and comparison of reliability levels of structures [14].

The design codes usually consider only one limit state function at the time. System effects are not considered. A structure can be idealized as either a series system, parallel system or a mixed system. The system effect will work differ-

ently on the two systems. To not consider the system effect for a series system will be non-conservative since the failure of one component causes the complete structure to fail. A statically determined truss bridge is an example of a structure that can be idealized as a series system. The opposite will be true for a parallel system. All the components have to fail to make the structure fail. An example will be several times statically indeterminate structures. A failure of one limit state function does necessarily not mean that the complete structure collapses.

Human errors are not considered in the reliability analysis. Most of structural failures are due to human error. Human errors are not taken into account when dimensioning structural components. They are not considered because they happen independently of the intended reliability level. An oversized beam is not safer than a normal-sized beam if the joint bolts are not fastened properly. Human errors frequently occur because of ignorance and insufficient knowledge [20].

3.2 Risk-based decision making

To establish an adequate safety level is all but trivial. How much personal risk people are willing to take seems to depend on degree of voluntary participation in the the risky activity, and the degree of personal influence on the risk. E.g., when climbing Mount Everest, the willingness to take risks is higher than when sitting on an airplane or crossing a pedestrian bridge [20]. Further, there seems to be a nonlinear relation between the willingness to take risks and the consequences associated with it. Different methods have been developed to establish an adequate safety level. Acceptance criteria can be based on socio-economic optimization and on people's individual preferences. Another approach is to use a fixed target value for the probability of failure as an acceptance criterion.

3.2.1 Socio-economic optimization

An optimization can be done based on a socio-economic consideration. The goal with the optimization is to find a solution that minimizes the expected cost for society. The socio-economic risk criteria states that one shall choose the probability of failure that minimizes the sosio-economic costs. The method is closely related to cost-benefit analyses that the Norwegian Public Road Administration uses for the evaluation of big infrastructure projects [55]. The big difference is that the probability of failure is a part of the consideration. Equation (3.7) is the basic equation that shall be optimized. C_{ET} are minimized subject to d. d is a variable that relates to the probability of failure, e.g., the height of a beam or the number of reinforcement bars. If the socio-economic optimization is used as a decision criterion, the optimal probability of failure is the probability that minimizes the expected cost [20, 40].

The expression that is going to be minimized is:

$$C_{ET}(d) = C_c(d) + C_o(d) + C_{i\&m}(d) + C_d(d) + C_f(d) \cdot p_f(d) \tag{3.7}$$

Where, C_{ET} total expected cost. d is the variable that is going to be optimized, e.g., the height of a beam. C_c cost of construction. C_o is the cost of operations. $C_{i\&m}$ is the cost of inspection and maintenance. C_d is the cost of demolition. C_f is the cost of failure. p_f is the probability of failure.

The costs appear at different points in time. The present value of all the different costs must be calculated to make them comparable to each other. The interest rate and the time period of analysis must be chosen. It is decided on a national level that the interest rate is 4 % and the time period of the analysis is 40 years for infrastructure projects [15].

Present value calculations:

$$C = \int_{t1}^{t2} c_0 \cdot (1+r)^{-t} dt \tag{3.8}$$

Where, C is the discounted cost. c_0 is the economic base cost. r is the 4% discount rate. $t1$ and $t2$ is the start and end time of the cost flow.

3.2.2 Risk acceptance

It can be convenient to give broad indicators over risk acceptance in society even though the nominal probability of failure not necessarily can be directly compared to actual structural failure rates or death rates. Some broad indicators based on Otway et al. [39] are given in table 3.1.

The values in table 3.1 correspond well with the values based on the "As Low As Reasonable Possible/Practicable (ALARP) principle given by ISO 3494 table G.1[50]. A probability of 10^{-4} is the intolerable limit for a member of the public. 10^{-5} is the upper limit, and risk reduction shall be carried out. 10^{-6} is broadly accepted.

People undoubtedly want their structures safe. The layman thinks of civil engineering structures as something substantial, and they shall not fail [34]. It can be a good idea to base the decision making on what people expect and wants. That is to keep structures at a reliability level so that people have a feeling that structural failure never happens to them.

Table 3.1: [39] Broad indicators over risk acceptance.

Risk of death per person per year	Typical response
10^{-3}	Immediate action is taking place. The risk is unacceptable to everyone.
10^{-4}	People spend money, especially public money, to control the cause (e.g., traffic signs and controls, police and fire department). Safety slogans show an element of fear, e.g., " The life you save may be your own".
10^{-5}	Risks are still considered by society. Mothers warn their children about most of these hazards (e.g., playing with fire, drowning, firearms, poisons). Safety slogan has a precautionary ring, e.g., "Keep medicines out of children's reach."
10^{-6}	Accidents are not of great concern for the average person. People may be aware of the risk, but they feel they will never happen to them. Phrases have an element of resignation, e.g., "Lightning never strikes twice" or "An act of God.".

3.2.3 Target reliability

Several different target reliability values have been suggested and used. The JCSS has based on economic optimization, made tentative target reliabilities related to a one-year reference period. Depending on the relative cost of the safety measure and the consequences of failure, the reliability index is ranging from 3.1 to 4.7 (G.5.2)[50].

The danish standard for probability assessment of existing bridges has suggested target values that are dependent on the material behaviour. It allows for a lower probability of failure if the failure is visible before a complete collapse. The Danish standard target values are presented in table 3.2.

Table 3.2: [63] The target reliability of the Danish standard.

Failure type	Ductile failure with remaining capacity	Ductile failure without remaining capacity	Brittle failure
β_t	4.26	4.75	5.20
p_f	10^{-5}	10^{-6}	10^{-7}

The Eurocode safety factors are optimized with the use of probabilistic models. They aim to satisfy a target β-index of 4.7 for the ultimate limit state with a yearly reference period (EN-NS 1990 table C2)[14]. The safety factors are carefully chosen to make sure that that is the case for so many design situations as possible.

3.3 Assessment of existing structures

3.3.1 Assessment strategy

The table is based on the suggestion given by JSCC [9]. The different phases represent separate stages of the assessment. If there is still doubt about the structural integrity after phase 1, it is recommended to move to phase 2. The costs associated with the measures tend to grow as the methods become complicated. Note that the degree of subjectivity is highly dependent on how much information is obtained. For instance, if design drawings can not be found. The analysis relies on a high degree of subjectivity. For example, one must assume the number of reinforcement bars.

Table 3.3: [9] Measures to improve the estimate of the probability of failure.

Measure	Description
Phase 0:	**First impression**
The layman's gut feeling	The layman's gut feeling is able to notice if something is wrong, but he is not able to say much about the probability of failure.
The expert's gut feeling	An experienced expert is able to tell more about a structure than the layman.
Phase 1:	**Preliminary evaluation**
Recover old documentation	Find relevant information such as design documentation, calculations, drawings and as-built drawings, documentation about maintenance and repairs. Find the geometrical and material properties of the structure. It can be necessary to use old standards to find information on material properties.
Consider the load situation	"Has the load situation changed?" is an important question to ask. The new standards that consider today's load situation are not necessarily compatible with the old materials. And old standards do not necessarily consider the new load situation. One can be in a situation where no standard is valid for the given situation.
Systematic visual inspection	Visual inspection of the bridge tells much about the structure. The Norwegian Public Road Administration's handbook V441 [51] can be a helpful tool. Look for possible damage, cracks, and corrosion, Measure crack lengths and widths.

Update information	Bayesian statistical method is the toolbox for combining old and new knowledge. Use the gathered information to update the calculation model.
Phase 2:	**Detailed investigations**
Detailed investigations	Measurements of carbonatization depth, chlorine content, and corrosion. Concrete cores can be taken from the structure and tested in order to find the concrete compression strength. Measurements of deformations and concrete cover.
Detailed structural analysis	Carry out a detailed structural analysis. Use reliability analysis to determine the safety of the structure or its most critical cross-sections. Analyses with nonlinear material behavior can be considered.
Phase 3:	**Call in a team of experts**
Site-specific measures	For bridges: proof loading and WIM (Weight in motion). Surveying of the real geometry. Intensify monitoring.

3.3.2 Preliminary documents

Assessment of existing structures is a difficult task. The clearness in matters of concepts and procedures is of prime importance when assessing existing structures [9]. Clients are confronted in these discussions with the possibilities and limits of the experts [20]. Table 3.4 contains proposed documents that should be implemented in the assessment process to keep the process as transparent as possible.

Table 3.4: [9] Preliminary documents.

Document	Description
Service criteria agreement	A contract between the client and the engineer must be made. The contract shall clarify the responsibilities. It must be defined what type of inspections are necessary? What analysis shall be performed? What is the degree of subjectivity of the statements of an existing structure? It is also beneficial to define the risk acceptance criteria before the analyses are performed so that the result of the analyses are not affected by someone's own interests. What is the risk of further using the structure? What type of measures can be taken?
Residual service life and utilization plan.	How long is the structure intended to serve its purposes? What shall the structure be used for?
Hazard scenarios	Identify the leading hazards. Is there any load situations that are of particular danger?
Safety plan	Come up with a plan to eliminate, avoid, or control the hazard scenarios. Sometimes the hazards must be accepted.
List of accepted risks	This is an important document. It clarifies who profits from accepting risks and who bears the consequences. Ideally, both the risk and the consequences should be carried by the same person or group.

Chapter 4

Preliminary documents

Much of this chapter originates from several meetings with representatives from the Norwegian Public Road Administration. Table 3.4 is a summary of the preliminary documents suggested by table 3.4. The elementary assumptions that make the basis for the analysis is a topic through the thesis. The essential assumptions are summarized, and the subjectivity of the assumptions is clarified.

Table 4.1: Preliminary document for the Stavå Bridge reassessment.

Keywords	**Service criteria agreement**
Inspection type	Several visual inspections has been carried out by the engineering consulting company Rambøll [7, 6]. Concrete cores were taken out of the structure [4]. The concrete compression strength were tested. Carbonatization depths, chlorine content and concrete cover have been measured [8].
Analysis type	An analysis corresponding to phase 2 in table 3.3 has been carried out. Two cross-sections have been analyzed with probabilistic methods. The analyses are based on linear material behaviour.

Degree of subjectivity	*Resistance:* The original design drawings are accessible [2]. The geometrical properties from the drawings are used. The concrete compression tests are used to obtain the concrete compression strength distribution (see: appendix B). One of the Rambøll reports states that the steel is of St.00 quality [6]. The probabilistic steel properties are provided by the Danish standard for probabilistic reassessment of bridges [63]. The properties correspond well with properties that were normal at the time [47, 43]. The subjectivity level is small. There are no reasons to believe that the drawings provide false information. *Load:* The elementary assumptions are based on the Eurocode 1-2 background document [30] and the Danish standard [63]. The assumption regarding the number of relevant vehicle and the weight distribution of each truck type in section 6.3.3 and 6.3.4 are based on personal assumptions guided by traffic flow data [59, 62], the Norwegian regulations on motor vehicles [41], conversation with truck drivers [35] and the Danish standard [63]. The assumption regarded the traffic amount after 2023 is based on speculation.

	Socio-economics: The elementary assumptions are "collective subjective," that is, assumptions that of nature are subjective, but are standardized on a national level. The basic costs are based on the Norwegian Public Road Administration's handbook on cost-benefit analysis [55]. The traffic flow model in section 5.4.1 is simplified and rely on subjective judgments guided by google maps, conversation with representatives from the Norwegian Public Road Administration [31] and conversation with Anders Straume, SINTEF [36].
Risk acceptance criteria	No risk acceptance criteria were established in the initial phase of the assessment. See section 3.2 for more information on risk acceptance criteria.
Risk of further use	The main risk involved in further use of the structure is the risk of structural failure and, in the worst-case, collapse. The traffic amount is ever-increasing, and the vehicles have gotten heavier. The risk might be too high.
Risk-reducing measures	The able risk-reducing measures are either to strengthen the bridge, weight restrictions, light regulations, strengthening the bridge, built an interim bridge or to close the bridge completely.

Keywords	**Residual service life and Utilization plan**
Residual service life	The bridge is going to serve as part of the national road network until 2023. Afterward, it shall be transferred from the national authority to the county municipality and serve as part of the local road network.

Utilization plan	It is of interest to keep the bridge open for as many transport classes as possible as long the bridge serve as part of the national road network. The bridge is intended to be kept open for traffic also after 2023. It may be used as a backup road for the new national road. No specific transportation classes are requested.

Keywords	**Hazard scenarios and Safety**
Hazard	The traffic load is considered to be dominant. Extreme heavy vehicles and large concentrated loads are considered a hazard for the integrity of the bridge.
Safety plan	The Norwegian Public Road Administration has made a plane for building an interim bridge which, in case of emergency, can be built. Road signs that encourage heavy vehicles to keep at least 50 meters distance have been installed on each side of the bridge.

Keywords	**List of accepted risk**
Involved groups	The situation regarding who bears the risk and who profits from risk acceptance is intricate for publicly owned structures. There are different interest groups with differing interests. In this case, there are five groups involved. Namely, the consultant engineer/-s (in this case student), the representative/-s form the Norwegian Public Road Administration, the government representative/-s, the taxpayers, and the road users. For some of the groups, their interests are two-sided.

Public decision making	Who is the final decision maker is cost dependent. The representative from the public road administration is normally the decision-maker, but he has a budget he must adhere to. If the costs are running too high, he must ask the government representative for more money. In this case, the government representative is the final decision maker.
The government representative	Also, the government representative has a budget to adhere to. His performance is measured based on cost-effectiveness. The extra spending used for bridge maintenance is visible on the balance sheet. The expected cost of failure is not visible. The bridge will most likely not fail, even if the probability of failure is too big. The government representative profits from accepting the risk, but bears small consequences.
The consultant engineer (student)	The consultant engineer has a professional responsibility. Structures shall not fail. The engineer will be charged for making a professional error and can, to some degree, be liable for damages. (In this case, the student does not carry any responsibility for the bridge, and he has nothing to gain for accepting too big risks.)
The representative from the Norwegian Public Road Administration	The representative form the Norwegian Public Road Administration is in a squeeze. His interests are two-sided. On one side, it is never pleasant to ask for more cash. On the other hand, he is the formal decision-maker. A big responsibility lies on his shoulders. Especially if the results from different engineers are diverse and scattered. He also runs the risk of being accused of making a professional error.
The taxpayers	The taxpayers must pay both for the bridge maintenance and the bridge failure if that should happen.

The road user	The road user, or to be more precise, the individual or the individuals that unfortunately find themselves on the bridge when it fails or, in the worst case, collapse. The traffic load is the dominating load. Someone will most likely be on the bridge when it fails. In the worst case is that two busloads full of peoples. That are 90 peoples. They have everything to lose and runs the risk of losing their lives.

Chapter 5

Decision alternatives and cost-effectiveness

In this chapter, the different decision alternatives that were derived through meetings with representatives from the Norwegian Public Road Administration [31] are presented. The risks associated with the decision alternatives are evaluated. And the socio-economic consequences are investigated. The socio-economic calculations are based on a standardized cost-benefit method for evaluating infrastructure projects in Norway [55].The difference is that the probability of structural failure is part of the consideration. This type of cost-benefit-risk evaluation is not a standard approach used by the Norwegian Public Road Administration for evaluating bridges. However, cost-benefit-risk assessment is not entirely unknown to them. The same methodology is used for assessing the benefit of geological safety measures along Norwegian roads. The Norwegian Public Road Administration has together with SINTEF, developed the program EFFEKT, which is used for cost-benefit analysis. This program has an own module for evaluating the risk associated with avalanches [3, 36].

The result of the socio-economic considerations for the period between 2020 and

2023 is summarized in table 5.1. The calculation method and the elementary assumptions are described in the following sections. The background for the decision alternatives and a detailed description of them are given in section 5.2. The risk of introducing the decision alternatives is described in section 5.2.2. The basis for the socio-economic considerations is described in section 5.3. The assumption regarding the traffic model and the final economic calculations for the period between 2020 and 2023 is presented in section 5.4.

5.1 Summary of the socio-economic considerations.

Table 5.1: Summary of the period between 2020 and 2023.

A0 – Do nothing	
Impact	The traffic flows as normal
Description of risk	The combination of the ever-increasing traffic amount and vehicle weight and the uncertainty associated with the properties of the old materials makes the uncertainty great. The risk might be too high.
Risk mitigation	The risk is unchanged.
Cost:	
Construction (C_c)	The A0 alternative is the benchmark, the reference point, for the cost calculations.
Socio-economic (C_{se})	0 NOK
Expected failure ($C_f \cdot p_f$)	Not calculated jet.
Total (C_{ET})	-
A1 – Weight reduction	

Impact	The heaviest trucks must either drive another rout or carry less load.
Description of risk	The number of heavy trucks is reduced, but one cannot expect that everybody follows the rules. The probability of an extreme load event will be reduced.
Risk mitigation	The risk is to some degree reduced.
Cost:	
Construction (C_c)	Magnitude of under 1 million NOK
Socio-economic (C_{se})	346 million NOK
Expected failure ($C_f \cdot p_f$)	
Total ($\boldsymbol{C_{ET}}$)	More than 346 million NOK

A2 – Traffic light regulation	
Impact	Reduced traffic capacity and congestion.
Description of risk	The alternative will eliminate the possibility of a meeting event. Barricades can assure that the vehicles drive centric over the bridge. The potential load that the bridge is exposed to is strongly reduced.
Risk mitigation	The risk is strongly reduced.
Cost:	
Construction (C_c)	The magnitude of 1 million NOK.
Socio-economic (C_{se})	Minimum 51 million NOK, based on a conservative first estimate.
Expected failure ($C_f \cdot p_f$)	-
Total ($\boldsymbol{C_{ET}}$)	More than 51 million NOK

A3 – Strengthening work

Impact	The bridge must be closed for at least 4 to 6 weeks, or 8 weeks with night-time work.
Description of risk	The strengthening of the bridge can reduce the risk for collapse, but it can also relocate forces to places where there have never been forces before.
Risk mitigation	It can if done correctly reduce the risk. It will at least keep the risk constant for a period.
Cost:	
Construction (C_c)	The magnitude of 10 million NOK
Socio-economic (C_{se}) Night work:	Between 53 – 79 million NOK Between 6.9 – 15.9 million NOK
Expected failure ($C_f \cdot p_f$)	-
Total ($\boldsymbol{C_{ET}}$) Night work:	17 – 79 million NOK 21.5 – 30.9 million NOK

A4 – Build an interim bridge	
Impact	The traffic flows as normal
Description of risk	It is assumed that the bridge is built so that it satisfies the Eurocode. I.e., probability of failure of $1.3 \cdot 10^{-6}$.
Risk mitigation	The risk is reduced to an appropriate level.
Cost:	
Construction (C_c)	42 million NOK
Socio-economic (C_{se})	0 NOK
Expected failure ($C_f \cdot p_f$)	663 NOK
Total ($\boldsymbol{C_{ET}}$)	42 million NOK

A5 – Close down the bridge	
Impact	The traffic must detour for several years.
Description of risk	The risk becomes the property of the detour rout.
Risk mitigation	The bridge is taken out of operation.
Cost:	
Construction (C_c)	Demolition cost of 10 million.
Socio-economic (C_{se})	2237 million NOK
Expected failure ($C_f \cdot p_f$)	0 NOK
Total (C_{ET})	Above 2237 million.

From an economic point of view, it is a bad idea both to choose to close down the road, to introduce weight restriction and traffic light regulations. The socio-economic cost of these decision alternatives exceeds alone, the total cost of building an interim bridge. The expected cost of failure for the interim bridge is negligible given that it has a β-value of 4.7. Hence, to build an interim bridge will be a better decision than introducing the above mentioned decision alternatives. Only to do nothing, to strengthen the bridge and to build an interim bridge are worth further consideration.

5.2 The decision alternatives

The decision alternatives were deduced in collaboration with representatives from the Norwegian Public Roads Administration [31].
Screening meetings were arranged during the initiation phase of the master work. As indicated in chapter 1, the traffic situation is expected to change during 2023 due to the construction of a new road. Thus, the Stavå bridge shall no longer serve as part of the E6 but as a local county road. The boundary conditions for the economic analysis changes when the new road opens. For this

reason, it is decided to consider different alternatives at two different points in time. The stage concerns the decision that must be made as soon as possible. There are no roads in the surrounding of the bridge that suited for detouring in the period between 2020 and 2023. Some vehicles are expected to detour for hours if the bridge must close. The second stage concerns the decision after the bridge is finished. In the period after 2023, the new E6 can be used for detouring. There is practically no detour at all. A decision tree is used in figure 5.1 to present different alternatives.

5.2.1 The alternatives

A0 The A0, do nothing alternative, is to keep the bridge exactly as it is. Nothing is done to improve the bridge integrity, and the vehicle weight limit is kept the same.

A1 The A1, weight restriction alternative means that the weight and the axle load of the vehicles are lowered compared to today's value. For instance, the axle load limit can be lowered from 10 tons to 8 tons, and the total weight can be lowered from 50 tons to 40 tons. The heaviest vehicles must either be detouring or carry less load.

A2 The A2, traffic light regulation alternative means that the bridge is rebuilt to a one-way bridge. Traffic can flow only in one direction at the time. Barricades make sure that the vehicles drive centric over the bridge. The alternative leads to congestion.

A3 The A3, strengthening work, means that the weakest parts of the bridge must be strengthened. The bridge must be closed for at least 4-6 weeks, or 8 weeks if the work is done by night.

A4 The A4, to build an interim bridge means to construct a temporary bridge that is going to serve as a replacement for the Stavå bridge until the new road is finished. The Norwegian Public Roads Administration has already made a plan for building an interim bridge. The considered interim is a single span simply supported steel truss bridge of the type Mabey Universal [54]. The plan is to build the interim bridge on the side of the existing Stavå bridge. The traffic flows as normal over the existing bridge during the construction of the interim bridge.

A5 The A5, close down the bridge alternative, means that the Stavå bridge is closed down permanently. All the traffic must detour until the new road is finished.

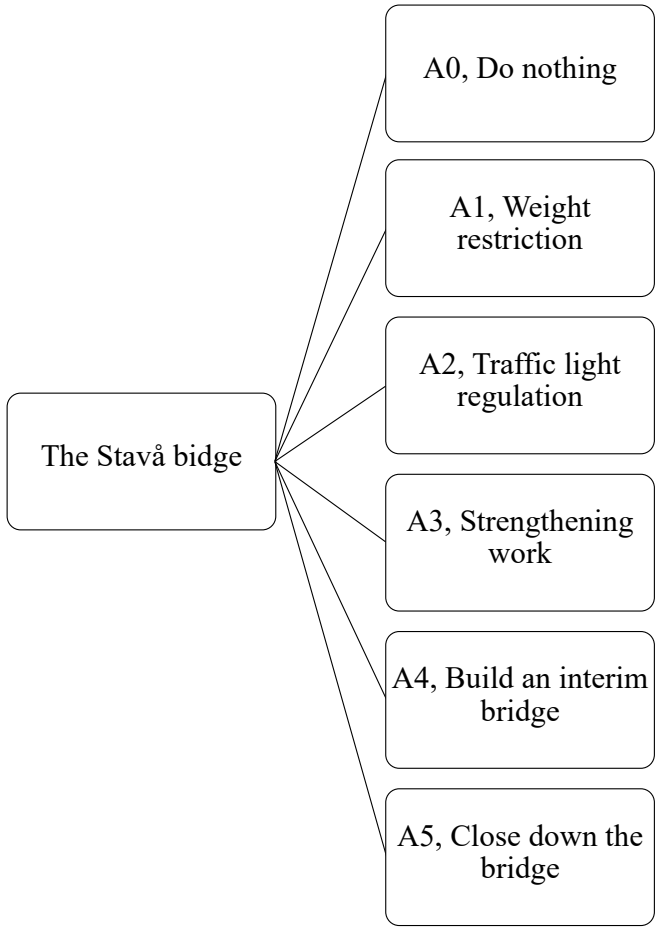

Figure 5.1: The 2020 decision alternatives.

5.2.2 Identification of risks

The decision alternatives will, in some way or another, affect the probability of failure.

A0 For A0, the status quo is kept. The traffic amount has been ever-increasing since the time the construction of the bridge was completed. The vehicles are also getting heavier. The uncertainty regarding the material properties is big. The bridge is slowly degrading, which makes the bridge weaker and weaker over time. The risk might be too high.

A1 It is expected that the A1, weight reduction alternative to some degree reduces the number of the heaviest vehicles. However, it can not be expected that everybody follows the weight restriction. The Stavå bridge becomes a weight limit bottleneck that prevents all the transport between Oslo and Trondheim from utilizing the load capacity. The risk is expected to be slightly reduced.

A2 The A2, traffic light alternative with physical barricades, reduces the risk. The traffic drives nearly centric over the bridge. The load transfers with a 50-50 distribution between the two sides of the substructure.

A3 The A3, strengthening work alternative can, if done correctly, reduce the risk. However, there is also a chance that the strengthening redistributes forces. If the stiffness ratio between structural elements is changed the forces can be redistributed into sections where there have never been large forces before. It must at least be assumed that the strengthening work terminates the degradation of the bridge for a period of time.

A4 To build an interim bridge, A4, reduces the risk if it is built sufficiently strong. The strength of the bridge can be chosen. In this master thesis, it is assumed that the interim bridge has a safety level that corresponds to the Eurocode safety level. I.e., a β-value of 4.7, which corresponds to a probability of failure of $1.3 \cdot 10^{-6}$.

A5 The A5, close down the bridge alternative, certainly reduces the risk of bridge failure. The risk becomes a property of the detour routes.

5.3 The basis for the economic considerations

5.3.1 Economic optimization

The ultimate goal with the economic considerations is to minimize the total expected cost (C_{ET}) for the rest of the lifetime of the bridge. Equation (3.7) is the basis for the economic optimization. Certain modifications to the equation must be made. The optimization problem is discrete. There is no continues variable that shall be optimized, but discrete, separate decision alternatives. A bridge failure and many of the decision alternatives lead to detouring or waiting time. It has a cost that must be considered. A socio-economic cost (C_{se}) is introduced to the equation. The road is publicly owned, and the decisions are made on behalf of the society. The A0 alternative is used as the benchmark for the socio-economic cost. The socio-economic cost of the A0 alternative is per definition zero. The economic cost is a relative cost. The cost of all the other decision alternatives is measured against the cost of A0. Further, the cost of operation (C_o) and the cost of inspection and maintenance ($C_{i\&m}$) are considered to be about equal for all the alternatives. The difference of C_o and $C_{i\&m}$ between the decision alternatives is non-dominant compared to the other costs. Therefore, C_o and $C_{i\&m}$ are neglected. The equation that shall be optimized is equation (5.1).

$$C_{ET} = C_c + C_{se} + C_f \cdot p_f \tag{5.1}$$

$$C_f = C_d + C_c + C_{se} \tag{5.2}$$

Where, C_{ET} is the total expected cost. C_{se} is the socio-economic cost. C_f is the cost of failure. C_d is the cost of demolition. C_o is the cost of construction. p_f is the probability of failure per year.

5.3.2 The socio-economic costs

The socio-economic costs are calculated using the method given in the Norwegian Public Roads Administration handbook V712, which is a handbook for impact assessment and cost-benefit analysis [55]. The method is the standard method for evaluating the value of transportation projects in Norway. The socio-economic costs consist of one part that is related to the number of extra kilometers that must be driven. A second part that relates to the time extra time used on transportation. And a third part that is related to the cost of the extra accidents caused by detouring. Additionally, the handbook has costs that are related to the excess greenhouse gas emission and loss of property value due to air and noise pollution. However, the calculations are simplified, and these costs are neglected. The considered costs are given by equation (5.3).

$$C_{se} = C_k + C_t + C_a \tag{5.3}$$

Where, C_k is the kilometer cost. C_t is the time cost. C_a is the accident cost.

Kilometer costs

The handbook V712 gives a cost that relates to each extra kilometer driven by a vehicle. The handbook distinguishes between passenger cars and heavy vehicles. Table 5.4 summarizes the kilometer costs. The kilometer cost includes, among others, the cost of vehicle maintenance, gas, and capital costs.

Table 5.4: The basis for the kilometer cost [2016NOK].

Type	Cost [NOK/km]
Passenger cars	1.74
Heavy vehicles	4.10

Time costs

The time cost relates to the time lost by the persons in the vehicles. For passenger cars, the handbook distinguishes the costs based on the length of the travel and the travel type. The travel length can either be short (0-70 km), medium (70-200km), or long (200- km). It is in the calculations assumed that all travels are of medium length. The type of travel can either travel that is done while working, between home and work, or at leisure. The second column in table 5.5 gives the share of the different types of travel. The average number of people in one car depends on the type of travel. The average number of people is given in the third column. The fourth column gives the cost for one person to lose one hour. The fifth column gives the average cost for one lost hour per vehicle. At last, the weighted average cost between the different travel types is calculated.

Table 5.5: Passenger car time cost calculation [2016NOK].

Travel type	Share	Persons in each car	NOK/(person·hour)	NOK/(hour·vehicle)
Work travel	0.09	1.2	449	538.8
From and to work	0.15	1.2	217	260.4
Leisure	0.77	2.2	169	371.8
			Weighted average:	**373.838**

The heavy vehicle time cost includes the cost of the driver. It includes also the cost of time dependent operating costs, such as administration. Table 5.6 makes the basis for the time costs.

Table 5.6: The basis for the time cost[2016NOK].

Type	NOK/(hour·vehicle)
Passenger cars	373.8
Heavy vehicles	676

Accident costs

It is assumed that the accident rate for the extra kilometers driven is equal to the average accident rate for all the roads. The handbook V712 gives the cost per fatality and seriously injured person [55], which is given by the second column in table 5.7. The number of accidents given in the third column is the average number over the five last years [46]. The total yearly cost of accidents is calculated in column four. In the fifth column, the total cost is divided on the total annual kilometers are driven, which was 46000 million kilometers in 2018 [45].

Table 5.7: Basis for the accident cost [2016NOK].

Accident type:	NOK/accident	Accidents/year	NOK/year	NOK/km
Death	30 200 000	123	3 714 600 000	0.08
Serious injured	11 200 000	651	7 291 200 000	0.16
		Totalt:	11 005 800 000	**0.24**

5.3.3 Construction cost

The cost of construction is calculated by equation (5.4). The construction cost is the cost for either building or installing the decision alternatives, or for building an interim bridge in case of bridge failure. The bridge is publicly owned. The financing of construction is done through the tax bill. The cost of financing through the tax bill is 0.20 NOK per 1 NOK financed [15].

$$C_c = (1 + C_{tax})C_{c_0} \tag{5.4}$$

Where, C_{tax} is the tax cost. C_{c_0} is the cost of the construction by it self.

5.3.4 Present value and time period of the analysis

The third quarter of 2020 is used as a reference point for economic considerations. The costs in the handbook V712 is given as the 2016 price level. The prices are inflation-adjusted using the price index for road infrastructure projects [44]. All the costs in the previous tables are multiplied by 1.0974. The future costs appear at different times. The present value is used to calculate the current value of future costs. The discount rate that shall be used for public projects is set by the government to be 4% [15]. All the future costs are discounted. Equation (5.5) is used to calculate the present value. If the cost flow is discrete, the integral is changed by a summation sign. The time period of the analysis is 40 years for infrastructure projects in Norway [15].

Present value calculations:

$$C = \int_{t1}^{t2} c_0 \cdot (1 + r)^{-t} dt \tag{5.5}$$

Where, C is the discounted cost. c_0 is the economic base cost. r is the 4% discount rate. $t1$ and $t2$ is the start and end time of the cost flow.

5.4 The period between 2020 and 2023

5.4.1 Traffic model and detouring

A traffic flow model must be established to quantify the socio-economic losses due to an implementation of the different decision alternatives, and the cost of

failure. The model is kept simple. It is without the reach of this master thesis to develop an advanced traffic flow model. Reasonable detour routes must be established to calculate the cost of a bridge close down.

The position of the bridge is marked with a red circle in the maps in figure 5.2a. The western route is the E6. The route in the middle is the Norwegian national road 3 (Rv 3) trough Østerdalen. The eastern route is the deviation route heavy vehicles must drive if the Stavå bridge must be closed for traffic. There is one small road on the other side of the valley that can, in case of emergency, be used for deviation of the passenger cars. The location of interest is zoomed in in figure 5.2b. Note that the road available for deviations is the westernmost road in this figure.

(a) Overview map. **(b)** Zoomed map.

The shortest and least time-consuming route between the two major cities Oslo and Trondheim, is the Rv3 route. It is expected that many of the vehicles that drive the Rv3 are driving between the two cities. A natural choice for detouring if driving this route is to use the easternmost route in figure 5.2a. For the

calculations, it is assumed that all the heavy vehicles that follow this route must detour the easternmost route, as shown in figure 5.2a.
The situation is a little bit more complicated for the vehicles that drive the E6, which is the westernmost route in figure 5.2a. These vehicles can both be driving from the eastern and western parts of Norway. If they are driving from the Oslo region in the east, they can use the Rv 3 and use the detour the easternmost route given in figure 5.2a. If they are driving from the west (Bergen, Molde, Stryn, Ålesund, and others...), they can use the coastal road. The coastal route has some ferry connections. The rout is more time consuming, but it is shorter than the original route. It is assumed that the heavy traffic that drives the E6 route must drive one extra hour in case of a bridge close down. No extra kilometers are added.
It is assumed that all passenger cars drive the short detour route on the other side of the valley, which is shown in figure 5.2b. The effects of the assumptions are summarized in table 5.8. Google maps are used to find the extra kilometers and to estimate the lost time caused by detouring.

Table 5.8: Traffic deviation assumptions.

Vehicle type	AADT	Extra kilometers	Lost time [min]
Passenger vehicles	3804	7	25
Heavy vehicles Rv 3	851	38	56
Heavy vehicles E6	570	0	60

5.4.2 The daily socio-economic costs

The daily socio-economic cost of a bridge close down is calculated by equation (5.6). The calculation result is summarized in table 5.7. The result is used for the further calculations. One can see from the table that the cost is dominated by the cost of lost time.

The total daily cost calculations:

$$C_{se,d} = \sum_{i=1}^{3} C_{k,i} + C_{t,i} + C_{a,i} \tag{5.6}$$

Where:

$$\begin{aligned} C_{k,i} &= c_k \cdot (\text{AADT})_i \cdot d_{e,i} \cdot P_{index} \\ C_{t,i} &= c_t \cdot (\text{AADT})_i \cdot t_{l,i} \cdot P_{index} \\ C_{a,i} &= c_a \cdot (\text{AADT})_i \cdot d_{e,i} \cdot P_{index} \end{aligned} \tag{5.7}$$

Where,i is the cost from each detour route. c_k, c_t, and c_k is the basic cost values given by table 5.4, 5.6, and 5.7 respectively. (AADT) is the annual average daily traffic. d_e is the extra kilometers driven. t_l is the lost time. P_{index} is the inflation adjustment factor.

Table 5.9: Daily cost of bridge close down.

Vehicle type:	**Kilometer cost [NOK/day]**	**Time cost [NOK/day]**	**Accident cost [NOK/day]**	**Total cost [NOK/day]**
Private vehicles	50 838	650 155	6990	707 984
Heavy vehicles Rv 3	145 495	589 200	8490	743 185
Heavy vehicles E6	0	422 835	0	422 835
Total:	**196 333**	**1 662 191**	**15 481**	**1 874 004**

5.4.3 Cost calculations

At this stage, no accurate calculations of the probability of failure have been made. The first paragraph of this section considers the cost related to a bridge failure. Thereafter, the costs related to introducing the different safety measures are presented.

The expected cost of failure ($p_f C_f$)

The representatives from the Norwegian Public Road Administrations informed that the cost of building an interim bridge costs 35 million NOK. Additionally, it is assumed that the demolition cost is 5 million. Adjusted for the tax financing cost, which must be added to everything that is financed through the tax bill, the total cost of construction and demolition is 48 million. It is assumed that in case of bridge failure, it takes 60 days before a new interim bridge is built, and the road can open. The sum of 60 days of daily costs is 112 million NOK. The total cost of failure (C_f) adds up to 160 million NOK. The cost of potential fatalities and injuries by a bridge collapse is not included in the calculations.
In figure 5.3, the discounted expected cost of failure is plotted as a function of the probability of failure. Equation (5.5) is used for the discounting. The cost is discounted over 3.5 years. One can see from the figure that the expected cost spans from 100 NOK to about 5.2 million NOK.

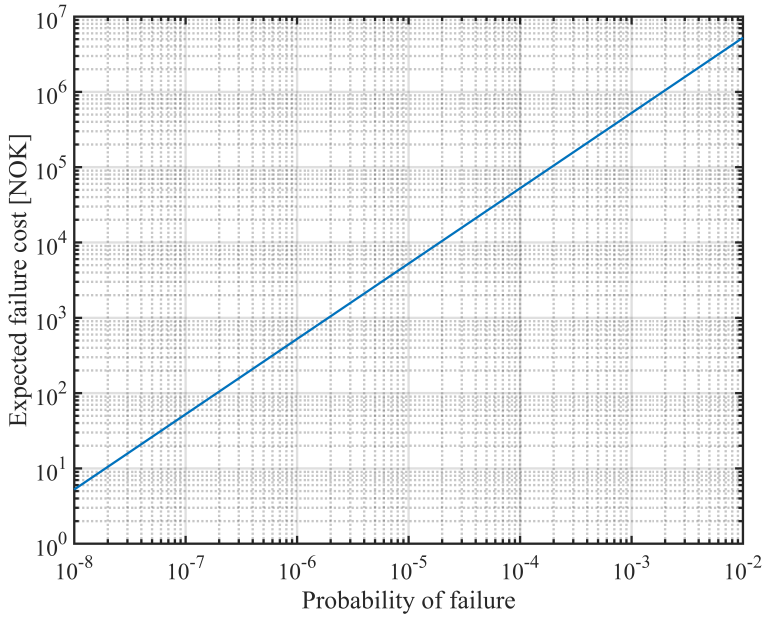

Figure 5.3: Discounted expected failure cost.

A0 The cost of doing nothing is 0 NOK. The A0 alternative is the benchmark for economic considerations.

A1 The Norwegian Public Roads Administration's report number 358 provides a calculation model to calculate the socio-economic benefit of increasing the permitted axle load [3] and total weight. The model is not really meant for calculating the cost reducing the axle load, but it is the best estimate that can be found. It is assumed that the benefit of increasing the axle load is equal to the cost of reducing the axle load. The heavy vehicles can not utilize the potential load capacity. The vehicles must drive more trips with less load. The model calculates the cost of extra trips. It is assumed that the permitted axle load is reduced to days 10 ton to 8 ton. The model divides the cost of lorries and semitrailer trucks. The AADT for heavy vehicles given by table 1.1 is 1336. It is for simplicity assumed that the AADT of semitrailers trucks is 1000, and the lorries are neglected. For a period of three and a half years, the discounted cost of reducing the axle load is 348 million NOK. The full calculation can be found in appendix A.1.

A2 A waiting time of only one minute per vehicle is used as a first estimate. The discounted cost 1 minute of time cost per vehicle over a three and a half year period adds up to 51 million NOK.

A3 The cost of strengthening work is uncertain, and it depends on which parts are needed to be strengthened. At this stage, no exact number for the cost of the strengthening work is given. However, the cost of closing down the bridge for four to six weeks is between 53 and 79 million NOK.

Approximately 10 % of the daily traffic volume passes the bridge between 22:00 and 06:00. The daily traffic amount is smaller in the winter than in the summer. The AADT is 3334 in January [62]. If the work is done at night in the winter, and the time consumption is 8 weeks the total socio-economic cost is $53 \cdot 2 \cdot 0.10 \cdot 3334/5140 = 6.9$ million NOK. The traffic is at it's worst in July. If the work is done at night in July the socio-economic cost is 15.9 million NOK. 5 million NOK is added to compensate for working at night. A magnitude of 10 million NOK must be expected for the strengthening work itself.

A4 The total costs of the interim bridge, including tax costs, are 42 million NOK.

A5 To close down the bridge for three and a half years is both for economic and politic reasons, barely an option at all. Three and a half years of daily costs add up to a discounted cost of 2237 million NOK.

5.5 The period after 2023

The period after 2023 is going to be revisited in chapter 8, after the structural analysis is carried out.

Chapter 6

Traffic load model

The previously discussed sensitive analysis highlights the strong effect that the load model has on the estimation of the probability of failure. This chapter is uses the Norwegian regulation on the use of motor vehicles [41] and Danish Road Directorates guideline for probability-based assessment of bridges [63] to develop customized load models that consider the number and the type of vehicle that drives over the bridge. Two distinct load models are going to be developed. The first one considers the traffic situation before the new road is finished. The second one considers the traffic situation after the new bridge is finished.

6.1 Legal regulations and road classification

An overview of the Norwegian road classification system is given in figure 6.1.

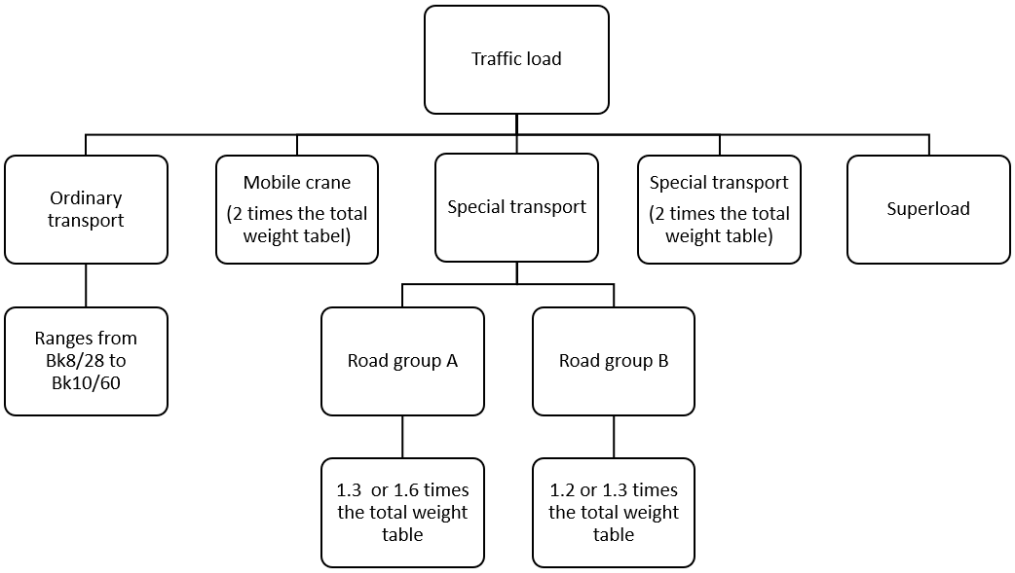

Figure 6.1: [56] Load classes.

All bridges have a classification for ordinary transport. The ordinary transport classification ranges from Bk6/28 to Bk10/60. The first number of the class indicates the allowed axle weight. The second number indicates the permitted total weight. Both figures are in metric tons. One can drive vehicles that satisfy the requirement for ordinary transport without any permission. Many of the roads are suitable for special transportation, and they are in addition to the ordinary class, classified into road group A or road group B. On these roads, one can search for permission to drive special vehicles that are heavier than ordinary traffic (typically Sv12/65 to Sv12/80). The difference between road group A and B is that road group A is more suited for heavy transport than road group B. The permission can either be given time-unlimited or time-limited. How much the load can be exceeded above the ordinary transport load depends on whether or not the permission is time-limited and on the road classification of the road. Further, the road can be classified for mobile cranes, special indivisible freight transport (Sv12/100), and superloads. Superload is a load that is greater than all

of the other load classes, and the cargo must be especially beneficial to society [41, 56, 53].

The Norwegian regulation on the use of motor vehicles

The Norwegian regulation on the use of motor vehicles regulates and specifies requirements for motor vehicles in Norway [41]. Chapter 5 regulates the weight and dimensions of motor vehicles. The axle load, the total weight and the dimensions of transport without any permission (ordinary transport) are regulated trough §5-4 to §5-7, transport with time-unlimited permission is regulated trough §5-8 (light or wide special transport), and transport with time-limited permission is regulated through the §5-9 and §5-10 (heavy or very wide special transport).

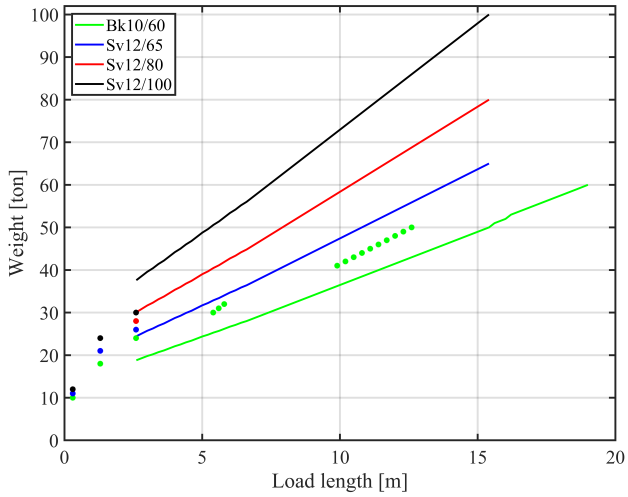

Figure 6.3: Maximum load. The green dots to the right are the semitrailer trucks. The three dots in the middle are the tipper trucks. The dots to the left are axle group loads. The green line is the total load table. The other lines are the total weight table multiplied with different multipliers.

There are mainly two criteria that limit the vehicle load. The first criterion is the axle load. There is a weight limit both for the axle, double axle, and triple axle loads. In figure 6.2, the three first dots are the single, double, and triple axle load. Note that the plot is only valid for Bk10/60 road group A roads. If the road had been classified into another class, for instance, Bk6/28, the plot would have looked different.

The second criterion is the permitted total weight of the vehicle. The allowed weight is for the special transport regulated through the total weight table, which can be found in § 5-8 clause 3 letter b [41]. The total weight table regulates the maximum load one can have within a certain length. The table gives values for the ordinary transport class, and the special transport classes are regulated by multiplying a number to the total weight table. For instance, is the permitted loads for the Sv12/100 found by multiplying the total weight table by 2. Transport with more than three axles in one axle group must satisfy the total weight table both for the single axle group and for the total axle distance, i.e., the total distance between the first and the last axle. If the distance between the axles in a multiple axle system is between 1.2 and 1.8 meters, the load on each axle can not exceed 1/3 of the permitted load for a triple axle system. For the Sv12/100 none of the axles can be closer than 1.3 meters. The total weight table is plotted figure 6.2. The first part of the green line, up to 50 tons, is the original total weight table for roads that are classified as Bk10/50. The blue line is the 1.3 times the total weight table (Sv12/65), which are vehicles that can be driven with a limited time restriction on Bk10/50 road class A roads. The red line is the 1.6 times the total weight table, and the black line is the 2 times the total weight table, which are vehicles that can be driven on Bk10/50 road class A roads with a time-limited restriction.

The restriction for the ordinary class is a bit more detailed. The total weight of the vehicle is regulated depending on the type of vehicle. The weight of a single-vehicle is regulated through table 2 [41], trucks with a full trailer (a

trailer that is supported both by front and rear axles) are regulated through table 3a [41], and trucks with a semitrailer (a trailer without a front axle) is regulated through table 3b [41]. Table 3a and b [41] gives many different load restrictions depending on the number of axles on the truck itself, the number of axles on the trailer, the distance between the axles in an axle group, and the distance between the last axle on the truck and the first axle on the trailer. Because of the vast number of combinations, only a few of them are plotted in figure 6.2. The three green points in the middle are the weight limitation for a four-axle vehicle (the tipper truck). The green points to the right are the weight limitation for a 3 axle truck with a 3 axle semitrailer (the semitrailer truck). Table 3b [41] gives the minimum distance between the last axle on the truck to the first axle on the trailer. The table is converted to give the total length between the first and the last axle. The length between the first and the second axle on the truck is fixed to 3 meters. The internal distance within the double axle group on the truck and the internal distances within the triple axle group is fixed to 1.3 meters. The distances can be seen in figure 6.4. As a reference, Volvo delivers its semitrailer trucks with different wheelbase options. The wheelbase (the distance between the first and the second axle) can be chosen to be between 3.0 to 3.9 meters [64].

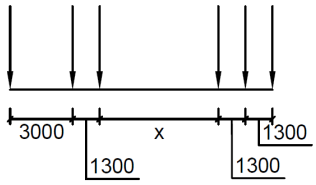

Figure 6.4: Converting table 3b values [mm].

The Bk10/60 class is regulated trough §5-5.3a. The last part, between 50 and 60 tons, of the green line in figure 6.2 is the load regulation given by §5-5.3a. The Bk10/60 regulation is an extension of the total weight table.
The load classes relevant for the bridge are summarized in table 6.1. The table

also shows the rules that are relevant to each of the load classes. The increase in the total weight is not proportional to the increase of the axle load.

Table 6.1: Load class summary.

Class name	Abbreviation	Dispensation	Time limited	Times the total weight table	Total weight [ton]	Maximum triple axle load [ton]
Ordinary transport	Bk10/50	No	No	1.00	50	24
Timber transport	Bk10/60	No	No	1.00	60	24
B-train	Bk10/60	No	No	1.00	60	24
Special transport	Sv12/65	Yes	No	1.30	65	26
Mobile crane	Sv12/65	Yes	No	2.00	65	28
Special transport	Sv12/80	Yes	Yes	1.60	80	28
Special transport indivisible freight	Sv12/100	Yes	Yes	2.00	100	30
Mobile crane	Sv12/72	Yes	Yes	2.00	72	30

The width of the vehicles

Vehicles are without any permission, in general, allowed to have a width of up to 2.55 meters. Vehicles that are transporting indivisible freight can without permission have a width up to 3.25 meters. Under special circumstances, it can be searched to drive a load that has a width of 4.20 meters.

6.1.1 Types of vehicles and their use

There is a great variety of different heavy trucks types with different axle combinations depending very much on the use of the truck. Trucks are, for instance, made for bulk, timber, vehicle, volume, fuel and gas, shipping container, sand,

and gravel transport. A common denominator is that everybody wants to optimize their profit and choose trucks optimized for their usage. For instance, if one is transporting load with high density, one only needs a sufficiently long truck to utilize the maximum load. On the other hand, if one is transporting voluminous goods, it is advantageous to have a truck that is as long as possible. Three different very typical trucks are chosen and will, later on, be used to study the load effects on the bridge.

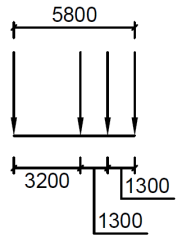

Figure 6.5: The silhouette of a tipper truck [mm].

The tipper truck is a truck often used for earthmoving on and between construction sites. It is desirable to have a compact truck that can be maneuvered on winding gravel roads. At the same time, the truck must be long enough to be permitted to drive a heavy load. It is of interest to have a rugged truck. This type of truck uses to have leaf springs, which are more solid than air suspension [35]. The figure 6.5 is a silhouette of the shortest tipper truck that is permitted to have a 32-ton total weight. The same axle arrangement, like that in figure 6.5, is often found on concrete trucks.

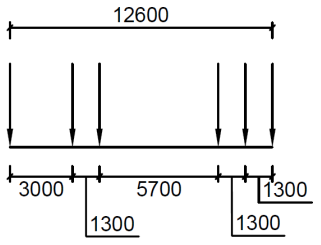

Figure 6.6: The silhouette of a semitrailer truck [mm].

The most common truck type for long-distance transport is a six-axle semitrailer truck. The truck itself has three axles (1 + 2), and the trailer has three axles. This is a type of truck that satisfies the Bk10/50 class. The figure 6.6 is the silhouette of the shortest semitrailer tuck that can have a 50-ton total weight. If the distance between the last axle on the truck to the first axle on the trailer is shorter than the 5.7 meters, the total weight must be reduced.

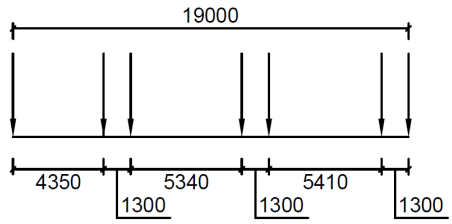

Figure 6.7: The silhouette of a B-train [mm].

The B-train (EuroCombi) is a type of truck that is relatively new in Norway. A trail arrangement started in 2008, and the final approval came in 2014. Since then, the number of B-trains on Norwegian roads has been ever-increasing [37]. The silhouette in figure 6.7 is the B-train with the smallest total wheelbase that can drive legal and with the least number of axles that can drive legally with a 60-ton total weight. Almost every truck used for long-distance transport has air suspension, which makes it possible for the driver to see the weight on each and every axle [35].

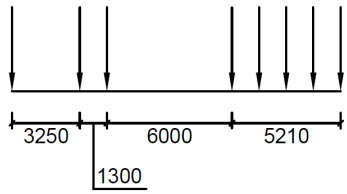

Figure 6.8: A vehicle that satisfies two times the total table [mm].

Furthermore, there is a great variety of axle combinations for special transport

classes. The silhouette in figure 6.8 is an example of a Bk12/100 truck. A truck with this axle configuration cannot utilize a 100-ton total weight, but the internal axle groups are fully utilized according to two times the total weight table. The five last axles are arranged so that they maximize the bending moment long an 8 meter long simply supported beam.

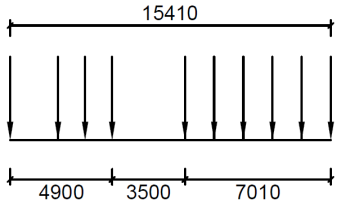

Figure 6.9: The shortest 100 ton vehicle [mm].

In general, will the load effect from a Bk12/100 truck that utilizes the maximum total weight be closer to the load effect of an idealized distributed load than a 6-axle semitrailer truck. The regulations allow a relatively higher increase in the total weight than the increase of the axle load. One needs at least 10 axles to be able to utilize a 100-ton total weight with an as short as possible vehicle, which is a 15.41-meter long vehicle. The vehicle is shown in figure 6.9 is the shortest vehicle that can legally have a 100-ton load.

6.2 Further considerations regarding the Norwegian load model

The characteristic static loads without the dynamic amplification given by the R412 handbook [53, 56] are plotted against the legal loads in figure 6.10. The handbook R412 dynamic load has a magnitude of 40% of one single axle load, which is 40 kN (4.08 ton) for Bk10/60 and 48kN (4.89 ton) for Bk12/100 [53, 56]. In figure 6.10, the pink dots closest to the Bk10/60 line are from the left,

the axle loads, the vehicle load at 7 meters, the Bk10/50 semitrailer load at 16 meters and at 18 meters the Bk10/60 semitrailer load respectively. The pink dots closest to the bk12/100 line are from the left, the axle loads, the vehicle load, and the semitrailer load, respectively. The density of the loads is plotted in figure 6.11. A short load is denser than a long load.

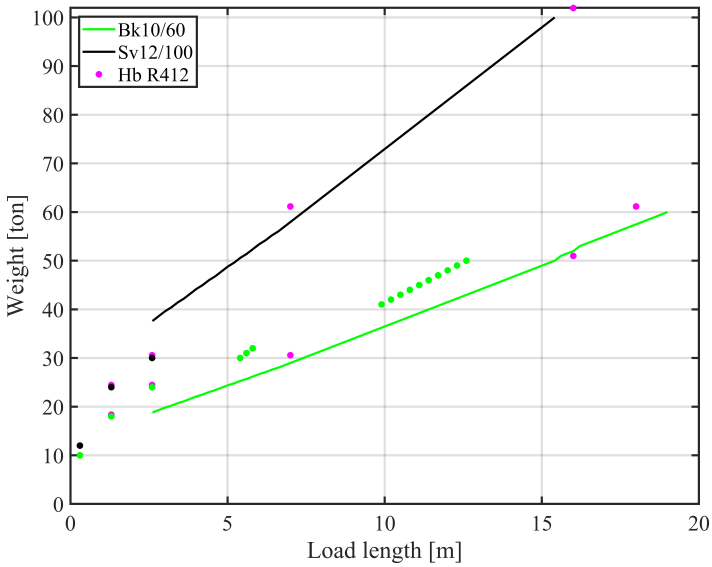

Figure 6.10: The Norwegian Public Roads Administration loads. The green dots to the right are the semitrailer trucks. The three dots in the middle are the tipper trucks. The dots to the left are axle group loads. The green line is the total load table. The black line is two times the total weight table. The pink dots are the Hb R412 static loads.

By comparing the maximum permitted load with the Norwegian Roads Administrations load model, it is evident that there is not full consistency between the load regulation and the load model. The Norwegian load model loads are close to the total weight table, but for the Bk10/50 ordinary transport, the total weight table does not give the maximum permitted load. The maximum loads are given by table 2, table 3a, and table 3b [41]. The few loads from the tables that are plotted in figure 6.10 and 6.11 is well above the total weight table. The charac-

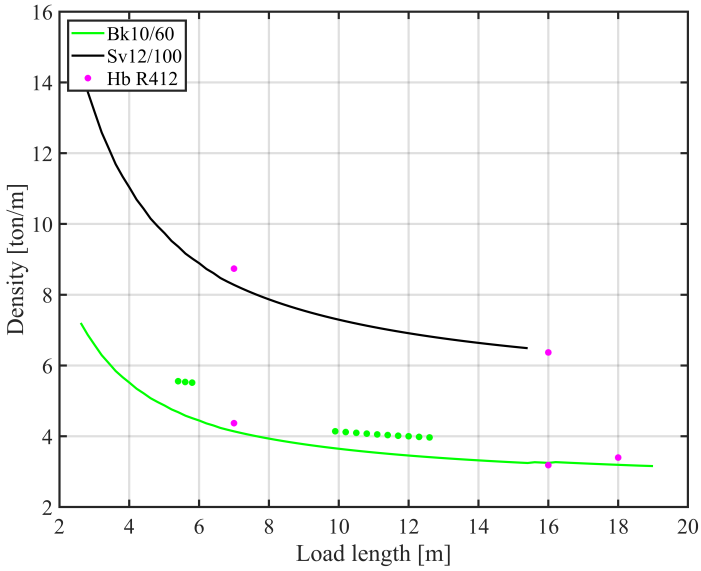

Figure 6.11: The Norwegian Public Roads Administration load density. The green dots to the right are the semitrailer trucks. The three dots in the middle are the tipper trucks. The dots to the left are axle group loads. The green line is the total load table. The black line is two times the total weight table. The pink dots are the Hb R412 static loads.

teristic load model loads are underneath the permitted load. The case is different for the Bk10/60 load. The Bk10/60 load is above the permitted load. The lack of consistency can lead to an underestimation of the load effect from a Bk10/50 (semitrailer) truck compared to a Bk10/60 (B-train) truck. As shown in chapter 7.3, the load effect on cross-section B-B is almost the same for both the tipper truck, the semitrailer truck, and the B-train. Therefore can none of the trucks automatically be neglected when estimating the number of relevant vehicles in section 6.3.2.

6.3 The probabilistic traffic load model

For the probabilistic modeling, the ordinary transport (Bk10/60) and special transport that satisfy two times the total weight table, i.e., the (Sv12/100) and mobile cranes (Sv12/72), are considered. The special transport is controlled first with the assumption that it can drive over the bridge simultaneously with ordinary traffic and then with the assumption that the special vehicle has to drive centric over the bridge.

A load model shall principally describe all possible traffic situations, ranging from free-flowing traffic to congested traffic. A full dynamic amplification can only be achieved with free-flowing traffic. In a completely congested traffic situation, dynamic amplification does not take place. As one can see from the load position in section 6.3.1, only one vehicle fits within the 8-meter beam span of cross-section A-A. For cross-section B-B, the situation is a little worse. An arch is sensitive to concentrated loads, and load on one side only. The Stavå bridge arch is slightly tilted. The northern support is in the vertical plane almost 2 meters higher than the southern support. Therefore, the vehicle must be placed on the northern side of the arch to provoke the most critical forces. The influence line of loads that contributes to an exacerbated stress state at the critical cross-section is therefore considered to be equal to 28.3 meters, which is the length between the top of the arch abutment column and the arch crown. The total length of a typical semitrailer truck is roughly 15-19 meters. The speed limit over the bridge is 80 km/h. If one assumes that it must be at minimum a 1-second gap between the vehicles driving at the speed limit, the distance between two vehicles is $(80/3.6 = 20.5)$ 20.5 meters. Two semitrailer trucks cannot be within the influence line at the same time $(15 + 20.5 = 35.5 > 28.3)$.
If a congested traffic situation is even close to the decisive load case, the traffic must be congested in both driving lanes on the north side of the arch only.

Arches perform well under evenly distributed load over the complete arch. A load on the south side will have a positive influence. One can maximally fit two semitrailer trucks within the influence line, and then the trucks must be parked as close as possible into each other. In such a situation, all the drivers have to ignore the sign, which tells that heavy vehicles must keep at least 50 meters distance. This situation is highly unlikely. At the same time, the dynamic amplification factor can be neglected. Due to this, the congested traffic situation neglected.

Breaking events are extremely unlikely to happen in combination with extreme loads. Breaking events are neglected without further reasoning.

6.3.1 The load position

Longitudinal

The critical cross-sections are found by the deterministic analyses. As mentioned in section 1.1 several recalculations have been conducted. Every report has, dependent on the analysis method, pointed at different critical cross-sections.
As previously mentioned, the structural analysis in this thesis is restricted to cross-sections A-A and B-B. The traffic load situations yielding the highest forces at the considered cross-sections are shown in figure 6.12. LA and LB refer to the traffic loads at cross-sections A-A and B-B, respectively. For cross-section A-A the worst load position is when the load, which is a triple axle system for the ordinary transport class, is placed almost in the middle of the 8.1-meter span. The influence line for which loads contributes negatively to the stress state is considered to be the 8.1-meter span.
The worst load placement for cross-section B-B is considered to be when a distributed load is placed, starting from the arches center, on the north side of the

arch [48]. For cross-section B-B, the influence line for which loads contribute negatively to the stress state is considered to be the 28.3-meter span shown in figure 6.12.
The property of the load for the two cross-sections and the different transport classes is considered more carefully in section 7.2.2.

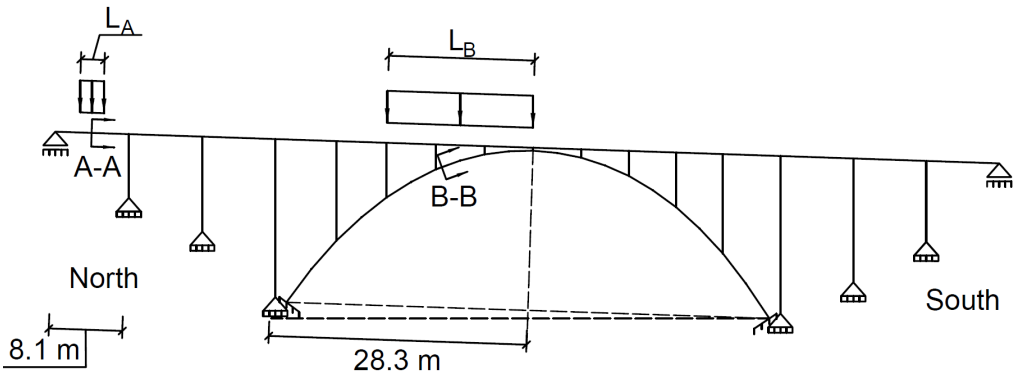

Figure 6.12: The load position.

Transverse

For the ordinary transport situation, the transverse vehicle position is assumed deterministic. Figure 6.13 shows the contour of two meeting trucks on the bridge. A standard truck is 2.5 meters wide without the side view mirrors. The distance from guard rail to guard rail is 6.0 meters. As one can see from the figure, there is not much space for a different transverse position.

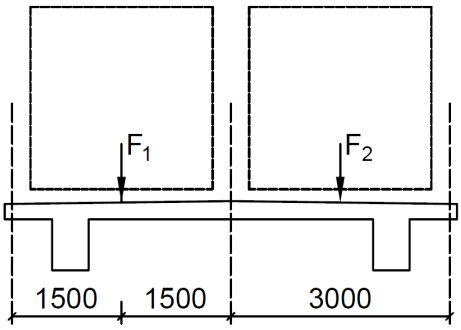

Figure 6.13: Traverse load position ordinary transport [mm].

The special transport trucks are, in many cases, even wider than ordinary trucks. It is questionable if a special transport truck and an ordinary truck can meet at the bridge at all. In the case where the special transport trucks are instructed to drive centric over the bridge, the vehicle position is treated as a normally distributed variable. The mean of the distribution is at the center of the beam, and the standard deviation is 0.5 meters. Figure 6.14 shows the probability density function of the random variable. A truck cannot drive outside the bridge. Therefore the resultant vehicle force is restricted to maximally 1.75 meters out from the center.

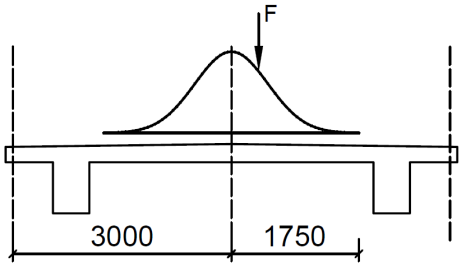

Figure 6.14: Traverse load position Bk12/100 [mm].

6.3.2 The extreme value distribution

The probability distribution for the traffic load is defined by equation (6.1). Where ν_1, ν_2, and ν_{12} are the intensity of the lane 1 traffic, the lane 2 traffic, and meeting events, respectively. T is the reference period; in this case, one traffic year. $F_1(q)$, $F_2(q)$ and $F_{12}(q)$ are the load effect form lane 1, lane 2 and simultaneous load in lane 1 and lane 2 respectively. When the simultaneous load effect ($F_{12}(q)$) is calculated, it is conservatively assumed that the load effect from each truck is the same as if they had met at the worst load position, which is the load positions shown in figure 6.12.
The traffic flow is assumed to be a Poisson process. Thus, it is assumed that the average rate of vehicles passing the bridge is constant, the occurrence of one vehicle does not affect the probability that another vehicle passes (independent events), and two vehicles cannot occur at the same time.

$$\begin{aligned} F_{max}(q) = &\exp\left(-(\nu_1 - \nu_{12})T(1 - F_1(q))\right) \\ &\exp\left(-(\nu_2 - \nu_{12})T(1 - F_2(q))\right) \\ &\exp\left(-\nu_{12}T(1 - F_{12}(q))\right) \end{aligned} \tag{6.1}$$

The intensity of meeting events can be calculated by equation (6.2).

$$\nu_{12} = \nu_1\nu_2\left(\frac{L_1 + l_1}{V_1} + \frac{L_2 + l_2}{V_2}\right) \tag{6.2}$$

L_1 and L_2 are the vehicle lengths, l_1 and l_2 are the influence lengths, and V_1 and V_2 are the vehicle speeds for lane 1 and lane 2 respectively.

6.3.3 The number of relevant vehicles

Vehicles that can utilize the permitted axle load

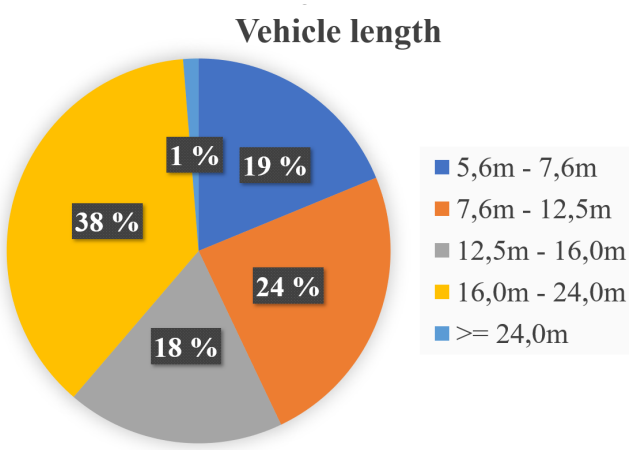

Figure 6.15: [60] Length distribution of heavy vehicles.

Only the heaviest vehicles are of interest. The passenger cars are neglected. The Norwegian Public Road Administration has automatic measuring stations that count and measure the length of the vehicles that paces the station. The data in figure 6.15 are from Garli, which is on the E6 some kilometers north of the bridge. The AADT of heavy vehicles over the bridge is 1337 (ref. table 1.1). The overall chassis length of the tipper truck is not less than 9.4 meters [65]. All the vehicle shorter than this is assumed not to be decisive vehicles. $100 - 19 - 24/2 = 69\%$ of the vehicles are assumed to either be semitrailer trucks, B-trains, or tipper trucks. Table A.2 and A.3 provides information on the share of the heavy vehicles that utilizes the permitted axle load, $0.73(1-0.35) = 48\%$. Finally, it is assumed that $0.48 \cdot 69 = 33\%$ of the heavy vehicles both utilizes the axle load and are either semitrailer trucks, B-trains, or tipper trucks. It assumed that 25% are tipper trucks, 50 % are semitrailers, and 25% are B-trains.

It is assumed that 200 Sv12/100 special transport vehicles drive over the bridge

every year.

Further assumptions

- The number of hours in which vehicles are using the road network is assumed to be 15 hours per day.
- The vehicle speed in both directions is assumed to be 80 km/h.
- Both vehicle lengths are assumed to be 19 m.
- The influence length is either 8.1 m or 28.3 m.

Intensities the relevant events

Table 6.2 shows the intensity for the ordinary transport. Table 6.3 shows the intensity for the special transport. ν_{12} is in table 6.3 the number of meeting events between a special transport vehicle and a ordinary transport vehicle. The numbers are round of upwards to the closest integer.

Table 6.2: The intensities for the ordinary transport, Bk10/60.

Bk10/60	**Year**	
Intensity [Trucks/year]	**2019**	**2023**
ν_1	117121	4517
ν_2	117121	4517
ν_{12} (Internal 8.1 m span)	803	3
ν_{12} (28.3 m)	1401	5

Table 6.3: The intensities for the special transport, Sv12/100.

Sv12/100	Year	
Intensity [Trucks/year]	**2019**	**2023**
ν_1	100	6
ν_2	100	6
ν_{12} (Internal 8.1 m span)	2	1
ν_{12} (28.3 m)	3	1

6.3.4 On the probabilistic property of each vehicle

On the benefit and disadvantages of driving with to heavy load

Most of the trucking companies benefit from driving overload. The more freight one can transport at once, the higher the profit becomes. On the other hand, the expenses of getting caught with overload are high. In Norway, the fine is 450 NOK per 100 kg overload the first 5000 kg, then 700 NOK per 100 kg [58]. In extreme cases, the companies or drivers can lose the license to drive trucks in Norway. Trucking companies can, and some do, speculate in overloading [57]. They optimize the profit with the expected cost of getting caught as a part of the equation. News articles about people getting caught are written regularly, and sometimes the fine exceeds 100 000 NOK [61].

Weight and axle configurations

The weight of each vehicle is assumed to be normally distributed. The axle arrangement and the length of the vehicles are made so that they just fulfill the regulation's minimum requirements for the given vehicle class. In this way, consistency between the different transport classes and between the different types of vehicles are provided. The vehicles are made with an axle spacing as short as permitted. The load on each axle in an axle group is assumed to be

equal on all the axles, even though one is allowed to have internal variations between the axles. One is, for instance, allowed to 11.5 ton on the drive axle. This assumption is also made in order to keep the calculations as consistent as possible. The static load effect on the bridge caused by a vehicle that just fulfills the regulations minimum requirements is assumed to be defined as the 50%-fractile of the vehicle weight distribution.

It is chosen to use different standard deviations for the different types of trucks. The tipper trucks do usually have leaf suspensions. The driver does not know the weight of the truck precisely. Experienced excavator operators know how many buckets one can fill into a truck without exceeding the weight limits [35]. However, they usually operate with the mean value, and the weight of soil is varying. A standard deviation of 4 is assumed for tipper trucks.

The long-distance trucks have, in most cases, air suspension. The driver knows the weight of the truck more precisely. The weight control of trucks operates with a safety margin that is meant to take into consideration that snow and ice can form on the truck. Sometimes the drivers use this safety margin to more load [35]. The heaviest special transport trucks are required to have air suspension. A standard of 2.5 tons is assumed for both the semitrailer truck, the B-train, and special transport trucks.

$$W_{tipper} \sim N(32, 4) \tag{6.3}$$

$$W_{semi} = W_{B-train} = W_{Sv12/100} \sim N(50/60/100, 2.5) \tag{6.4}$$

Where, W_{tipper}, W_{semi}, $W_{B-train}$, $W_{Sv12/100}$ is the probability distribution of the tipper, semitrailer, B-train, and special transport tuck respectively.

The dynamic amplification factor

The distribution given by the danish standard is used. The dynamic amplification factor is defined by equation (6.5) and (6.6).

$$K_t = 1 + S_t \tag{6.5}$$

$$S_t = N(\frac{41.5}{9.81w}, \frac{41.5}{9.81w}) \tag{6.6}$$

The model recognizes that the dynamic amplification factor is smaller for a big load than for a small load. The heavier the vehicle is, the more its dampers contribute to the damping of the complete system. Heavy vehicles also tend to have more axles than a lighter vehicle. All the axles can not hit a bump or a pothole at the same time. The magnification of the axle force will, with high probability, not coincide.
The extreme events are caused by vehicles with overloaded or destroyed dampers, making the damping small and the stiffness of the dampers big. At the same time must the vehicle hit a surface irregularity/-ies that have the right position and at the correct speed [27].
There are mainly two types of suspension for trucks and trailers. One of them is leaf spring suspension. The other is air suspension. Leaf spring suspension tends to be stiffer than air suspension, which in general leads the leaf spring suspension to provoke a higher dynamic amplification than the air suspension [27]. Air suspension has the advantage that the truck driver easy can know the axle loads of the truck.

The traffic load model uncertainty

The traffic load model uncertainty (I_t) is modeled as a normally distributed variable with the mean value of 1 and a coefficient of variation of 0.10, 0.15, or 0.20

depending on the circumstances. The danish standard recommends using 0.15 for special transport and 0.20 for ordinary transport. The traffic load model uncertainty is introduced to the calculation model by multiplying it to the load. The number of ordinary vehicles is in the case of the Stavå bridge known to much greater accuracy than the number of special trucks. It is chosen to use a CoV of 0.20 both for the ordinary traffic situation and for special transport.

Chapter 7

Assessment of load bearing capacity

This chapter contains a description of the mechanical model that is used. Several simplifications have been made and some load effects, due to temperature and wind, are neglected. A description of the simplifications and the neglected loads are given. The chapter is describing the considered load cases, and how the load is distributed and transferred to the critical cross-sections. At the end a probabilistic capacity assessment is carried out on the two critical cross-sections using Monte Carlo simulations. Matlab scripts have been developed and are used for the execution of the Monte Carlo Simulations.

7.1 The mechanical model

7.1.1 General assumptions and simplifications

Simplified models have been developed to determine the forces at the critical cross-sections. The models are partly based on analytical solutions and partly based on two-dimensional finite element modeling. The bridge beam is treated as a continuous beam on rigid supports. The arch deflection is not considered when calculating the forces in the beam. The arch is modeled a free-standing

arch, separately form the bridge beam. The stiffness of the bridge beam is neglected when calculating the forces in the arch. All the additional moments caused by the load are transferred to the arch only.
The assumption is conservative, at least with regard to the stresses in the arch. The deflection of the arch leads in reality to additional stresses in the bridge beam. The stiffness of the bridge beam is reduced compared to the stiffness of the arch. In this way, some of the extra moments are transferred to the arch. The bridge is ductile enough for moments to be redistributed. The assumption can be seen as a redistribution of moments from the bridge beam to the arch.

The modeling is based on a linear elastic analysis where all the elements are assumed to be uncracked, and the reinforcement ratio is assumed to be constant over the complete bridge. The bridge beam is modeled as a straight beam even though it, in reality, is slightly curved in the spans closest to the abutments. The geometry of the bridge is based on the original construction drawings.
The geometrical imperfections of the arch were measured. The measurements are given on an old as-built drawing. It is written on the drawing that some of the measurements are affected by wind [2]. Geometrical changes to the construction caused by creep, shrinkage, and alkali-silica reactions are not considered. Creep and shrinkage have a shrinking effect on the concrete. Alkali-silica reactions are leading to an expansion of the concrete [42]. The geometrical changes must in itself be treated as a probabilistic variable. It is outside the scope of this master thesis to make probabilistic models for creep, shrinkage, and alkali-silica reactions. For the reasons mentioned above the geometrical imperfections is neglected.

The restraint stresses that may have arisen as a consequence of the bitumen filled expansion joint are neglected. Temperature load and wind load are also neglected.

7.1.2 Force distribution

Transverse

The bridge beam is simplified as a single span statically determined beam, which is torsionally fixed by the cross members between the T-beams webs. The bridge beams mechanical substitute system can be seen in figure 7.1.

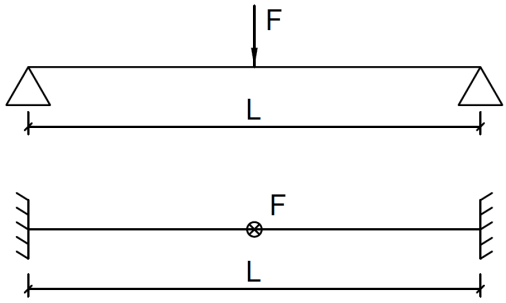

Figure 7.1: Idealization for the transverse force calculations.

The traverse force distribution is calculated by the use of the flexibility method, i.e., by defining and solving a compatibility condition. In figure 7.2, the cross-section is divided at the middle, and the unknown force is found by solving the equation.

$$\delta_{aa} = \delta_{ap} \tag{7.1}$$

Where, δ_{ap} is the deflection caused by the applied force P, and δ_{aa} is the deflection caused by the unknown force X_a. The deflection δ_{aa} has three components: δ_{aa1} is caused by bending, δ_{aa2} is caused by rotation, and δ_{aa3} is caused by transverse bending.

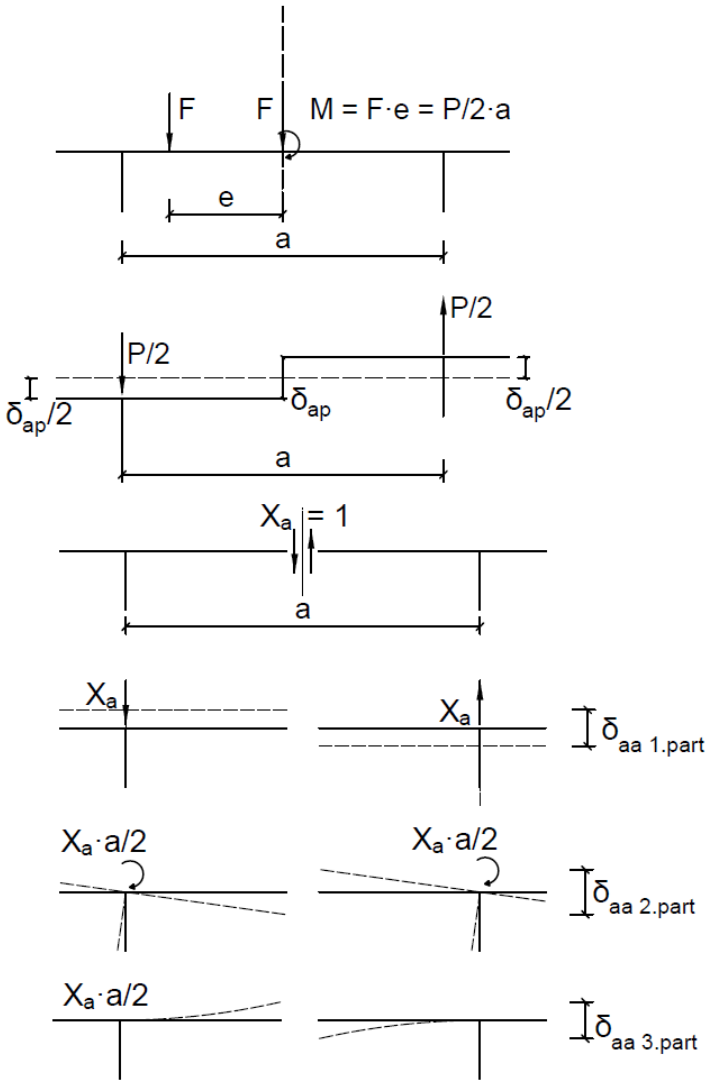

Figure 7.2: [5] The transverse force calculations method.

Solving the compatibility condition given by equation (7.1) gives the solution for X_a that is given by equation (7.2) [5].

$$X_a = \frac{\frac{P}{L}}{\frac{2}{L} + \frac{\pi^2 a^2 EI_{HBB}}{2L^3 GI_T} + \frac{\pi^4 a^3 EI_{HBB}}{24L^4 EI_{Plate}}} \tag{7.2}$$

Where, $P = \frac{2e}{a}$ when $F = 1$, L is the length of the span, a is the distance between the two webs , EI_{HBB} is the bending stiffness of half the bridge beam, GI_t is the torsional stiffness, and EI_{plate} is the bending stiffness of the complete middle plate.

The equilibrium calculation finally finds the force distributing to each side of the cross-section in equitation 7.3 and 7.4.

$$F_{HBB1} = 0.5 + \frac{P}{2} - X_a \tag{7.3}$$

$$F_{HBB2} = 0.5 - \frac{P}{2} + X_a \tag{7.4}$$

The geometrical measurements of the cross-section can be found in figure 7.25. The flange height varies between 210 mm and 250 mm. For the determination of the transverse force distribution, a constant cross-section height of 230 mm is assumed.

The solution of the transverse force distribution shall be found in a place between the solution one gets when the cross-section is considered completely rigid and when the force is calculated with the law of the lever. The ratio L/a is small for all spans. The stiffness in the longitudinal direction is rather big compared to the stiffness in the transverse direction. The transverse force distribution is quite close to the law of the lever arm solution.

The load distribution between the two sides of the bridge beam for the ordinary traffic situation is given by table 7.1. The transverse position of the trucks is probabilistic when the load position of the special transport class is assumed to be centric.

Table 7.1: Load distribution between the two sides of the bridge beam.

Cross-section	Span length [mm]	Beam 1	Beam 2
A-A	8067	0.8291	0.1709
B-B	4177	0.8394	0.1606

Longitudinal

The bridge beam is considered as a continuous beam on rigid supports in the longitudinal direction. The beam reaction forces are transferred through the columns, either to the ground or to the arch. Figure shows the bride beams mechanical model. The position of the critical traffic load is also shown.

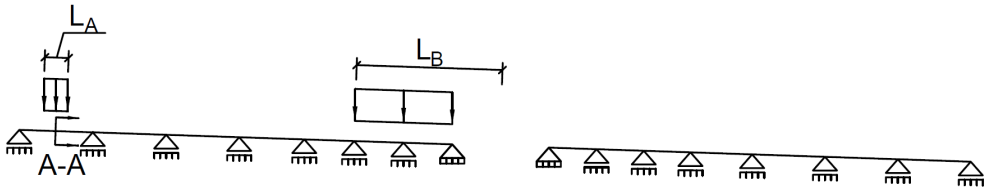

Figure 7.3: The top beam with traffic load.

The transition zone between the bridge beam and the arch is a challenge to model. The part of the traffic load that is on the transition zone is applied directly to the arch. The rest of the traffic load is applied to the bridge beam. It is chosen to model the transition between the arch and the bridge beam as a pinned support. The transition support reaction force is added to the arch as a distributed force. The other reaction forces are applied to the arch as point loads. Figure 7.4 shows how the traffic load is applied to the arch.

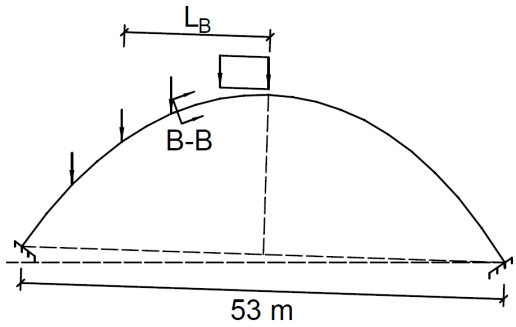

Figure 7.4: The arch with traffic load.

The bridge beam is divided in the middle of each span. The load effect of the beam sections and the columns are applied as point loads. The weight of the transition zone is applied as a distributed load.

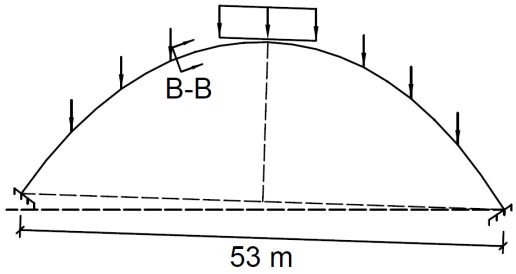

Figure 7.5: The arch with self weight.

7.1.3 The geometry of the arch

The finite element program Robot structural analysis is used to model the arch. Only one of the two arches is modeled. Two-dimensional elements are used. The geometry from the original construction drawings is used. The centerline of the arch is used as geometrical input. The drawings give 21 arch coordinates. The arch elements are straight between these points. Figure 7.6 shows how the arch is divided into straight elements. The cross-section of the arch is tapered. The cross-section height at the supports is 1910 mm. At the crown, the cross-

section height is 1100 mm.

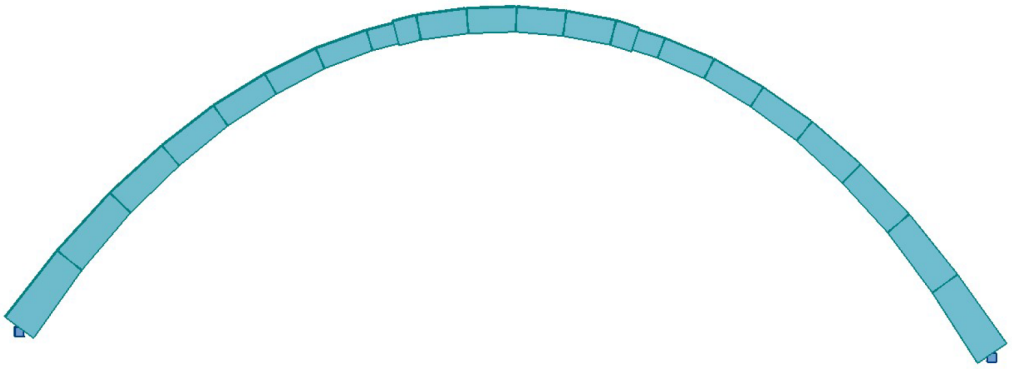

Figure 7.6: The geometry of the arch.

Figure 7.7 shows the transition between the bridge beam and the arch. The figure shows the reinforcement in the arch, but not the reinforcement in the bridge beam. Shear reinforcement connects the bridge beam to the arch. It is assumed that the arch is stiffer in the transition zone. The height of the arch set to be 1330 mm for the complete transition zone, which is the sum of the bridge beam flange and the arch height.

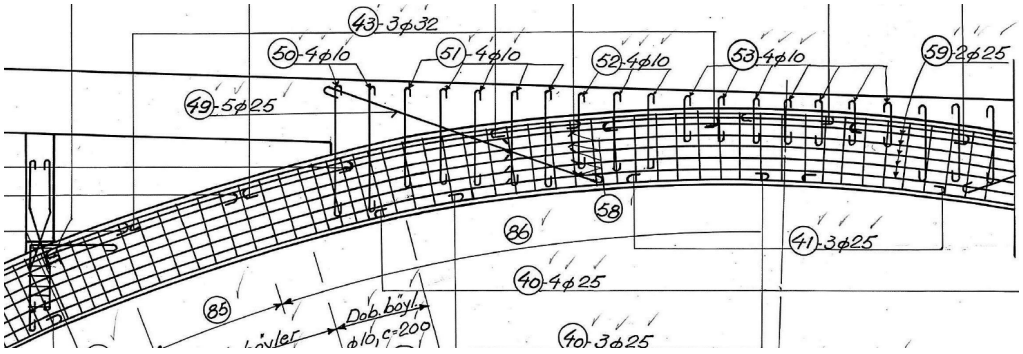

Figure 7.7: [2] The transition zone between the bridge beam and the arch.

The northern support of the arch is 1.8 meters higher than the southern support. The angle between the horizontal plane and the arch supports connecting the

line is 1.9 degrees. In figure 7.8, the surface coordinates of the arch are rotated 1.9 degrees around the crown. The arch is rotated so that both supports are on the horizontal plane. One can see that the arch is symmetric. Also, the column placement on the arch is symmetric. A hyperbolic cosine and a parabolic function are fitted so that the function, by definition, goes directly through the northern support and the top point of the arch. The hyperbolic cosine and the parabolic function are important because they are the anti-funicular form of an arch that is exposed to an evenly distributed load that is distributed over the complete arch and applied perpendicular to the supports connecting line. The hyperbolic cosine function is the anti-funicular form when the distributed load flows the shape of the arch [5]. The parabolic function is the anti-funicular form when the distributed load is straight. An anti-funicular formed structure is a structure that carries the applied force only by pure compression. However, gravity does not work perpendicular to the supports connecting line. The gravity works with a 1.9 degrees angle to the connecting line. One can decompose the gravity force into one component working perpendicular to the connection line and one component working parallel to the connecting line. The perpendicular component carried approximately by pure compression. The parallel component will introduce some moments in the arch.

7.2 Loads

7.2.1 Permanent and quasi permanent loads

The permanent and quasi permanent load properties

The permanent load, i.e., the self-weight, is modeled with a normal distribution. The mean concrete density is 25 kN/m^3 and the CoV is 0.05. The quasi-permanent loads, such as the guard rails and the asphalt is modeled with a normal distribution. The mean density of the asphalt is 25 kN/m^3 and the guard rail

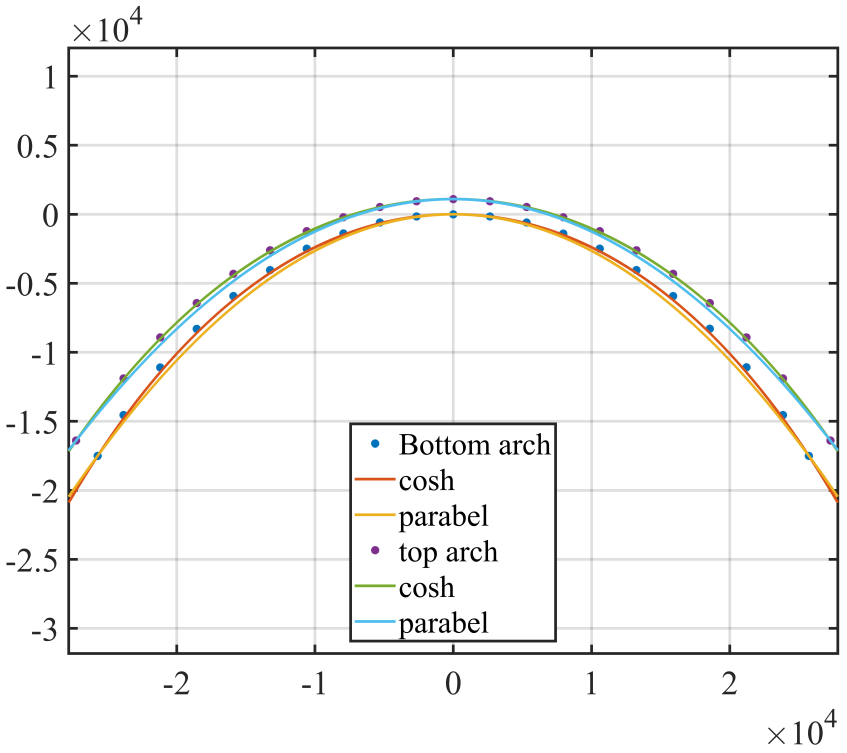

Figure 7.8: The form of the arch [mm].

is assumed to have a weight of 150 kg/m. The asphalt thickness was in 2007 measured to be 5 cm [6].The CoV is 0.1 for the quasi-permanent loads.

The geometry given by 7.21 is used for the calculations of the bridge beams self-weight. The calculated values are given by table 7.2 correspond to values for the half of the bridge beam.

Table 7.2: The half bridge beam self weight.

Material:	**Load [kN/m]:**
Asphalt	4,5
Gelander	1
Concrete	31,8
Sum:	37,3

The forces from the bridge beam and the columns applied on the arch are given by table 7.3. The correspond to the value from half the bridge deck. TZ is the force applied in the transition zone. As shown in figure 7.5, the transition force is distributed over the complete transition zone. The self-weight of the arch itself is calculated directly by robot structural analysis.

Table 7.3: Self-weight forces applied on the arch.

Column number:	**1**	**2**	**3**	**TZ**	**4**	**5**	**6**
Total force [kN]:	273,82	229,65	195,00	566,53	187,65	219,02	260,13

Model uncertainty

The model uncertainty for the permanent and quasi-permanent loads is assumed to be normally distributed. The mean value is 0 and the standard deviation equal to 5 % of the mean value of the sum of the permanent and the quasi-permanent load. The model uncertainty is added to the basic variable [63].

7.2.2 Traffic load cases

Cross-section A-A

From the previous studies, it was found that the worst load case for cross-section A-A is an axle group consisting of three axles. Almost every vehicle presented

in 6.1.1 has a triple axle group. The triple axle group is almost always at the back end of the vehicle. The vehicles are in one of the driving lanes driving of the bridge. The axle/-es in front of the triple axle system will not contribute to the span moment. In the other lane, the axles in front of the triple axle system can be in the second span. The other axles can reduce the span moment in span one. This positive effect is, however, neglected. The load effect from the second lane on the beam under lane one is much smaller than the load effect from the first lane on the beam under lane one. The positive effect is rather small. The calculations are also harder to carry through. The load effect from each single vehicle type must in such case be considered more closely.

The finite element program Robot structural analysis is used to find most unfavourable load position and calculate the load effect. The northern side of the bridge beam is modeled as a continuous beam. The triple axle load system is applied as a discrete movable load on the beam. Each load step is set to be 0.1 meters. The legal limit for a triple axle group load is 24 tons for the ordinary transport class. The 24-ton load is divided equally between each axle. Each axle has an 8-ton weight. The minimum permitted distance between the axles is 1.3 meters. The load case is shown in figure 7.9.

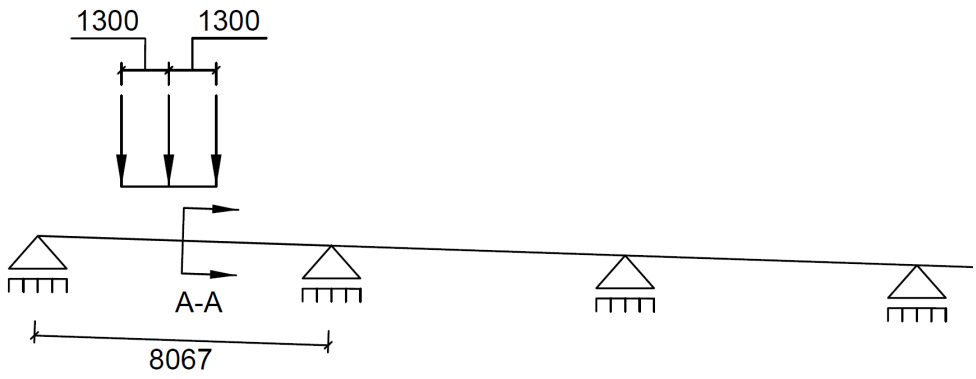

Figure 7.9: Load case for cross-section A-A ordinary transport [mm].

For the Bk12/100 special transport class, it is not given that a triple axle system gives the worst load case. As shown in section 6.1, the increase of the axle load is much smaller than the increase in the total weight. One can risk that an axle group consisting of more than three axles is a worse load case than a triple axle group. To approximately find the worst legal load case, the bridge span is idealized as a statically determined beam. The load is considered as an evenly distributed load. The substitute system can be seen in figure 7.10. As shown in figure 6.11, the density of the load (q) falls off as the length of the load gets bigger. The q used in the calculation is the q given by the 2 times the total weight table, which is the black line in figure 6.11. The distributed load is placed in the middle of the beam. The length c is the variable. Equation (7.5) is the equation for the maximum span moment [25].

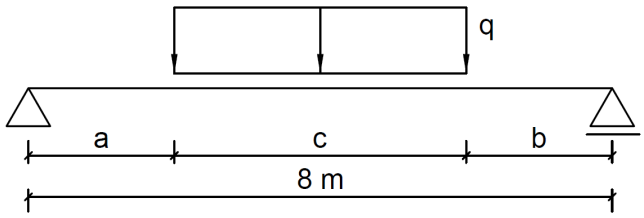

Figure 7.10: Bk12/100 load case calculations.

$$M_{max} = \frac{A^2}{2q} + Aa \tag{7.5}$$

Where, a is the distance between the first support to the start of the load, A is the first supports reaction force. A is found by equation (7.6).

$$A = qc(2b + c)2L \tag{7.6}$$

Where, L is the length of the span, b is the distance between the end of the load to the second support. c is the length of the load.

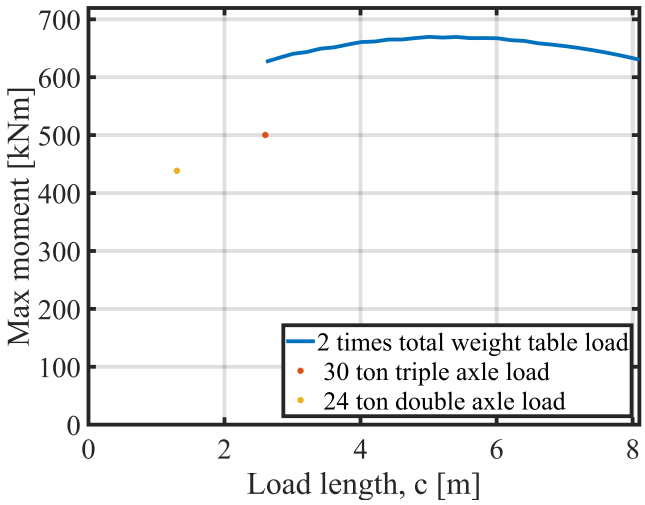

Figure 7.11: Worst load effect Bk12/100 calculation result.

Figure 7.11 shows the maximum span moment as a function of the length of the distributed load. One can see from the figure that the maximum load is caused by a 5 meters long distributed load. However, the distance between the axles must be at least 1.3 meters for the Bk12/100 load. It is chosen to use an axle group with 5 axles. The distance between the first and the last axle in the axle group is 5.21 meters, and the total permitted load within the 5.21 meters is 49.6 tons. The load is evenly distributed between the axles. Each axle has a 9.92-ton load. The final BK12/100 lode case for cross-section A-A is shown in figure 7.12.

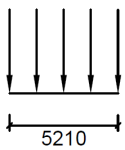

Figure 7.12: The final Bk12/100 cross-section A-A load case [mm].

Cross-section B-B

The deterministic load analysis carried out by Aas Jakobsen uses the Norwegian Public Road Administrations load model to find the worst load case [48]. This is used as input in the current study for. The dynamic amplification factor is also considered differently in this thesis. The characteristic load is, contrary to the Norwegian load model, expressed without the dynamic amplification factor. The load position that was found by the use of the Norwegian Public Road Administrations load model is used in further considerations, despite the fact that the worst load position can be a little different. One is not guaranteed that the very worst load position is found.

For the ordinary transport case, it is chosen to use the vehicles presented in section 6.1.1 as load cases. In figure 7.13, the first load case is the 32-ton tipper truck. Load case 2 is a 50-ton semitrailer. Load case 3a is the B-train from section 6.1.1. Load case 3b is a B-train where the trailer from load case 2 is used as part of a B-train. Additionally, a fourth load case is applied. The Bk10/50 and Bk10/60 load case from the Norwegian Public Road Administrations load model is applied without the dynamic amplification factor. The Norwegian standard treats the Bk10/50 load as a 500 kN load that is distributed over 16 meters. It treats the Bk10/60 load as a 600 kN load distributed over 18 meters. All the load cases are applied so that the back end of the vehicles are at the center of the bridge.

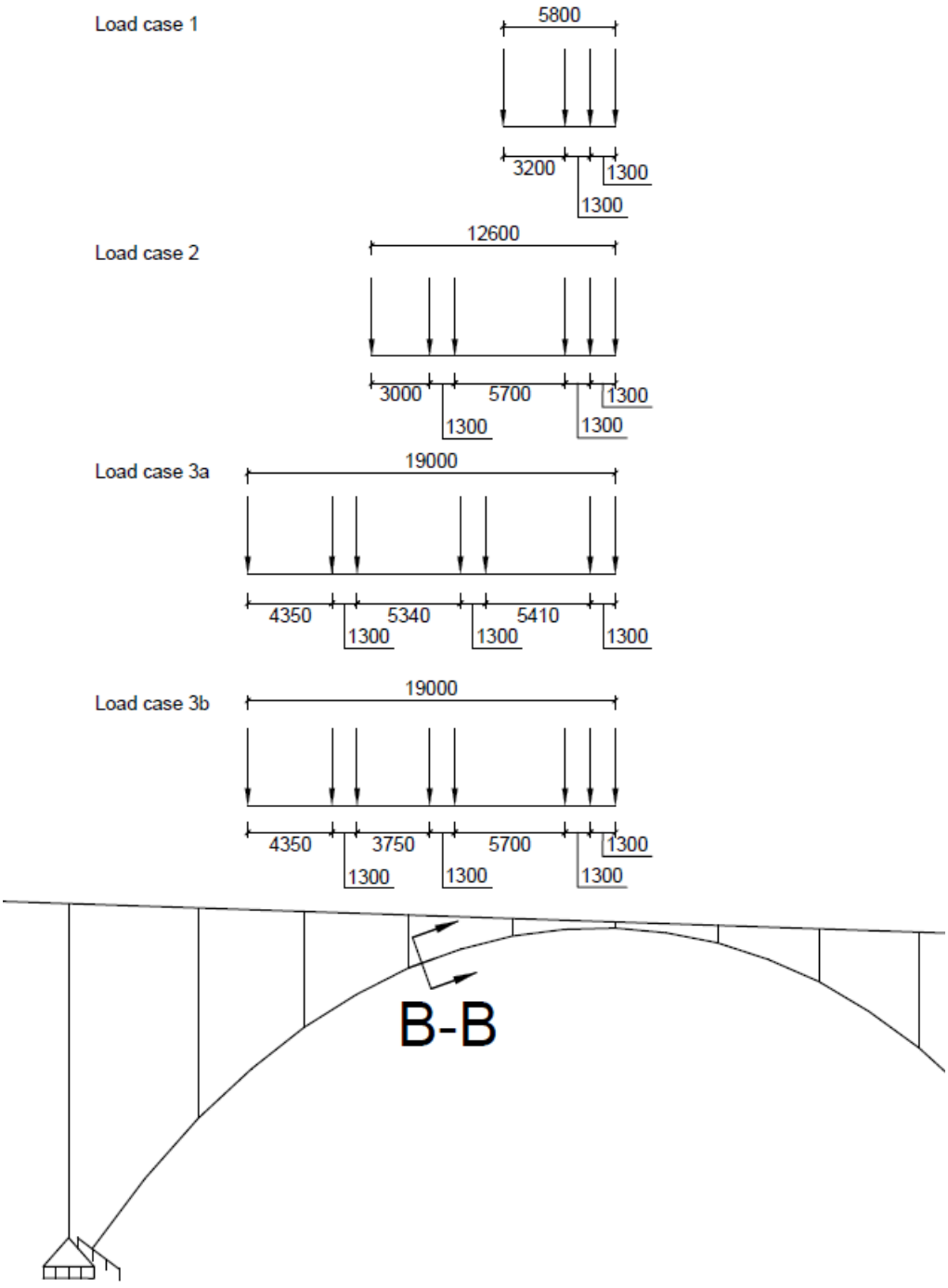

Figure 7.13: Load cases for cross-section B-B [mm].

The weight of each of the axles is given in table 7.4. The axle groups closest to the center of the bridge are loaded to the legal maximum. The load is evenly distributed between axles in one axle group. The single front axle is never fully utilized because of the total vehicle weight limitation. On can see that when the B-train (load case 3b) is built up with the semitrailer from load case 2, the first three axles must be loaded with a small load.

Table 7.4: The weight of each axle ordinary transport.

Axle nr:	**1**	**2**	**3**	**4**	**5**	**6**	**7**	**8**	**Total weight**
Load case:	**Axle weight [ton]:**								**limit [ton]:**
1	-	-	-	-	8,0	8,0	8,0	8,0	32
2	-	-	8,0	9,0	9,0	8,0	8,0	8,0	50
3a	-	6,0	9,0	9,0	9,0	9,0	9,0	9,0	60
3b	6,0	6,0	6,0	9,0	9,0	8,0	8,0	8,0	60

The Bk12/100 load case is applied in the same position as the load cases from the ordinary transport class. Table 7.5 gives the weight of each single axle of the Bk12/100 vehicle shown in figure 7.14. The first axle is limited by the single axle weight limit. The triple axle group in the middle is limited by the triple axle weight limit. The axle group is limited by the two times the total weight table.

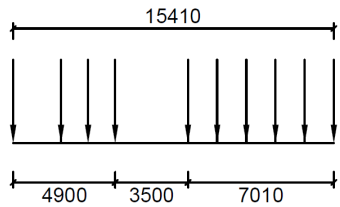

Figure 7.14: Load case Bk12/100 special transport cross-section B-B [mm].

Table 7.5: The weight of each axle Bk12/100 special transport.

Axle nr:	1	2	3	4	5	6	7	8	9	10	Total weight
Load case:	Axle weight [ton]:										limit [ton]:
5	12	10	10	10	9.67	9.67	9.67	9.67	9.67	9.67	100

7.3 Load effect

7.3.1 Cross-section A-A

The values are values for the half-bridge beam. The moment diagram for the characteristic self-weight and the static part of the ordinary transport tipple axle group are shown in figure 7.15 and 7.16. The moment diagram for the Bk12/100 special transport is shown in appendix C. It is important to notice that the characteristic load value only is a single arbitrary point on the probability distribution, which defines a certain fractile of the probability distribution. The characteristic cross-section moments are given in table 7.6.

Table 7.6: Characteristic cross-section A-A moments.

Characteristic load:	Moment [kNm]
Self weight	189
Ordinary transport traffic load	291
Spacial transport traffic load	493

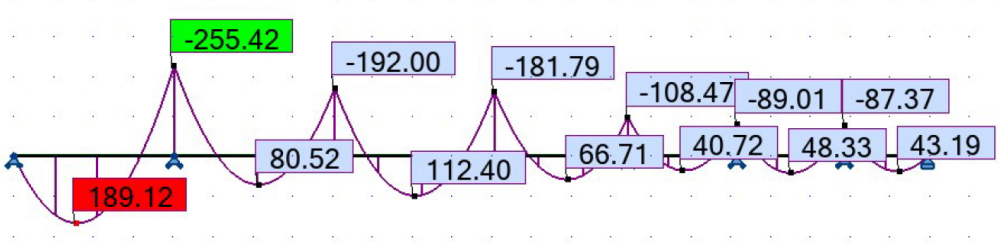

Figure 7.15: Self weight moment diagram [kNm].

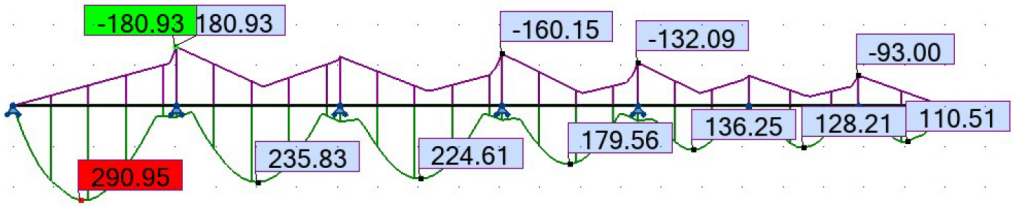

Figure 7.16: Triple axle group moment diagram [kNm].

7.3.2 Cross-section B-B

Several load cases have been studied. The moment and normalforce diagram for the self-weight and one of the traffic load cases are shown to give the reader an overview of the load situation. The other diagrams are found in appendix C. The characteristic loads are given by table 7.7.

Table 7.7: Characteristic moments and normalforces cross-section B-B.

Characteristic load:	**Moment [kNm]**	**normal force [kN]**
Self weight	282	1260
Ordinary transport:		
Load case 1	670	259
Load case 2	695	326
Load case 3a	668	343
Load case 3b	679	345
Load case 4a	631	336
Load case 4b	574	301
Special transport:		
Load case 5	1263	590

The table shows that the self-weight is dominant for the normal force in the arch. The traffic load is dominant for the moment. The load effect form the three different vehicles are very similar. The B-train (load case 3) causes the smallest

moment and the biggest normal force. The semitrailer truck (load case 2) gives the biggest moment. One can also see that the Norwegian Public Road Administrations load model underestimates the load effect from a Bk10/50 semitrailer truck (load case 4b) compared to the load effect from a Bk10/60 B-train (load case 4a).

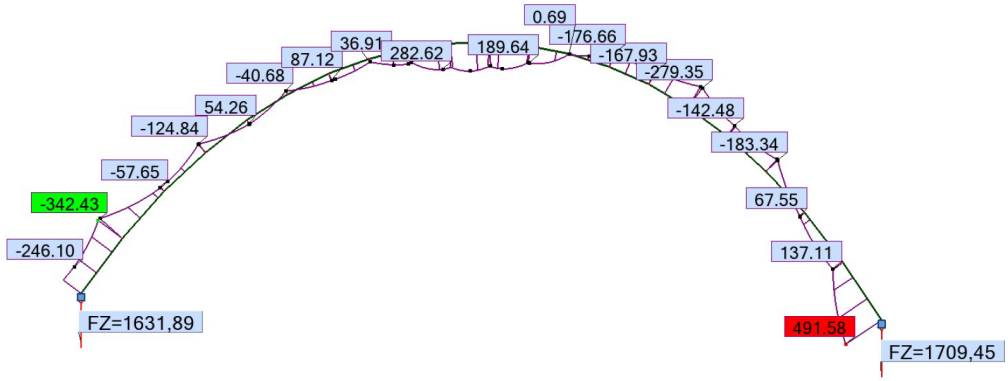

Figure 7.17: Self-weight moment diagram [kNm].

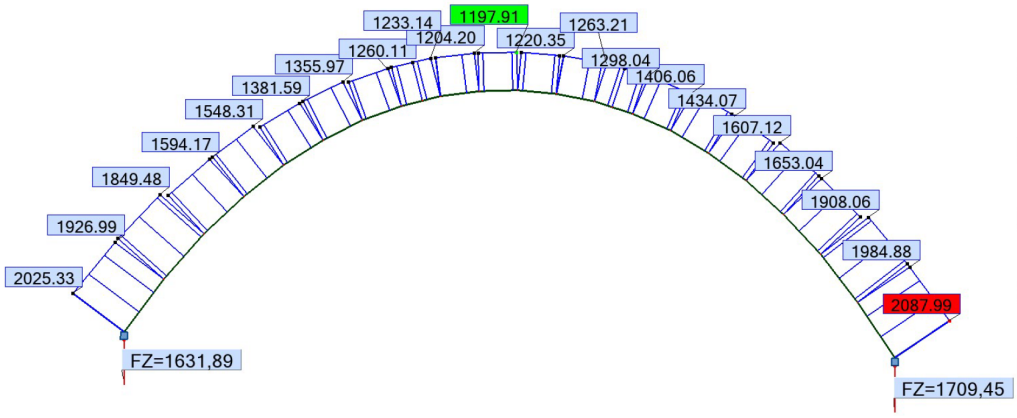

Figure 7.18: Self-weight normal force diagram [kN].

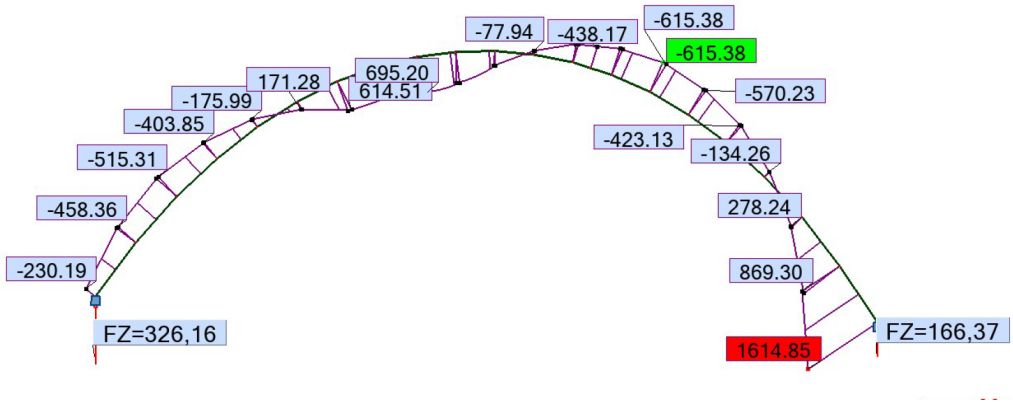

Figure 7.19: Semitrailer truck moment diagram [kNm].

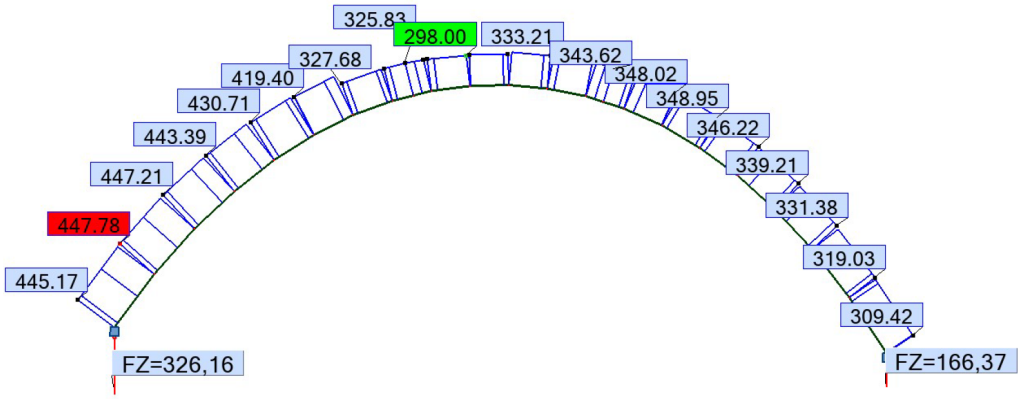

Figure 7.20: Semitrailer truck normal force diagram [kN].

7.4 The material modeling

7.4.1 The material properties

The concrete compression strength

Old drawings from the time when the bridge was built state that the concrete which was used is B-concrete [2]. B-concrete is associated with an in situ cylin-

der compression strength of 11.5 MPa. Further information on the calculations of the concrete compression strength can be found in appendix B. The measured characteristic concrete strength is equal to 10.37 MPa when the statistical uncertainty is taken into account. The concrete compression strength distribution is nearly log-normal with a mean value of 17.37 and a CoV of 0.3.

The reinforcement yield strength

The earlier reports on the condition of the bridge state that the reinforcement steel quality is St.00, i.e., unclassified steel, which usually has the same properties as St.37 [43]. The reinforcement bars are plain. The same steel classification system was used in Denmark and Norway at that time. The Danish standard provides information on the reinforcement distribution. For reinforcement bars with diameter greater than 16 mm, the steel yield strength is modeled as log-normal distributed with mean 293 MPa and standard deviation 25 MPa. This steel quality is quite different from the steel that is used in modern structures. Among others the ratio between the ultimate tensile strength and the yield strength is very big. According to the Danish standard, the ultimate tensile strength can be represented by, a log-normal distribution with a mean value of 431 MPa and a standard deviation of 25 MPa. The characteristic yield strength (f_{yk}) is given to be 225 MPa, and the characteristic ultimate tensile strength (f_{uk}) is given to be 360 MPa. The characteristic corresponds to the 0.1%-fractile of the probability distribution [63]. The ratio between the two is $360/225 = 1.6$. Eurocode 1992-1-1 annex C prescribes a minimum ratio of 1.15 [13]. The characteristic steel resistance is defined in the Eurocode as the 5%-fractile. The small deviation between the definitions makes a small difference between the numbers, but they are almost directly comparable to each other. According to the Norwegian standard NS 227; Rules for reinforced concrete construction design, which was the standard valid at the time the bridge was constructed, the reinforcement steel must have a minimum elongation of 20% [43].

7.4.2 Degradation

The modeling of the degradation is based on the studies of Enright and Frangopol [28]. Certain modifications are made in order to account for the observed degradation of the bridge. The time-variant resistance is modeled by multiplying the initial probabilistic resistance to a deterministic resistance degradation function.

$$R(t) = R_0 \cdot g_{deg}(t) \tag{7.7}$$

Where, $R(t)$ is the time-variant resistance. R_0 is the initial resistance. $g(t)$ is the resistance degradation function.

$$g_{deg}(t) = 1 - k_1 t + k_2 t^2 \tag{7.8}$$

Where, t = elapsed time in years.

For reinforced concrete bridge beams subjected to corrosion of steel reinforcement the table 7.8 given values are suggested by Enright and Frangopol [28]. The corrosion for the reinfocement does not take place from day one. The carbonatization front must reach the reinforcement before it is possible for the reinforcement to corrode. In table 7.8, T_i is the corrosion initiation time. k_1 and k_2 is the degradation constants. $E[g_{deg}(t)]$ are the expected value of $g(t)$.

Table 7.8: [28] Degradation rate variables.

Degradation rate	$\boldsymbol{E(T_i)}$ **[yr]**	$\boldsymbol{E(k_1)}$	$\boldsymbol{E(k_2)}$	$\boldsymbol{E[g_{deg}(75)]}$
Low	10	0.0005	-	0.9675
Medium	5	0.005	-	0.6500
High	2.5	0.01	0.00005	0.5378
Nondegrading	-	-	-	1.0000

The bridge is located at a place with a relatively dry and cold climate, and the corrosion process will be slow. It is assumed that the degradation rate is low. The cross-section A-A main beam has no visible damages that lead to a reduction of the capacity. However, it is informed that the maximum measured carbonatization depth is 45 mm [8, 7]. The carbonatization front has reached both the shear reinforcement and the moment reinforcement. The concrete cover over the moment reinforcement is 42.5 mm. The depth of the carbonatization can be found by equation (7.9) [42]. The initial corrosion time is found by equation (7.11) to be 68 years after the construction was completed, i.e., the corrosion was initiated in 2010.

Carbonatization depth function:

$$C_d(t) = K\sqrt{t} \tag{7.9}$$

K is found by solving equation (7.10).

$$\begin{aligned} 45 &= K\sqrt{2018 - 1942} \\ K &= 5.1618 \end{aligned} \tag{7.10}$$

The initial corrosion time is found by equation (7.11).

$$T_i = \frac{42.5}{5.1618} = 68 \text{ year} \tag{7.11}$$

The cross-section A-A degradation is calculated using equation (7.8). The results are shown in table 7.9.

Table 7.9: Cross-section A-A degradation.

Year	2019	2023	2033	2043	2053	2063
$g_{deg}(t)$	0.9955	0.9935	0.9885	0.9835	0.9785	0.9735

The carbonatization front has not reached the reinforcement of the arch [8]. The average carbonatization depth is 23 mm. The average concrete cover is 50 mm. The carbonatization front will not reach the arch reinforcement in many years. Other damages are observed. The concrete of the arch is poorly compacted some sections. Spalling of the concrete is observed. It is assumed by the assessment report that the damages reduce the effective cross-section of the arch by 5-6% [7]. The degradation rate suggested by Enright and Frangopol is strictly speaking only valid for a cross-section subjected to bending. The cross-section B-B degradation process is modeled as a reduction of the concrete cross-section A-Area. It is assumed that the degradation was initiated the day the construction of the bridge was finished, and that the degradation is a linear process. The degradation rate is assumed to be $(0.05/75)$ 0.00067 per year. The following assumptions leads to the table 7.10 presented degradation.

Table 7.10: Cross-section B-B degradation.

Year	2019	2023	2033	2043	2053	2063
$g_{deg}(t)$	0.9487	0.9460	0.9393	0.9327	0.9260	0.9193

7.4.3 The material model uncertainty

The material model uncertainty (I_m) is modeled as a log-normal variable with a mean value of 1 and the CoV is calculated by equation (7.12).

$$V_{I_m} = \sqrt{V_{I_1}^2 + V_{I_2}^2 + V_{I_3}^2 + 2(\rho_1 V_{I_1} + \rho_2 V_{I_2} + \rho_3 V_{I_3})V_m} \tag{7.12}$$

I_1 is a variable that considers the accuracy of the calculation model, I_2 accounts

for the uncertainty of the material properties, and I_3 takes into consideration how certain one can be that the described material actual is used in the construction. V_m is the coefficient of variation for the material parameter.

Table 7.11: [63] Model uncertainty factors.

Accuracy of the calculation model			
	Good	Normal	Poor
V_{I_1}	0.04	0.06	0.09
ρ_1	-0.3	0.0	0.3
Material property deviation			
	Small	Medium	Large
V_{I_2}	0.04	0.06	0.09
ρ_2	-0.3	0.0	0.3
Material identity			
	Good	Normal	Poor
V_{I_3}	0.04	0.06	0.09
ρ_3	-0.3	0.0	0.3

I_1 is recommended to be normal when an acknowledged calculation model is used. I_2 is, in general, assumed to be large for the concrete compression strength, but it can be reduced when compression tests are used to verify the concrete compression strength distribution. I_2 is, in general, assumed to be medium for the reinforcement steel yield strength. I_3 is recommended to be normal when the material information comes from project material, etc. original drawings. The identity uncertainty can be assumed to be good when the information comes from as-built documentation and bad if the information is based on estimates.

The concrete compression strength distribution is predicated based on concrete

compression tests, and the statistical uncertainty is considered. The geometrical information comes from original drawings. The concrete cover is also measured [8]. The measurement results are consistent with the information provided by the drawings. It is chosen to use a CoV of ($\sqrt{3(0.06)^2} = 0.104$) both for the concrete compression strength and reinforcement yield strength.

7.5 Summary of the probabilistic properties

Table 7.12: Summary of probabilistic properties.

Variable	Abbreviation	Distribution	Mean [MPa]	Std./CoV
Material:				
Concrete compression strength	f_c	ca. Log-Normal	17,37 [Mpa]	0,3
Steel yield strength	f_y	Log-Normal	293 [Mpa]	25 [MPa]
Material model uncertainty:				
Concrete strength	I_c	Log-Normal	1	0,1039
Steel strength	I_y	Log-Normal	1	0,1039
Loads:				
Truck load	W [ton]	Normal	w [ton]	4/2,5 [ton]
Dynamic addon	S_t	Normal	41,5/(9,81·w)	41,5/(9,81·w)
Dynamic amplification factor	$K_t = (1 + S_t)$	-	-	-
Concrete weight	G_p	Normal	25 [kN/m^3]	0,05
Quasi permanent load	G_{qp}	Normal	variable	0,10
Eccentricity Sv12	ECC	Normal	0	0,5 [m]
Eccentricity Bk10	ECC	Deterministic	-	- [m]
Load model uncertainty:				
Traffic load	I_t	Normal	1	0,20
Self weight	I_g	Normal	0	0,05

7.6 Assessment of the Cross-section A-A capacity

The assessment of the cross-section A-A capacity is a a calculation of the span moment. The assessment is carried out on half the bridge beam as a single T-beam assessment. The geometry is simplified. The edge beam is neglected. The

height of the flange varies between 210 mm and 250 mm. The calculation is performed with a 230 mm constant height. The geometry of the cross-section without the edge beam is shown in figure 7.21.

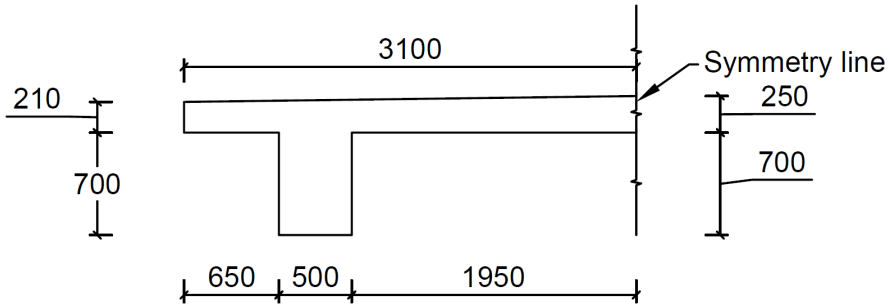

Figure 7.21: Cross-section A-A [mm].

The limit state function for cross-section A-A is given on the simplest form by equation (7.13).

The limit state function is given by:

$$M_R - M_S \leq 0 \tag{7.13}$$

Where, M_R is the moment resistance. M_S is the moments caused by the loads. M_S consist of one traffic load part ($M_{S,TL}$) and one self-weight part ($M_{S,G}$).

$$M_S = M_{S,TL} + M_{S,G} \tag{7.14}$$

Effective width

The stress distributes differently over the width of the flange. An effective flange width is calculated to adjust for the stress distribution. The effective width of the cross-section is calculated using the EC2, 5.3.2.1 [13] rules. The effective cross-section is shown in figure 7.22.

[13] EC2, 5.3.2.1:

$$b_{eff} = \sum b_{eff,i} + b_w \leq b \tag{7.15}$$

$$b_{eff,i} = 0.2b_i + 0.1l_0 \leq 0.2l_0 \tag{7.16}$$

and,

$$b_{eff,i} \leq b_i \tag{7.17}$$

$$l_0 = 0.7l_1 \tag{7.18}$$

Where, $l_1 = 8.067$ m, is the beam span.

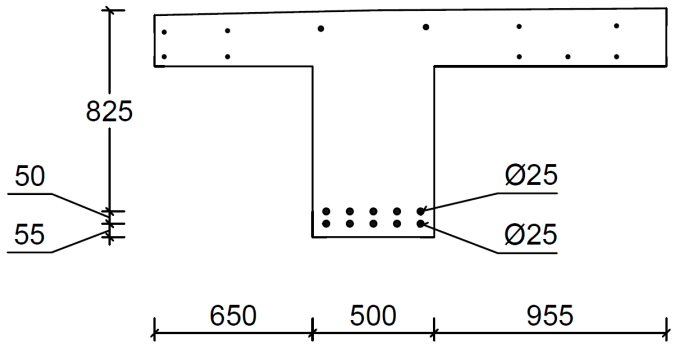

Figure 7.22: Effective cross-section A-A [mm].

7.6.1 Resistance (M_R)

Relation between internal stresses and moment resistance

Together with the roads administration, it was decided that the assumptions made in the Eurocode 2 [13] should be used, although paragraph 3.2.2(3) states that the code only is valid for reinforcement with a yield limit between 400-600 MPa.

The following is assumed:

- Full bond between the reinforcement and the concrete.
- Plane strain sections remain plane (Navier's hypothesis).
- A bi-linear stress-strain relationship ([13] EC2 3.1.7(2)).
- The concrete has no tension capacity.

The assumptions lead to the following general relation between stress and strain. Figure 7.23 shows a cross-section with both tension- and compression reinforcement and the relation between stress and strain. The maximal permitted concrete strain on the upper edge of the compression zone is $\varepsilon_{cu3} = 3.5 \cdot 10^{-3}$ ([13] EC2 table 3.1). The concrete compression zone is idealized to have a rectangular form with a length equal to 0.8 times the real triangle formed compression zone ([13] EC2 3.1.7(3)).

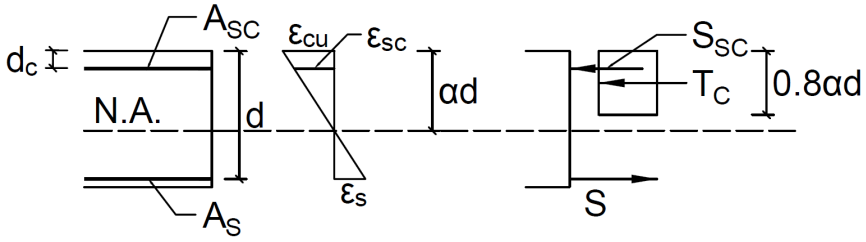

Figure 7.23: [49] Relation between strain and moment.

Moment resistance

For a general concrete cross-section exposed to a pure moment, there are two failure modes. The first failure mode is reinforcement yield failure. The second mode is the concrete compression strength failure. The compression flange of the cross-section is wide compared to the amount of tensile reinforcement and the yield strength of the tensile reinforcement. The cross-section A-A also has some compression reinforcement. The probability of a concrete compression

failure is negligibly small compared to the yield failure mode. The moment resistance given a yield failure is expressed by equation (7.19). The reinforcement strain is big before the ultimate strain of the concrete is reached. The compression flange is only partly utilized. Figure 7.24 shows to the right a partly utilized flange. The size of the compression zone depends on the concrete compression strength. The compression reinforcement is neglected. To the left, one can see the force couple and a moment arm. In the calculations, the moment arm is restricted not to be smaller than 735 mm. Then the compression flange is fully utilized and counted as a failure.

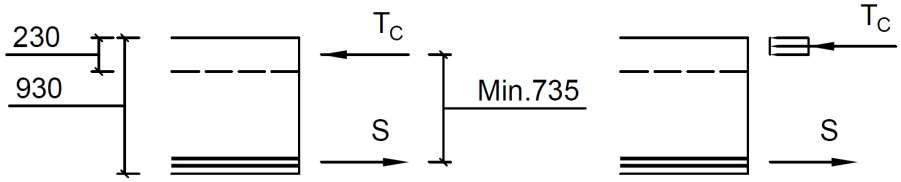

Figure 7.24: The limit state cross-section A-A [mm].

The moment resistance in the mid span is given by:

$$M_R = g(t) I_y f_y A_s (d - 0.5 \frac{I_y f_y A_s}{I_c f_c b_{eff}}) \tag{7.19}$$

Where d is the distance from the top of the beam to the center of the tensile reinforcement.

7.6.2 Stresses (M_S)

Traffic load ($M_{S,TL}$)

The traffic load extreme value distribution is generated using Monte Carlo techniques. As shown by equation (6.1), one must in principle consider both the load action from meeting events and the load action from one lane traffic only. The number of vehicles that passes the bridge in one lane is very big in the pe-

riod until 2023. It is very computationally demanding to simulate all the traffic. The meeting events can be calculated directly. The one lane only traffic must be extrapolated. Only the tipper trucks are considered for the extrapolation. It seems like the tipper trucks are dominant both for cross-section A-A and B-B. The tipper truck has the biggest standard deviation and the ratio between the load effect caused by the truck and the weight of the vehicle is bigger for the tipper truck than the two other trucks.

For the special transport traffic both meetings with ordinary traffic and special transport in one lane only are considered.

The load effect from the meeting events is the sum of the load effect from lane one and the load effect form lane two. The combined load effect from one meeting event is calculated with equation (7.29). All the random variables in the equation is independent from each other.

$$M_{TL,12} = M_{TL,1} + M_{TL,2} \tag{7.20}$$

Where, $M_{TL,12}$ is the moment in the controlled cross-section caused by one meeting event. $M_{TL,1}$ is the moment caused by the load in driving lane 1. $M_{TL,2}$ is the moment caused by the load in driving lane 2.

$$\begin{aligned} M_{TL,12} = D_{tran,1} \cdot \frac{M_{1,k}}{W_{t1,k}} \cdot I_t \cdot W_1 \cdot (1 + S_{t,1}) \\ + D_{tran,2} \cdot \frac{M_{2,k}}{W_{t2,k}} \cdot I_t \cdot W_2 \cdot (1 + S_{t,2}) \end{aligned} \tag{7.21}$$

Where, $D_{tran,1}$ and $D_{tran,2}$ is the ratio of the load from lane 1 and lane 2 that transfers to the controlled cross-section. $M_{1,k}$ and $M_{2,k}$ characteristic traffic load moment from the vehicle in driving lane 1 and 2 respectively. $W_{t1,k}$ and $W_{t2,k}$ is the characteristic weight of the vehicle in lane 1 and lane 2 respectively. I_t is the traffic model uncertainty. W_1 and W_2 is the vehicle weight distribution. $S_{t,1}$ and $S_{t,2}$ is the dynamic amplification.

In section 6.3.3, it was assumed that tipper trucks contributes to 25 %. The semi-trailers contributes to 50 %. B-trains contributes to 25 % of the relevant meeting events. The vehicle order in each lane is random, which makes it possible for all types of vehicles to meet.
The final load distribution is generated numerically by equation (7.22). It is very important to notice that the extreme value distribution describes the probability that most extreme event during a complete year will not exceed a certain value.

Numerical generation of the traffic load extreme value distribution:

$$M_{TL,\max} = \max(\boldsymbol{M_{TL}}) \tag{7.22}$$

Where, $\boldsymbol{M_{TL}}$ is a $m \times n$-matrix. m is the number of single/meeting events, and n is the number of random realizations. The extreme value distribution $M_{TL,\max}$ is found by the maximum of each column of $\boldsymbol{M_{TL}}$.

The 2020 one lane only traffic is used as the basis for the extrapolation. The 2020 one lane only traffic is generated by using the same technique as described above. The maximum likelihood method is used to fit a Gumbel distribution to the generated data. The distribution is extrapolated using the properties of the Gumbel distribution given by equation (7.23). The mean for one reference period depends on n, which is the number in which another reference period repeats. For instance, the heavy vehicle traffic amount in 2020 is $n = 1336/75 = 17.81$ times the traffic amount in 2023. The standard deviation of the distribution is independent from the considered reference period. The same method was used when making the Eurocode traffic load model [30].

$$\mu_{X_{nT}^{max}} = \mu_{X_T^{max}} + \frac{\sqrt{6}}{\pi}\sigma_{X_T^{max}} \ln(n)$$
$$\sigma_{X_{nT}^{max}} = \sigma_{X_T^{max}} = \text{constant} \tag{7.23}$$

Self weight ($M_{S,G}$)

The properties of the self-weight load is described in section 7.2.1. The self-weight load effect distribution is calculated by equation (7.24) and 7.25.

$$G_{sw} = G_p + G_{qp} \tag{7.24}$$

Where, G_p is the permanent part of the self-weight. G_{qp} is the quasi-permanent part of the self-weight.

$$M_G = \frac{M_{G,k}}{G_{sw,k}} \cdot G_{sw} + I_g \tag{7.25}$$

Where, $M_{G,k}$ is the characteristic self-weight moment. $G_{sw,k}$ is the characteristic self weight. G_{sw} is the self-weight distribution. I_g is the self-weight model uncertainty.

7.7 Assessment of the cross-section B-B capacity

The assessment of cross-section B-B is a different kind of problem compared with cross-section A-A. The cross-section B-B is subjected to both a moment and a normal compression force. The compression capacity and the tensile capacity of concrete are not equal. Superposition of normal forces and moments does not work. A M-N interaction diagram must be made. The geometrical properties of the cross-section B-B is shown in figure 7.25.

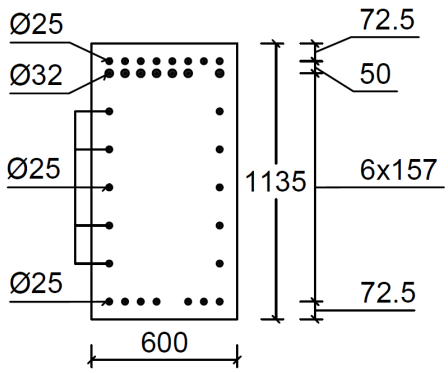

Figure 7.25: Cross-section B-B [mm].

The cross-section A-A assumptions given in section 7.6.1 are applied also to cross-section B-B. The arch is curved. The stress distribution over the cross-section due to bending is strictly speaking not linear. This effect is neglected. The stress distribution is assumed to be linear over the cross-section. In addition, the concrete strain shall on average not be bigger than $\varepsilon_{c3} = 1.75 \cdot 10^{-3}$ ([13] EC2, table 3.1 and 6.1(6)). The Young's modulus of the reinforcement steel is $E_s = 200000$ MPa. The steel yields when $\varepsilon_s = f_y/E_s$.

M-N interaction diagram

Figure 7.26 makes the basis for the derivation of the M-N interaction diagram. The figure, shows to the left that both a normal force and a monument are applied to the cross-section. The strain state of the cross-section is expressed as a function of x, which is the variable. The cross-section must be in equilibrium for every chose of x. In the middle of figure 7.26, the x is bigger than the height of the cross-section. The strain at the center of the cross-section is kept at $\varepsilon_{c3} = 1.75 \cdot 10^{-3}$. The average strain requirement is satisfied for every chose of x. To the right in figure 7.26, the x is smaller than the height of the cross-section. The strain at the top of the cross-section is locked at $\varepsilon_{cu3} = 3.5 \cdot 10^{-3}$. The maximal strain requirement presented in section 7.6.1 is satisfied for every chose of

x. The mathematical calculations for the M-N interaction diagram are presented in appendix D. The x is discretized. Only eight values for x are chosen.
The diagram is determined by an equilibrium consideration.

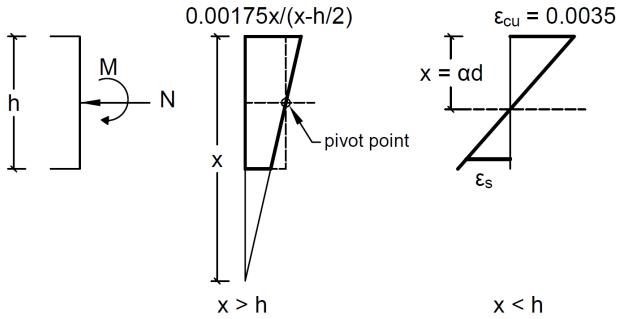

Figure 7.26: [49] M-N diagram derivation.

Limit state function

The M-N interaction diagram defines the limit curve for all allowable combinations of moment and normal force. All combinations on the inside of the curve are tolerated. All the combinations on the outside of the diagram are failures. One must figure out whether or not the moment-normal force combination caused by the load is outside the M-N diagram curve. Figure 7.27 shows an example of a M-N diagram. A load data point is placed outside the curve. A line is drawn from origin through the load data point. The intersection between the line and the M-N diagram is calculated. The structure fails if the the distance between origin and the intersection point is shorter than the distance between origin and the load data point.
The limit state function is given by equation (7.26). It is defined in terms of the line distances.

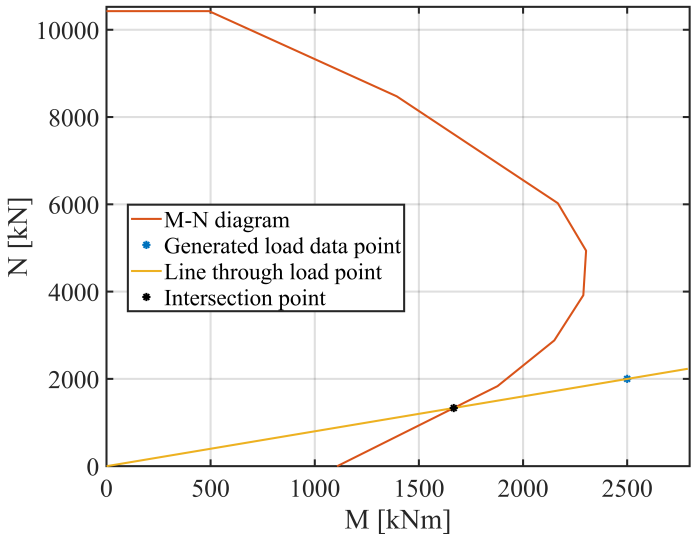

Figure 7.27: Example of a discrete M-N diagram.

Limit state function:

$$L_R - L_S \leq 0 \tag{7.26}$$

Where L_R is the distance of the line between origin and the intersection point. L_S is the distance between the origin and the generated load point.

7.7.1 Resistance

The M-N diagram is a function of the cross-section geometrical properties, the steel yield strength, the Young's modulus of the steel and the concrete compression strength. The geometrical properties and the Young's modulus are treated as deterministic values. The geometrical properties is shown in figure 7.25. The yield strength of the steel and the concrete compression capacity is treated as probabilistic values. The degradation factor is introduced to the calculations by reducing the with of the cross-section.

$$b_{eff} = g_{deg}(t) \cdot b \tag{7.27}$$

Where, b_{eff} is the effective width. $g_{deg}(t)$ is the degradation function. b is the original cross-section width.

7.7.2 Load effect

Traffic load

$$M_{TL,12} = M_{TL,1} + M_{TL,2} \tag{7.28}$$

Where, $M_{TL,12}$ is the moment in the controlled cross-section caused by one meeting event. $M_{TL,1}$ is the moment caused by the load in driving lane 1. $M_{TL,2}$ is the moment caused by the load in driving lane 2.

$$\begin{aligned} M_{TL,12} = D_{tran,1} \cdot M_{1,k} \cdot \frac{1}{W_{t1,k}} \cdot I_t \cdot W_1 \cdot (1 + S_{t,1}) \\ + D_{tran,2} \cdot M_{2,k} \cdot \frac{1}{W_{t2,k}} \cdot I_t \cdot W_2 \cdot (1 + S_{t,2}) \end{aligned} \tag{7.29}$$

Where, $D_{tran,1}$ and $D_{tran,2}$ is the ratio of the load from lane 1 and lane 2 that transfers to the controlled cross-section. $M_{1,k}$ and $M_{2,k}$ characteristic traffic load moment from the vehicle in driving lane 1 and 2 respectively. $W_{t1,k}$ and $W_{t2,k}$ is the characteristic weight of the vehicle in lane 1 and lane 2 respectively. I_t is the traffic model uncertainty. W_1 and W_2 is the vehicle weight distribution. $S_{t,1}$ and $S_{t,2}$ is the dynamic amplification.

The extreme value distribution for the traffic load is generated in the same way as shown by equation (7.22). The traffic load is causing both a moment and a normal force. One can not have an extreme moment without also having a extreme normal force. The moment and the normal force is assumed to be fully

correlated. The normal force distribution is modeled as a scaling of the moment extreme value distribution.

$$N_{TL_max} = \frac{N_k}{M_k} \cdot M_{TL,max} \tag{7.30}$$

Where N_k is the characteristic normal force. M_k is the characteristic moment given by table 7.7.

Self-weight

The self-weight is also causing both a normal force and a moment in the arch. One can not have a moment without a normal force. The normal force and the moment are assumed to be fully correlated. Both the normal force and the moment are normally distributed. The moment distribution is a scaling of the normal force distribution. Mean of the distributions is given by 7.7. The CoV is the same as for cross-section A-A.

$$\begin{aligned} N_{SW} &= N(282,\ CoV_{a-a} = 0.067) \\ M_{SW} &= \frac{M_k}{N_k} \cdot N_{SW} \end{aligned} \tag{7.31}$$

Total load effect

The total load effect for the moment and the normal force is calculated by equation (7.32). The total load effect is the sum of the load effect from the traffic load and the self-weight.

$$M_{tot} = M_{TL,max} + M_{SW}$$
$$N_{tot} = N_{TL,max} + N_{SW} \tag{7.32}$$

Chapter 8

Results

8.1 Calculation results

This chapter is going to present the result of the analysis. First, the resultants from the different traffic situations are presented. Then the effect of the different decision alternatives is presented. At last, the socio-economic considerations form chapter 5 are revisited.

8.1.1 Cross-section A-A

Table 8.1 and 8.2 show the cross-section A-A results. The calculations are intentionally carried out with the degradation constant (g_{deg}) fixed at the 2020 level. The effect of the reduction on the traffic amount becomes visible. Table 8.1 shows that the Sv 12/100 class is the decisive load class with the 2020 traffic assumptions. The load caused by the ordinary traffic class in one lane only is just slightly worse. One can see that there is a relatively big gain of requiring special transport to drive centric over the bridge.
The situation changes with the assumed 2023 traffic. The ordinary transport class becomes decisive. The load effect form one lane only traffic is worse than

Table 8.1: Cross-section A-A, 2020 traffic situation results.

Load type	**EC definition: Characteristic load [kN]**	**β-index**	**p_f**
Bk10/60 - Meeting events	752.9	3.09	$1.0 \cdot 10^{-3}$
Bk10/60 - One lane only	847.1	2.43	$7.5 \cdot 10^{-3}$
Sv12/100	-	**2.38**	$8.7 \cdot 10^{-3}$
Sv12/100 - Centric	-	3.43	$2.9 \cdot 10^{-4}$

the meeting event traffic in table 8.1. The meeting events are left out in table 8.2. It is not decisive.

Table 8.2: Cross-section A-A, 2023 traffic situation results.

Load type	**EC definition: Characteristic load [kN]**	**β-index**	**p_f**
Bk10/60 – One lane only	753.8	**3.03**	$1.2 \cdot 10^{-3}$
Sv12/100	-	3.10	$9.6 \cdot 10^{-4}$

The characteristic values from the Eurocode load standard are used as a benchmark to control that the generated load effect is trustworthy. The 99.9%-fractile of the distribution. This definition is used for the generated data. Three Eurocode values are included. The first value in table 8.3 does not include the adjustment factor from the national annex. The second value includes the adjustment factor from the national annex. The adjustments factor suggested by the Eurocode background documents for normal heavy traffic [21] is used for the calculation of the third value. If one compares the characteristic values in table 8.1, and 8.2 to the Eurocode values, one can see that the characteristic values from the generated data are some smaller than the two first values. The third Eurocode value is found in the middle of the generated traffic data for 2020 and

Table 8.3: Cross-section A-A, comparison of characteristic values of different load standards.

Load type	Characteristic load [kN]
Eurocode	935.8
Eurocode N.A.	877.9
Eurocode NHT.(1)	806.1
The Norwegian R412 load model	374.7

(1) With the use of adjustment factors for normal heavy transport from [21].

2023.

Only the characteristic values for the Bk 10/60 class are given because the Eurocode 1-2 load model 1 only considers ordinary traffic. Special vehicles are treated separately (See: Eurocode 1-2 annex A [11]). The number of vehicles is very different. Hence, the probability distributions are also different. It would have been misleading to compare the Sv 12/100 characteristic value with the others.

The characteristic value given by the Norwegian Public Road administration load model is unknown. Still, much points to that the characteristic value is based on the legal maximum with and an average dynamic amplification factor. The Norwegian Public Road Administration HB R412 load model has a characteristic load that is smaller than half the value of the other load models.

8.1.2 Cross-section B-B

The Sv 12/100 transport class is decisive both for the 2020 and the 2023 traffic situation. The ordinary one lane only traffic is worse than the ordinary meeting traffic. One can see that the gain from driving centric over the bridge is huge. The number of simulations was 10^{-7}, and none of them was a failure. No exact probability of failure was found, but it is less than 10^{-7}.

The meeting events and the special traffic that drives centric over the bridge is left out from the 2023 calculations, since they are not decisive.

Table 8.4: Cross-section B-B, 2020 traffic situation.

Load type	EC definition: Characteristic load [kN]	β-index	p_f
Bk10/60 – Meeting events	1808.2	3.85	$5.9 \cdot 10^{-5}$
Bk10/60 – One lane only	1911.8	3.56	$1.9 \cdot 10^{-4}$
Sv12/100	-	**2.84**	$2.3 \cdot 10^{-3}$
Sv12/100 - Centric	-	-	$< 10^{-7}$

Table 8.5: Cross-section B-B, 2023 traffic situation.

Load type	EC definition: Characteristic load [kN]	β-index	p_f
Bk10/60 – One lane only	1669.8	4.34	$7.2 \cdot 10^{-6}$
Sv12/100	-	**3.60**	$1.6 \cdot 10^{-4}$

8.2 Effect of the different decision alternatives

The β-index is smaller for cross-section A-A than for cross-section B-B. The cross-section A-A calculations are less time-consuming and easier to handle than the cross-section B-B calculations. A-A is considered to be decisive, and the cross-section is more suitable for studying the effects of the different decision alternatives. In the following section, only cross-section A-A is considered.

8.2.1 A0, Do nothing

The initiation of the length reinforcement corrosion was calculated to be in the year 2010. The moment capacity has been falling since then. In the period between 2010 and 2023, the SV12/100 traffic is used. The new road is planned to be finished in 2023. The traffic amount is expected to decrease, and the one-lane only ordinary traffic becomes decisive. The change in the traffic amount

causes the jump in figure 8.1. The degradation is expected to continue until the end of the period of analysis.

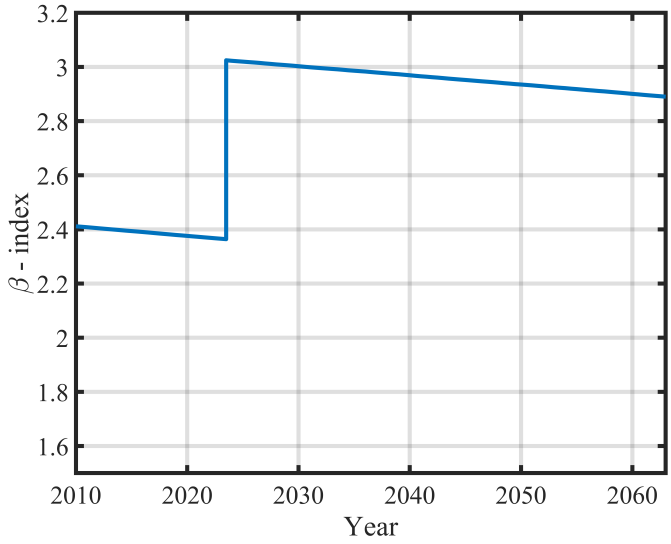

Figure 8.1: The effect of doing nothing.

8.2.2 A3, Strengthening the bridge

There are 5 reinforcement bars in the bottom row of the cross-section. The effect of strengthening the bridge is studied by adding reinforcement bars to the bottom row. This can, in reality, be done by bolting an equivalent steel plates or CRFP (carbon fiber reinforced polymer) plates to the underside of the bridge beams. One can see from figure 8.2 that one only need 5 extra reinforcement bars of the same bad quality steel to bring the β-index well above 5. The 2020 special transport traffic situation is used for the calculations.

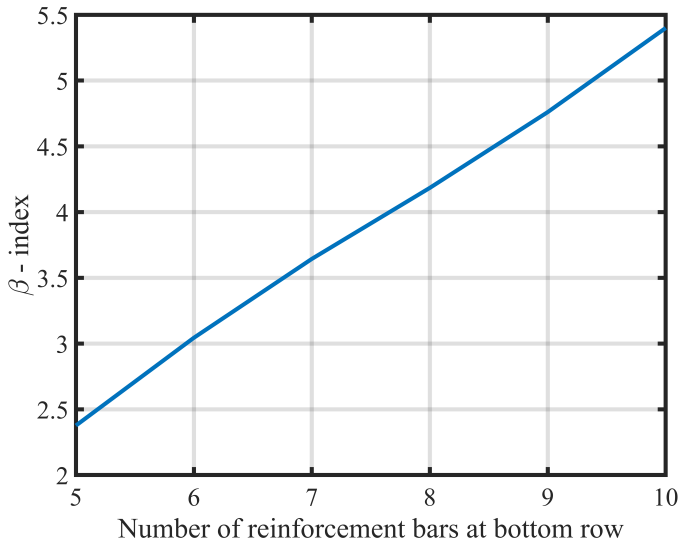

Figure 8.2: The effect of strengthening the bridge.

8.2.3 A1, Weight restriction

The bridge class is for this alternative reduced from Bk10/60 to Bk8/32. The total weight of the tipper truck is reduced from 32 tons to 24 tons. The triple axle system load is reduced from 24 tons to 16 tons [41]. The weight restriction alternative is because of the economic considerations in chapter 5 not considered as an alternative before 2023. The x-axis in figure 8.3 starts in 2023. The degradation process is expected to continue. The curve is falling off towards 2063.

8.2.4 A2, Light regulation

Figure 8.4 shows the result of introducing light regulation. The same probability distribution as for the special transport that was required to drive centric over the bridge is used to describe the transverse position for the vehicles. It means that there are not installed any extra barricades. The choice was found to be

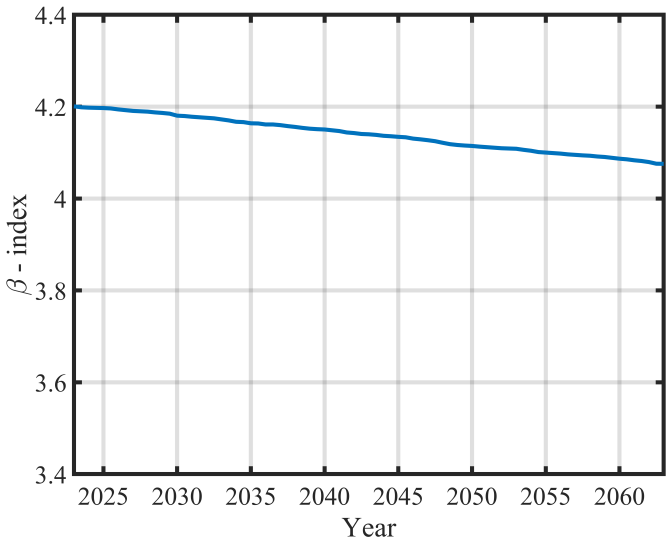

Figure 8.3: The effect of weight restriction.

uneconomical in chapter 5 and is considered to be an option only after 2023. The one way only ordinary traffic with the 2023 intensity is used for the calculations.

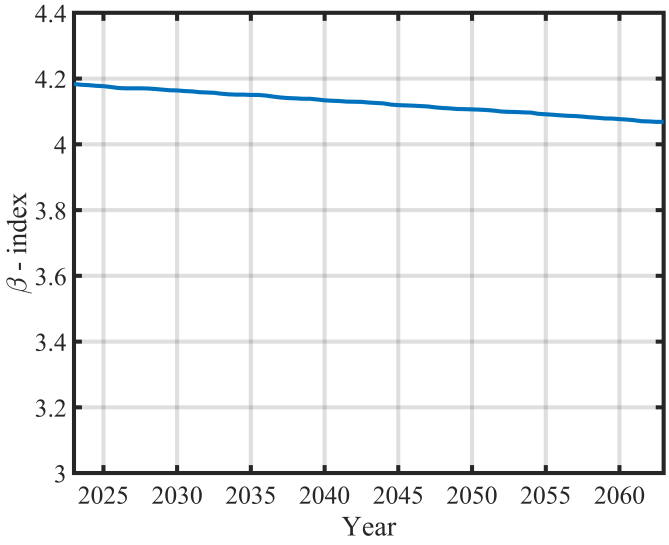

Figure 8.4: The effect of light regulation.

8.2.5 Considerations regarding cross-section B-B

A few results are also made for cross-section B-B. They are made to show insensitivity for concrete degradation and to show the sensitivity of the modeling of the arch.

Degradation

The degradation coefficient that is expected degradation of 2063 is applied together with the 2023 special traffic load. By comparing the results from table 8.5, one can see that the β-index only falls off by 0.02, which is a small number.

Table 8.6: Cross-section B-B, 2023 traffic situation, 2063 degradation.

Load type	**EC definition: Characteristic load [kN]**	**β-index**	p_f
Sv12/100	-	**3.58**	$1.7 \cdot 10^{-4}$

All the failures happen in the bottom part of the MN-diagram. Therefore, the degradation of the concrete is of such small importance. The steel yields this part of the diagram. Hence, the capacity of the steel will be of much greater significance than the concrete compression strength. The concrete compression strength is of greater importance for the upper part of the diagram. In figure 8.5, all the load realizations are plotted. The diagram is plotted with a concrete compression strength of 10 MPa and a steel yield strength of 293 MPa. The diagram is just one realization and is made for illustrative reasons. One can see that the load realizations are in the bottom part of the diagram. That will be the case independent of the choice of the steel yield strength.

On the sensitivity of the arch

The arch is particularly sensitive. Only small deviations in the way the self-weight was added to the arch change the moment distribution over the arch

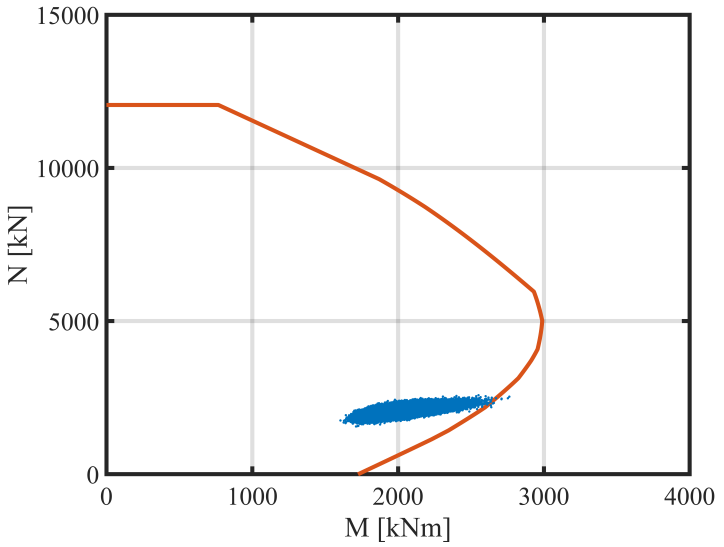

Figure 8.5: A NM-diagram plotted against the load effect realizations.

completely. Table 8.7 shows how a changing moment affects the probability of failure. The special transport load of 2019 is used. A moment of 282 was used for the analysis. The number seemed to be mildly conservative (at least when creep is neglected).

Table 8.7: Arch sensitivity.

Moment [kNm]	**β-index**	p_f
300	2.76	$2.9 \cdot 10^{-3}$
282	2.84	$2.3 \cdot 10^{-3}$
87	3.68	$1.2 \cdot 10^{-4}$
20	3.92	$1.4 \cdot 10^{-5}$
0	4.03	$2.8 \cdot 10^{-5}$

8.3 Revisiting the economic considerations

In this section, the economic considerations are revisited. It was established in chapter 5 that the alternative A1, weight reduction, A2, Traffic light regulation, and A5, Close down the bridge are bad economic decisions. They are not a part of the further considerations. The costs in table 8.8 is transferred from table 5.1. For alternative A3, the socio-economic cost of night work is much smaller than the cost of closing the bridge completely. The night cost is used. As one can see, the do-nothing alternative is considered to be the least costly alternative in the period between 2020 and 2023.

Table 8.8: Costs between 2020 and 2023.

Alternative: **Cost [mill.NOK]**	**A0,** **Do noting**	**A3,** **Strengthening**	**A4,** **Interim bridge**
C_c	0	20	42
C_{se}	0	11	0
$C_f \cdot p_f$	4.5	0.001	0.001
$\boldsymbol{C_{ET,2023}}$	**4.5**	31	42

The values in table 8.9 are the costs between 2023 and 2060. It is assumed that it is unnecessary to do something with the bridge in this period if it is strengthened in the first period. It is also assumed that the interim bridge must be taken down after 2023 and that the Stavå bridge must be strengthened in the next period if alternative A4 is chosen. At the bottom row, the costs of the first period are added to the costs from the second period.

Table 8.9: Costs between 2023 and 2060.

Alternative: **Cost [mill.NOK]**	**A0,** **Do noting**	**A3,** **Strengthening**	**A4,** **Interim bridge**
C_c	0	0	20
C_{se}	0	0	0
$C_f \cdot p_f$	4.8	0.003	0.003
$\boldsymbol{C_{ET,2060}}$	4.8	0.003	0.003
$\boldsymbol{C_{ET,tot}}$	**9.3**	31	62

8.3.1 Socio-economic acceptance criteria based on optimization

The socio-economic risk criteria are plotted in figure 8.6. On the horizontal are one low (10 mill.NOK) and one high (60 mill.NOK) estimate for the cost of construction of the safety measure. The graphs are the discounted expected cost of failure plotted as a function of the β-index. They are based on three different estimates for the cost of failure. The first (in blue), is the initially calculated cost. The second (in orange) is 5 times the initially computed cost. The third (in yellow) is 210 times the initial cost. They are made to show how the cost calculations effects the solution. According to the socio-economic risk acceptance criteria, one shall accept the risk if the expected cost of failure is smaller than the cost of construction. I.e., when the expected cost of failure is underneath the horizontal line.

The cost of failure is as a simplification kept the same throughout the entire period of analysis 3.

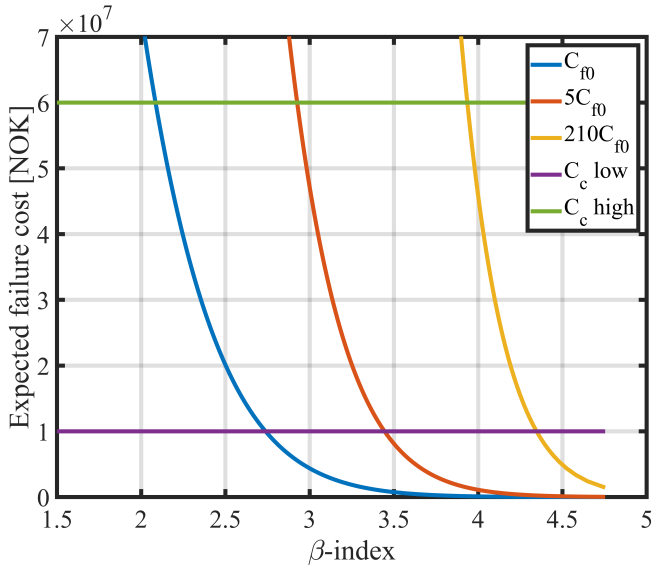

Figure 8.6: Socio-economic risk acceptance criteria based on optimisation.

Chapter 9

Discussion

9.1 Discussion

Any analysis is not better than the underlying assumptions. That is also a challenge in this master thesis, both regarding the socio-economic considerations and the structural analysis. Some of the most critical assumptions are discussed in this chapter.

9.1.1 The socio-economics

The socio-economic analysis was carried out with a simplified traffic model. The time cost could have been underestimated. It was assumed that it takes 60 days to build an interim bridge and re-open the road. This number is uncertain. The costs double if the time to re-opening doubles. The Public Roads Administration has only one lane interim bridges in stock that can span over the river valley. The time cost related to the reduced traffic flow until a new permanent solution is not considered. Neither is the extra tear and wear on the loads that must handle the detouring traffic. Some of the roads are not built to handle heavy traffic volumes. One must expect emergency service costs, investigation

costs, and possible lawsuit costs if the bridge collapses. All these costs add up and 5 times accedes of the initially calculated cost does not look completely impossible (without having made an attempt to quantify these effects).

The socio-economic analysis was carried out with a simplified traffic model. The studies could have been carried out with a more accurate traffic model. The cost of detouring is only based on simple considerations. The calculations had been more accurate if a proper traffic model had been established with the use of the program EFFEKT. The calculations had been 100% according to the Norwegian official calculation method. The results had then been fully comparable to other cost-benefit analysis results.

9.1.2 The load

The extreme value distribution is deducted from an underlying distribution, which is put together by a static load distribution and a dynamic amplification distribution. Both the static load and the dynamic amplification distribution are assumed to be normally distributed. Extreme value predictions are particularly sensitive to false assumptions. Three main problems must be addressed : (i) The dynamic amplification factor is a part of the extreme value expression. (ii) It is not trivial that the underlying distributions are normal. (iii) The extrapolation of the extreme value distribution do not converge.

(i) The dynamic amplification factor of the traffic load can be broken down into two main categories: properties that relate to the bridge and properties that relate to the vehicle dynamics. Road bumps and potholes belong to the first category. They do not change too much from vehicle to vehicle. A smooth road provokes less dynamic amplification than a bumpy road. If the bump or pothole gets too big, road maintenance work is implemented out of road safety reasons.It can

be argued that not all the dynamic effects shall be a part of the extreme value distribution.

(ii) The normal distribution implies that the driver is uninformed. He must not know or react to any signs that indicate that his truck is hugely overloaded. The assumption may be unrealistic because to provoke the extreme loads, one needs both to (a) have an overloaded truck and (b) the suspension can not work correctly. (a) The engine begins to struggle as the truck gets heavier. It gets harder and harder to keep the speed uphill. The vehicle can not be extremely heavy without being fully loaded. One is impossible not to notice that the truck is fully loaded. (b) The suspension must more or less be broken, which effects dramatically affects the driving comfort. The more extreme the situation is, the easier it becomes for the driver to notice that something is wrong.

(iii) The extreme value distribution does not converge. As one can see from equation (7.23), the mean value of the distribution never converges. The mean value is proportional to the natural logarithm of the number of trucks. The extreme load value goes towards infinity as the number of vehicles that drives over the bridge goes towards infinity. However, the growth is slow.

Mathematically expressed:

$$\lim_{n\to\infty} \mu_{X_{nT}^{max}} \propto \lim_{n\to\infty} \ln(n) = \infty \tag{9.1}$$

The extreme value distribution does not have an upper limit; the weight of trucks has. The truck becomes completely fully loaded at some point. One of the truck divers told that when he was working on a tunnel project, they used to fill the truck to its maximum. Stones were falling off the truck, as he started to drive. They measured the weight of the truck. It weighed 42 tons [35]. A further ex-

ceedance will only be possible if the load is exceptionally dense, e.g., lead or uranium, or if the truck is specially made to carry more load. Tipper trucks made for mining operation has an extra high truck bed can have a total weigh more than 60 tons [33]. Also, the dynamic amplification factor has an upper limit. The road will be improved if it gets too bumpy. If any upper limit is introduced to the vehicle weight distribution or the dynamic amplification distribution, the extreme value distribution will eventually converge towards this limit. In this regard, one can do better by finding the hazards scenarios, and by defining the limits both for the total weight and the dynamic amplification factor.

The Eurocode methodology is applied as a basis for the site-specific load model. It is clear that the loads from the own Stavå bridge specific load model compare well to the Eurocode loads that use the adjustment factors suggested by the background documents [21]. One can argue that the Eurocode load model philosophy is not the way to go forward. It does neither take into consideration human-load interaction, nor the physical limitations of the vehicles. A better alternative may be to think in hazard scenarios and try to reduce the hazards. Ludescher has utilized this design philosophy and defined maximal values for the dynamic amplification factors to use for verification of the load-bearing capacity of bridges [26]. In the case of the Stavå bridge, an overloaded tipper truck with leaf suspension that hits bumps that set the bridge in motion is the hazard. One can easily reduce the risk of the worst-case scenario by ensuring that there are no bumps. One shall keep the asphalt plain.

Calculations based on hazard scenario thinking

The specially made tipper truck that can carry a weight of 60 tons is used as a worst-case hazard scenario. The load on each axle is 15 tons. The dynamic amplification factor is suggested to be 1.4 for vehicles with a weight of up to 300 kN. The amplification factor falls linearly off until it becomes 1 when the weight of the vehicles reaches 1500 kN [26]. For the meeting scenario, it is assumed that the hazard truck meets an ordinary 50-ton semitrailer truck. Everything else in the analysis is kept the same.

Table 9.1: Calculations based on hazard thinking.

Cross-section:	**DAF**	β**-index**	$\mathbf{p_f}$
A-A	1.32	**3.03**	$1.2\ 10^{-3}$
A-A	1.4	2.7	$3.5\ 10^{-3}$
A-A(meeting)	1.11	3.43	$3.0\ 10^{-3}$

It can be argued that this hazard vehicle can be breaking and that it can make a sharp turn. When the vehicle turns sharply, all the weight is put on the outermost wheels. These effects are not considered.

Nevertheless, the load Eurocode assumptions work well. The results compare well the results obtained by the hazard scenario method.

9.1.3 The mechanical modeling

Some points regarding the mechanical model must be emphasized. Namely, (i) the assumption regarding the steel properties and the (ii) the sensitivity of the arch modeling.

(i) The reinforcement steel was assumed to have an elastic-perfect plastic material behaviour.I.e., the reinforcement bars do not mobilize any more resistance after the yield limit is reached. The strain hardening effect is neglected. The effect of strain hardening can be significant [19]. The ratio between the ultimate tensile strength and the yield strength is potentially large for the steel used in the Stavå bridge. On the other side, even more assumptions, and corresponding uncertainties, must be introduced into the model. One can not take it for granted that the steel has good yield properties. After all, the bridge was built under the war in 1942. The high-quality steel was used for something else.

(ii) The sensitivity of the arch was found to be significant. Small changes to how the self-weight was applied caused large changes the moment distribution over the arch and, thus, the probability of failure. Not only model deviations can change the moment distribution. The effect of creep, shrinkage, alkali-silica reactions, temperature gradients, changed boundary conditions, and internal density differences in the concrete can have an impact. The arising moments are closely related to the shape of the arch. One can always find an optimal form that leads to zero moments for a corresponding set of forces. The arch is already built, and there are most likely moments in the arch. The moments can be counteracted by applying forces at the correct location on the arch. The effects mentioned above will not necessarily worsen the moment distribution over the arch.

Chapter 10

Conclusions and further work

10.1 Conclusion

The main aim of this thesis was to find out what to do with the Stavå bridge. Several decision alternatives have been studied. The decision alternatives have been assessed under both socio-economic and structural considerations.

It has been emphasized that the assumptions are of significant importance for the result. Some of the essential assumptions have been discussed. A common denominator for the assumptions is that they are based on standard assumptions. Hence, the β-indexes and the probability of failure can be compared to the risk acceptance criteria proposed in chapter 3. Cross-section A-A is with the used calculation methods considered to be the most critical cross-section. It has a β-index of 2.38 for an Sv12/100 special transport class and a β-index of 2.43 for the Bk10/60 ordinary traffic class. The β-index of cross-section B-B is 2.84 for the Sv12/100 special transport class and 3.56 for the Bk10/60 ordinary transport class.

Danish standard for probability-based assessment of bridges recommends a β-

index of 4.26 for ductile failures with remaining capacity. The Eurocodes are calibrated with the use of a beta value of 4.7. The low as reasonable possible set a β-index of 3.72 as an intolerable limit for a member of the public.

The β-index for both the cross-sections and for both the Bk10/60 and the Sv12/100 transport class is to low. Based on the findings, it is recommended to implement measures to reduce the probability of failure. The socio-economic considerations indicate that to strengthen the already existing bridge is the cheapest alternative.

10.2 Further work

An alternative to the conclusion is proceeding to phase 3 from table 3.3. One or more of the measures can be implemented. The suggested measures for further assessment are (i) weight in motion (WIM) measurements, (ii) carry out proof load testing or/and (iii) measure the real geometry. (iv) The socio-economic analysis can be improved.

(i) The load model in this master thesis is a top-down model. It is derived from the legal regulations and traffic volume data. WIM is an approach to find the real bridge specific traffic load effects. Strain sensors are installed on the specific bridge, and the load effects are measured directly. A. O'Connor and E. Eichinger have made a framework describing how one can implement WIM measurements for probabilistic assessment of bridges [38]. WIM measurements have been used to calibrate specific adjustment factors to the Eurocode traffic load model that are valid for low traffic short span bridges.

(ii) Proof load testing is an intuitive method to find out if a bridge is safe or not. The method is to load the bridge with a heavy load and see if the bridge can

stand the load. Proof load is used to update the estimate of the probability of failure. The danger of ruining the structure while conducting the test increases as more and more load is applied. There is a trade-off between the expected reduction to the probability of and the chance of ruin. One should do an optimization before the test is carried out to find the optimal load. M.H. Faber et al. provides the theoretical framework for how one can calculate the optimal proof load and how one can update the probability of failure based on the result from the proof load test [17].

(iii) The geometry used for the modeling is the geometry from the original construction drawings. The result regarding the probability of failure is sensitive to how the arch is model. It can be sensible to measure the geometry of the arch, and use the exact geometry in the structural model.

(iv) The socio-economic calculations could have been better. The traffic flow model is based on simple considerations. The costs further down the chain of events could have been included. The cost calculations could have been more accurate if the program EFFEKT had been used. As mentioned in chapter 5, the cost-benefit analysis program EFFEKT already includes a module for avalanches. The colleagues in SINTEF seemed to have an interest in finding new applications for the program EFFEKT [36].

Appendices

Appendix A

On the alternatives for the bridge

A.1 The calculations of the weigth reduction cost

The calculations follows the the procedure given in the Norwegian Public Roads Administrations report number 358 section 13 [3]. The calculation procedure was made at that time it was of interest to increase the axle load.

$$AADT_t = 1000\, trucks/day \tag{A.1}$$

Axle load	Payload
8	21.1
10	28.1

Table A.1: Relation between axle load and payload.

Axle load	Trucks [%]
8	92
10	73

Table A.2: Part of the trucks that technically can utilize the axle load.

Transport type	Trucks [%]
Between regions	35

Table A.3: Part of the trucks that do not utilize the total axle load.

Transport type	Average trip length [km]
Between regions	120

Table A.4: Average trip length.

The reduction of the traffic work is calculating using equation A.2.

$$RED = 365 \cdot AADT_t \cdot \frac{PL_{after} - PL_{before}}{PL_{after}} \cdot TUAL \cdot (1 - NUAL) \cdot TL \quad \text{(A.2)}$$

Where:

RED = Reduction of traffic work [Truck kilometers/year].

$AADT_t$ = Annual average daily traffic of trucks.

PL_{after} = Payload after increasing the payload.

PL_{before} = Payload before increasing the payload.

$TUAL$ = Part of the trucks that technically can utilize the axle load.

$NUAL$ = Part of the trucks that do not utilize the total axle load.

TL = Average trip length.

$$RED = 365 \cdot 1000 \cdot \frac{28.1 - 21.1}{28.1} \cdot 0.73 \cdot (1 - 0.35) \cdot 120 = 5.177 \cdot 10^6 \quad \text{(A.3)}$$

The yearly mileage is given by equation A.4 and is given as [1000 km/year].

$$YM = 34.465 \cdot \ln(TL) - 46.314 \tag{A.4}$$

$$YM = 34.465 \cdot \ln 120 - 46.314 = 118.67 \tag{A.5}$$

Axle load	Permitted total weight
8	32
10	44

Table A.5: Relation between axle load and permitted total weight.

The unit price is calculating using equation A.6 and is given as [NOK/Truck kilometer].

$$UP = 2.064 \cdot ((768.747 + 3.77 \cdot YM) \cdot \frac{0.8399 + 0.00536 \cdot TW}{YM} \tag{A.6}$$

Where:
TW = Total permitted weigth of the truck.
YM = The yearly mileage of a truck.

$$UP_{after} = 22.75 \tag{A.7}$$

$$UP_{before} = 21.39 \tag{A.8}$$

The weighted unit price is calculated using equation A.9 and is given as [NOK/Truck kilometer].

$$VUP = \frac{UP_{before} - (1 - \frac{PL_{after} - PL_{before}}{PL_{after}}) \cdot UP_{after}}{\frac{PL_{after} - PL_{before}}{PL_{after}}} \tag{A.9}$$

$$VUP = \frac{21.39 - (1 - \frac{44-32}{44}) \cdot 22.75}{\frac{44-32}{44}} = 17.76 \tag{A.10}$$

The social economic benefit of increasing the permitted axle load from 8 to 10 ton is calculated using equation A.11. The answer is given as [mill NOK/year]. The benefit becomes a cost if one intend to decrease the permitted axle load from 10 to 8 ton. The prices in the report are given with 2013 value. The consumer price index is used to adjust the prices.

$$SEB = RED \cdot VUP \cdot PA = 5.177 \cdot 10^6 \cdot 17.76 \cdot \frac{111}{95.9} = 106.4 \tag{A.11}$$

The discounted cost is calculated with equation A.12 and the answer is given as [mill. NOK].

$$DC = \int_0^{3.5} 106.4 \cdot (1.04)^{-t}\, dt = \underline{348} \tag{A.12}$$

Appendix B

On the previous findings

B.1 The concrete compression distribution

B.1.1 The concrete strength

The concrete standard that was valid at the time the construction of the bridge took place is the NS 227; Rules for execution of works with reinforced concrete. NS 227 (§10 table II) [43] defines a B-quality concrete as a concrete that has a mean compressive strength of $\mathbf{230\ kg/cm^2}$ (22.5 MPa) measured on 20x20x20 cm cubes or $\mathbf{253\ kg/cm^2}$ (24.8 MPa) measured on 10x10x10 cm cubes. The concrete compressive strength defined in the Eurocode 2 is the compressive strength from cylinder specimen tests. The old number has to be converted. The converting formulas given by NS-EN 1992-1-1 table 3.1 are used to convert the mean cube strength to the mean cylinder strength, and the mean cylinder strength to the characteristic cylinder compressive strength. A B-concrete has a characteristic cylinder compressive strength of 13.5 MPa. This value is again equal to an in situ compressive strength of 11.5 MPa. Meaning that core specimen from the bridge has to have a compressive strength equal to

or greater than 11.5 MPa to satisfy the requirements for a B-quality concrete (NS-EN 13791 chap.6) [12].

NS 227 middle cube strength [kg/cm^2]	**NS-EN 1992-1-1 characteristic cylinder strength [MPa]**	**In situ characteristic cylinder strength [MPa]**
253	13.5	11.5

Table B.1: B-quality concrete.

B.1.2 The concrete compression tests

Four concrete cores were in 2006 taken out from the top side of the bridge deck, and the compression strength was tested[2].

Core	**1**	**2**	**3**	**4**	**Average**
Compression strength [MPa]	19.3	15.2	11.7	22.4	17.2

Table B.2: [2] Concrete core test results.

B.1.3 Calculation method

The maximum likelihood method is used to obtain the probability distribution for the concrete compression strength. The results from the concrete core testing given in table B.2 are used. The concrete compression strength is assumed to be log-normal distributed. The number of samples is small, making the statistical uncertainty large. The parameters' statistical uncertainty is assumed to be normally distributed. The expected values are obtained from the MLM, and the standard deviations are obtained from the Fisher information matrix. The Fisher information includes the possibility that the standard deviation and the mean can be smaller than zero. The standard deviation is only defined for positive numbers, and a mean smaller than zero is impossible from a physical point of view.

Figure B.1 shows that there is a chance that the standard deviation is less than zero. To avoid problems, only the part of the PDF greater than 0 is considered. The remaining part of the PDF is normalized so that the volume under it is equal to 1.

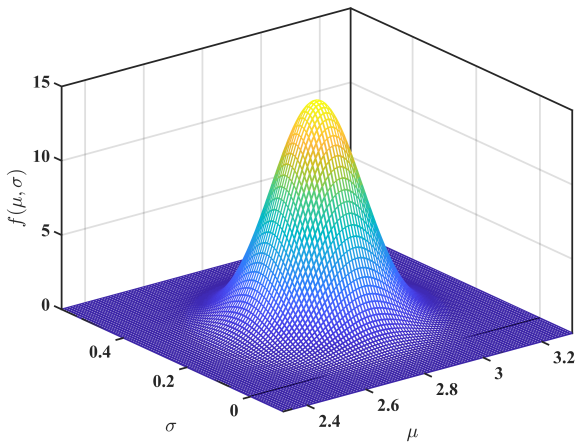

Figure B.1: The joint PDF of the statistical uncertainty.

The maximum likelihood function is defined as:

$$L(\mu_L, \sigma_L|\hat{x}_1, \hat{x}_2, \hat{x}_3, \hat{x}_4) = \prod_{i=1}^{4} f_X(\hat{x}_i|\mu_L, \sigma_L) \tag{B.1}$$

Sometimes it can be easier to work with the log-likelihood function defined as:

$$l(\mu_L, \sigma_L|\hat{\mathbf{x}}) = \ln[L(\mu_L, \sigma_L|\hat{\mathbf{x}})] = \sum_{n=1}^{4} \ln[f_X(\hat{x}_i|\mu_L, \sigma_L)] \tag{B.2}$$

For the log-normal distribution $f_X(\hat{x}_i|\mu_L, \sigma_L)$ is defined as:

$$f_X(\hat{x}_i|\mu_L, \sigma_L) = \frac{1}{(2\pi)^{0.5}\hat{x}_i\sigma_L} \exp\left[-\frac{1}{2}\Big(\frac{\ln \hat{x}_i - \mu_L}{\sigma_L}\Big)^2\right] \tag{B.3}$$

Where μ_L and σ_L is the parameters that are going to be optimized by finding the maximum of the log-likelihood function. The maximum can be found by partial derivation:

$$\frac{\partial l(\mu_L, \sigma_L|\hat{\mathbf{x}})}{\partial \mu_L} = 0\ , \quad \frac{\partial l(\mu_L, \sigma_L|\hat{\mathbf{x}})}{\partial \sigma_L} = 0 \tag{B.4}$$

The statistical uncertainty is assumed to be normal distributed. The mean is the values obtained by the maximum likelihood method and the standard deviation can be obtained in the covariance matrix ($\mathbf{C}$), which can be find by:

$$\mathbf{C} = \mathbf{H}^{-1} = \begin{bmatrix} -\frac{\partial^2\ l(\mu_L,\sigma_L|\hat{\mathbf{x}})}{\partial^2 \mu_L^2} & -\frac{\partial^2 l(\mu_L,\sigma_L|\hat{\mathbf{x}})}{\partial \mu_L \partial \sigma L} \\ -\frac{\partial^2 l(\mu_L,\sigma_L|\hat{\mathbf{x}})}{\partial \mu_L \partial \sigma L} & -\frac{\partial^2 l(\mu_L,\sigma_L|\hat{\mathbf{x}})}{\partial^2 \sigma_L^2} \end{bmatrix}^{-1}_{\mu_L=\mu_L^*,\ \sigma_L=\sigma_L^*} \tag{B.5}$$

Finally the new distribution can be found by integrating the statistical uncertainty:

$$f_X(x) = \iint f_X(x|\mu_L, \sigma_L) f(\mu_L, \sigma_L|(\mu_L^*, \sigma_L^*)^T, \mathbf{C})\, d\mu_L\, d\sigma_L \tag{B.6}$$

B.1.4 Concrete compression strength distribution

The concrete compression strength distribution is presented in B.2 and B.3. The distribution has a mean of 17.37 MPa and a CoV of 0.3. To give an impression of the statistical uncertainty, the distribution both with- and without the statistical uncertainty is shown. The characteristic concrete strength (f_{ck}) is 10.37 MPa.

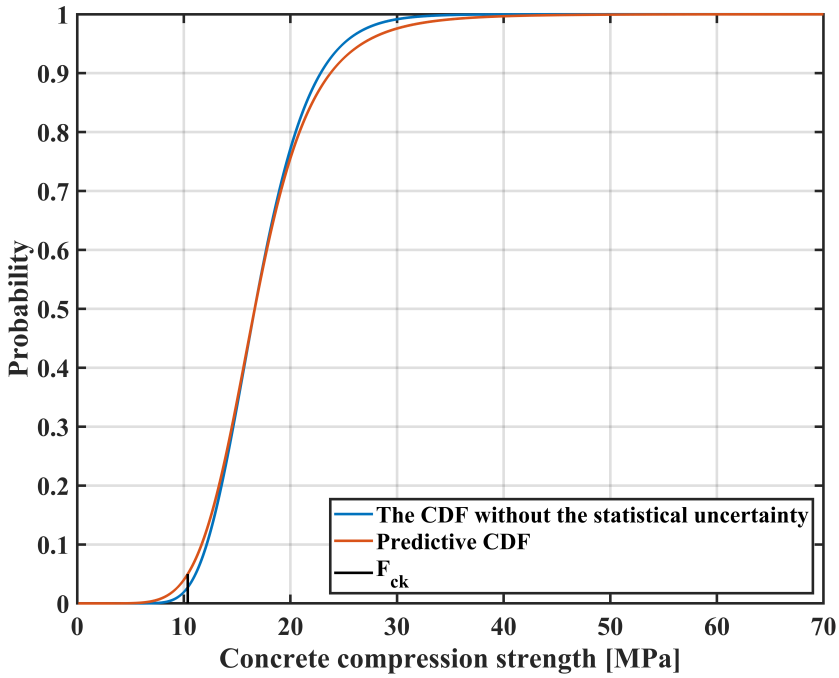

Figure B.2: The CDF obtained from the concrete cores.

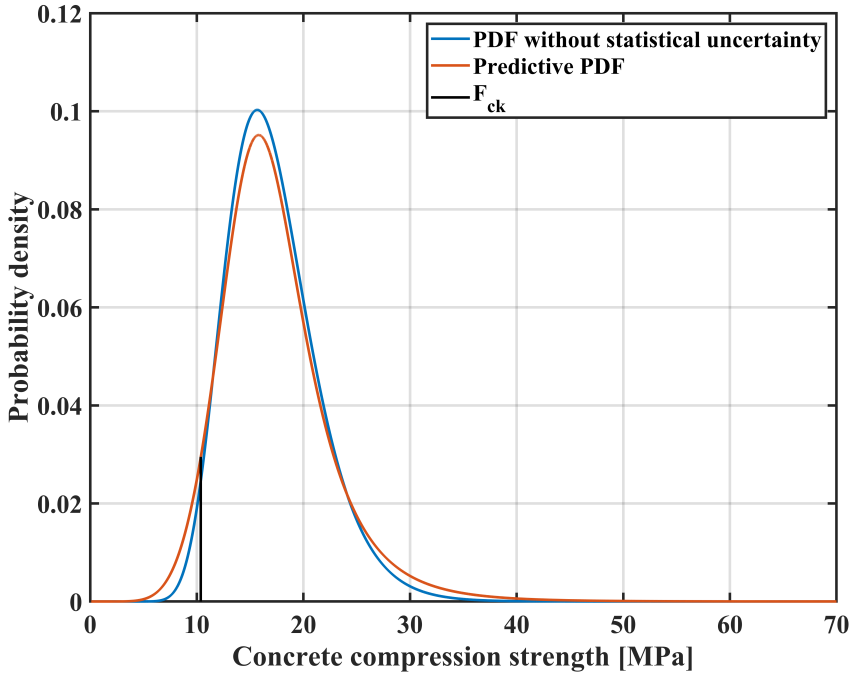

Figure B.3: The PDF obtained from the concrete cores.

B.2 Historic load models end the Eurocode load model

B.2.1 The Norwegian Public Road Administration's traffic load model

The handbook R412[56] provides a load model where a wheel-, an axle-, a double axle-, a triple axle-, a vehicle, and a trailer load have to be considered. The dynamic effects are included in the load cases. The loads can be placed in any possible position. Only the load case that gives the greatest load effect is to be considered. The wheel- and all the axle loads are considered as point loads. The

distance between the axles is 1.3 meters. For the triple axle the largest point load can be either in the first-, second- or third position. The vehicle- and the trailer load are considered as evenly distributed loads. An additional point load is to be placed within the limits of the evenly distributed load. The loads are placed on a silhouette of one part of the Stavå bridge bridge deck. The Norwegian load model distinguish between different road classes. The magnitude of the loads depends on the bridges classification. The magnitude of the forces given in the figure are the forces corresponding to the normal trailer load (Bk10/60).

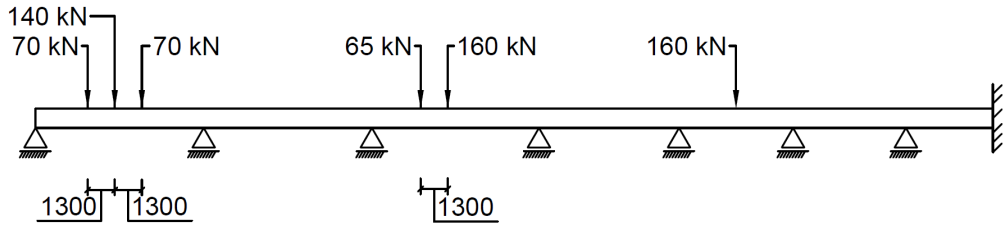

Figure B.4: The value of all the three axle loads [mm].

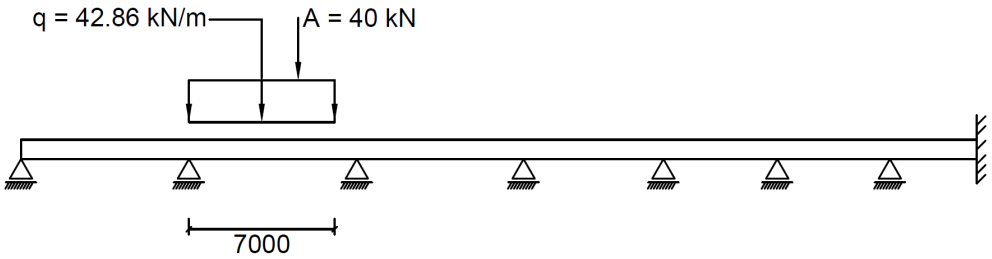

Figure B.5: The vehicle load.

There can be an evenly distributed load of 6 kN/m behind or/and in front of the trailer load if this is unfavorable.

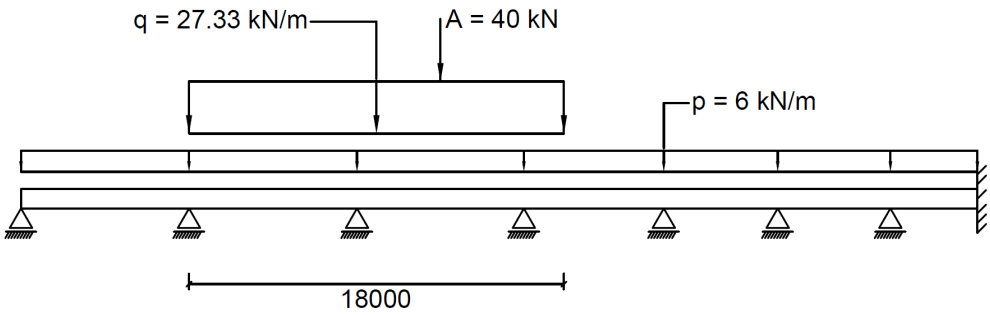

Figure B.6: The trailer load with cars in front and behind [mm].

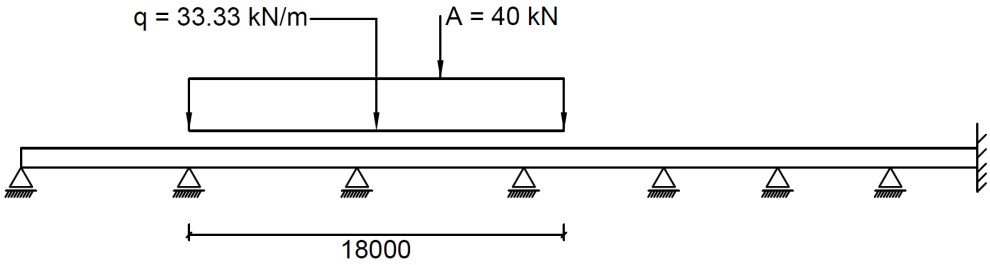

Figure B.7: The trailer load without cars in front and behind [mm].

B.2.2 1930-1947 Load class 1 traffic load model

The bridge was originally designed to satisfy load class 1 form 1930 [2]. The load class is given in figure B.8. All the numbers in the figure have to be multiplied by 1.35 to take care of the dynamic effects (Hand book 239 chap. 2.2.2)[52].

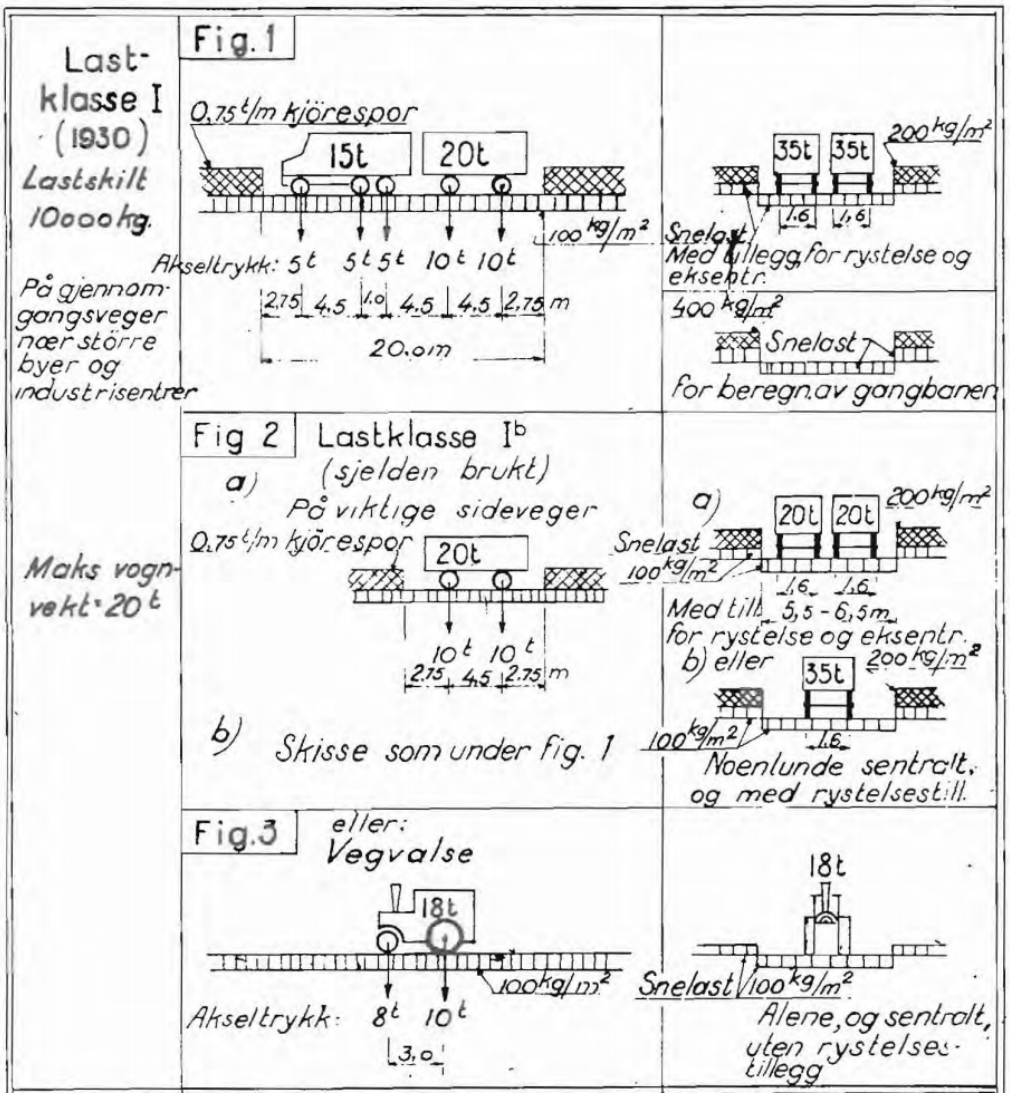

Figure B.8: [52]. 1930-1947 Load model 1.

B.2.3 The Eurocode 1 traffic load model

The Eurocode load model 1 divides the bridge into noional lanes. How many lanes a bridge is divided into depends on the width. A six meter bridge is divided into exactly two lane. In each lane one shall apply one uniformly distributed load

(UDL) and one tandem system (TS) load, i.e. two axles at a row. The distance between the axles is 1.2 meter. The load in the first row is bigger than the load in the second row. Table B.3 gives the magnitude of the forces for each lane.

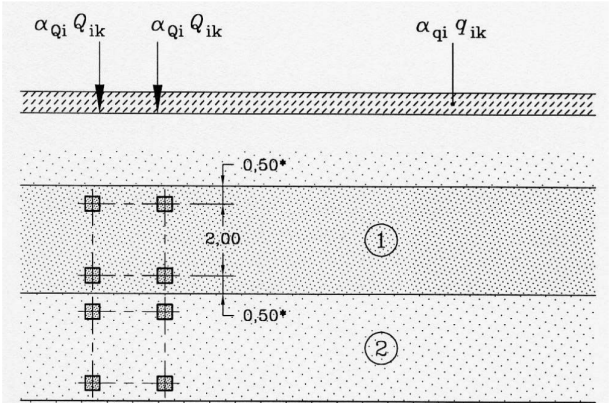

Figure B.9: EC1-2: Fig. 4.2a [11].

Location	**Tandem system TS**	**UDL system**
	Axle loads Q_{ik} (kN)	**q_{ik} (kN/m^2)**
Lane number 1	300	$0.6 \cdot 9 = 5.4$
Lane number 2	200	2.5

Table B.3: EC1-2: table 4.2[11]. Axle loads.

B.3 FORM calculation method

The cross section is a T-beam and the flange is in compression. The limit state function for the discussed cross section is given as:

$$g(\mathbf{x}) = m_{mod}(f_y A_s(d - 0.5\frac{f_y A_s}{f_c b_{eff}})) - s_q - s_g \tag{B.7}$$

m_{mod} is the model uncertainty, f_y is the steel strength, A_s is the reinforcement area, f_c is the concrete compression strength, b_{eff} is the effective width of the flange, d is the distance from the top of the beam to the reinforcement area center, s_q is the traffic load and s_g and the self weight.
The limit state function is transformed into the U-space:

$$\begin{aligned} g(\mathbf{u}) = &\exp(\sigma_M u_M + \mu_M)\exp(\sigma_Y u_Y + \mu_Y)A_S \ ... \\ &\cdot (d - 0.5\frac{\exp(\sigma_Y u_Y + \mu_Y)A_S}{\exp(\sigma_C u_C + \mu_C)b_{eff}}) \ ... \\ &- (b_Q t - \frac{1}{a_Q}\log(-\log(\Phi(u_Q)))) - (\sigma_G u_G + \mu_G) \end{aligned} \tag{B.8}$$

The β-index is found by solving eqn. B.9.

$$\beta = \min_{u \in \{g(\mathbf{u})=0\}} \sqrt{\sum_{i=1}^{5} u_i^2} \tag{B.9}$$

$$\mathbf{u} = \beta\alpha \tag{B.10}$$

$$\alpha = \beta^{-1}\mathbf{u} \tag{B.11}$$

Appendix C

Force diagrams

C.1 Cross-section A

C.1.1 Dead load

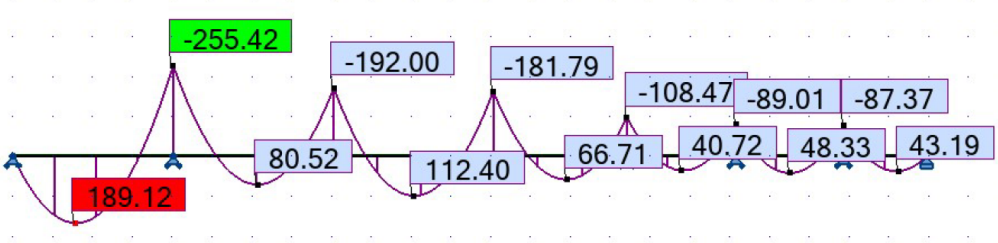

Figure C.1: Dead load moment diagram [kNm].

C.1.2 Ordinary traffic

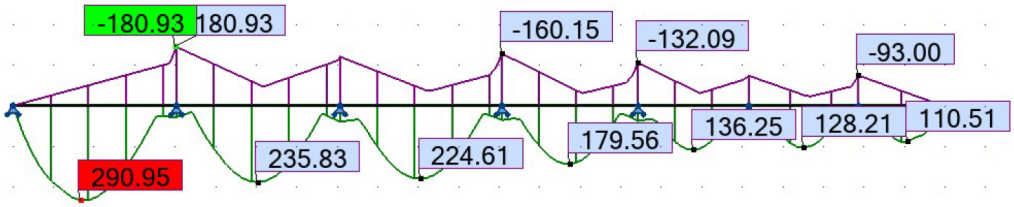

Figure C.2: Triple axle group envelope moment diagram [kNm].

C.1.3 Special transport

Control of the calculations

The calculations are controlled to see that the 5 meter distributed load causes a worse load effect than the 7 meter distributed load described by the Norwegian Public Road Administration's load standard.

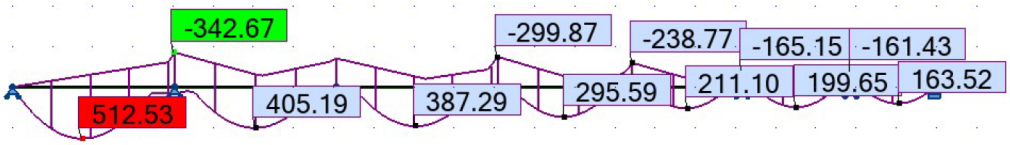

Figure C.3: 5 meter distributed load envelope moment diagram [kNm].

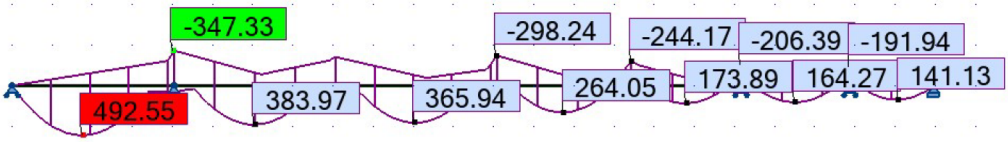

Figure C.4: 7 meter distributed load envelope moment diagram [kNm].

Modeled as 5 point loads

The load is then modeled as 5 point loads instead of a distributed load. One can see that 5 point loads causes less load effect than the distributed load.

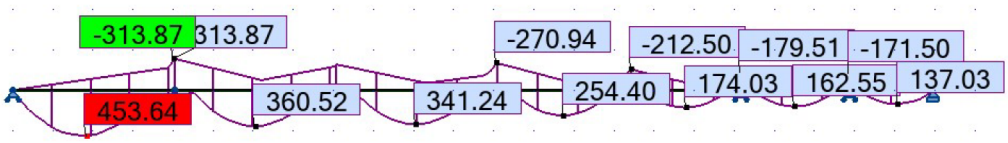

Figure C.5: The worst axle number envelope moment diagram [kNm].

Eurocode loads

The loads are calculated according to the Eurocode 1991-2 [11] load model 1, which is described in appendix B. The same transverse distribution as the one described in chapter 7 is used.

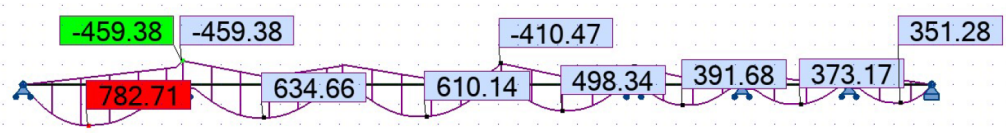

Figure C.6: The Eurocode load model 1 axle load part [kNm].

Figure C.7 shows the result without the adjustment factor from the Norwegian national annex.

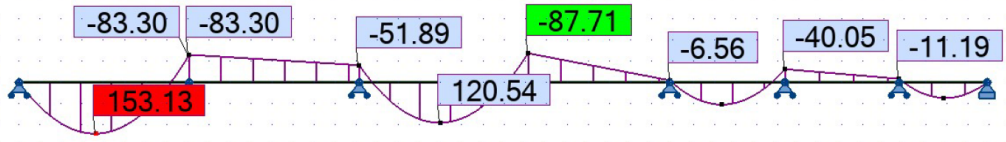

Figure C.7: The Eurocode load model 1 distributed load part [kNm].

The Norwegian Public Road Administration's HB R412 load model

The load shown in figure C.8 is caused by the triple axle system described in appendix B

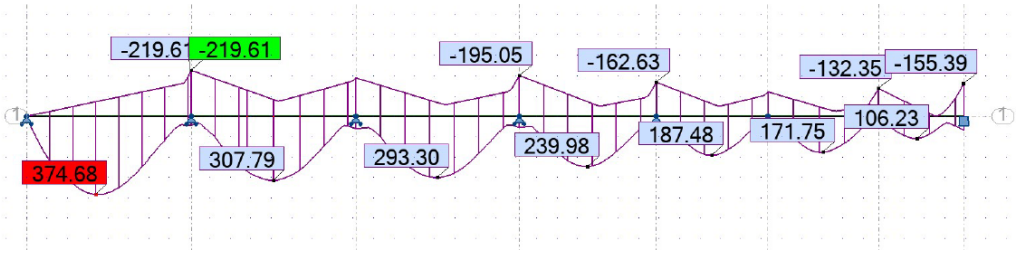

Figure C.8: The Norwegian Public Road Administration's load model [kNm].

C.2 Cross-section B

C.2.1 Dead load

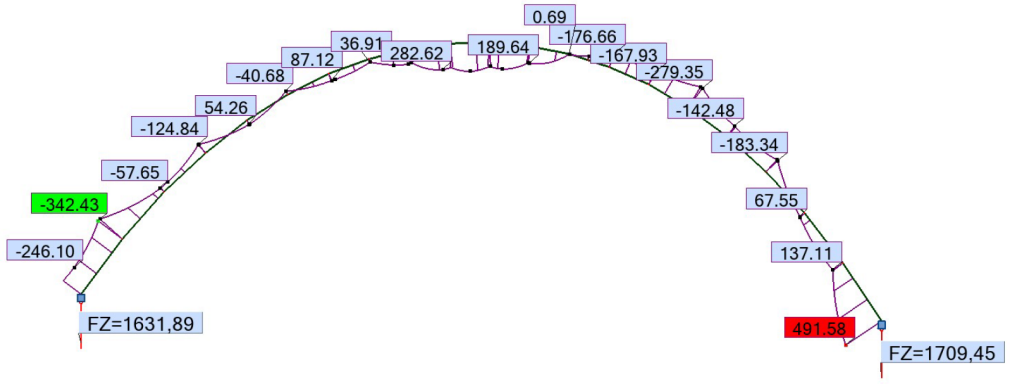

Figure C.9: Dead load moment diagram [kNm].

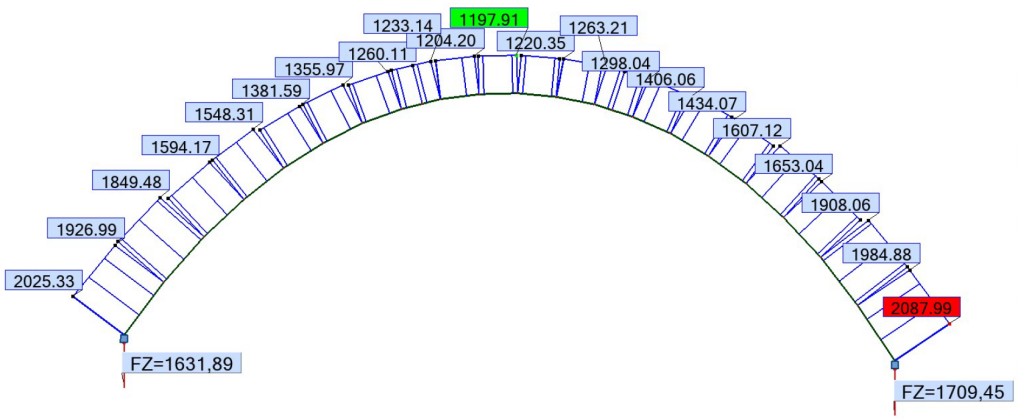

Figure C.10: Dead load normal force diagram [kN].

C.2.2 Ordinary transport

Load case 1:

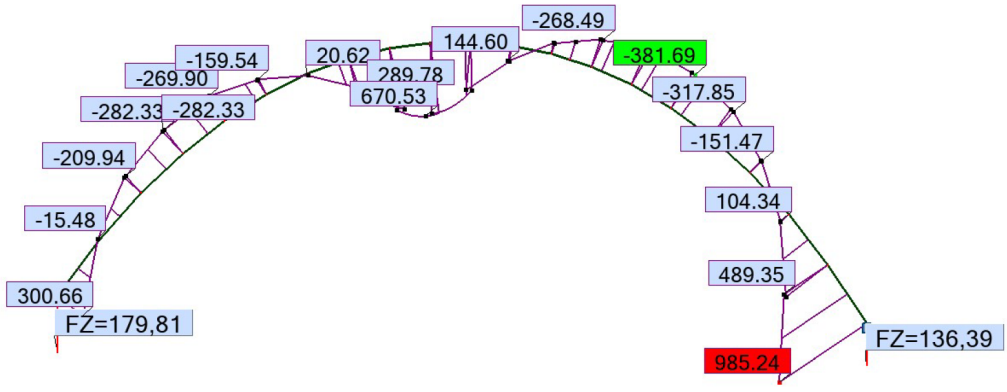

Figure C.11: Tipper truck moment diagram [kNm].

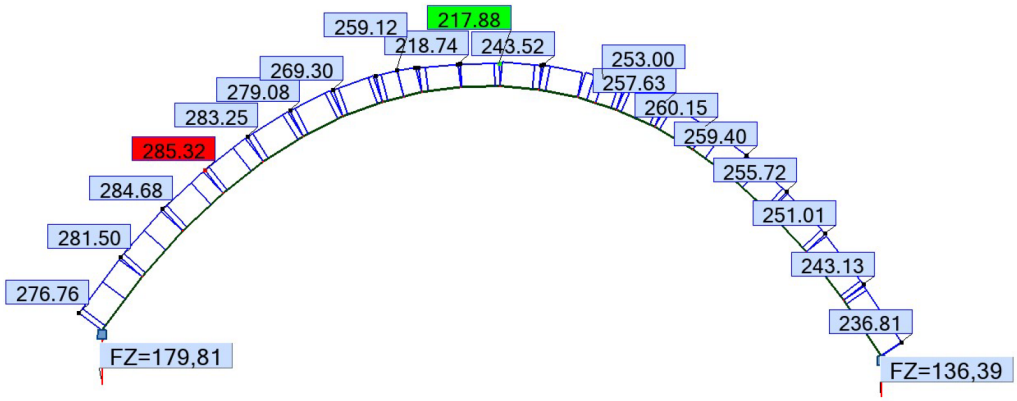

Figure C.12: Tipper truck normal force diagram [kN].

Load case 2:

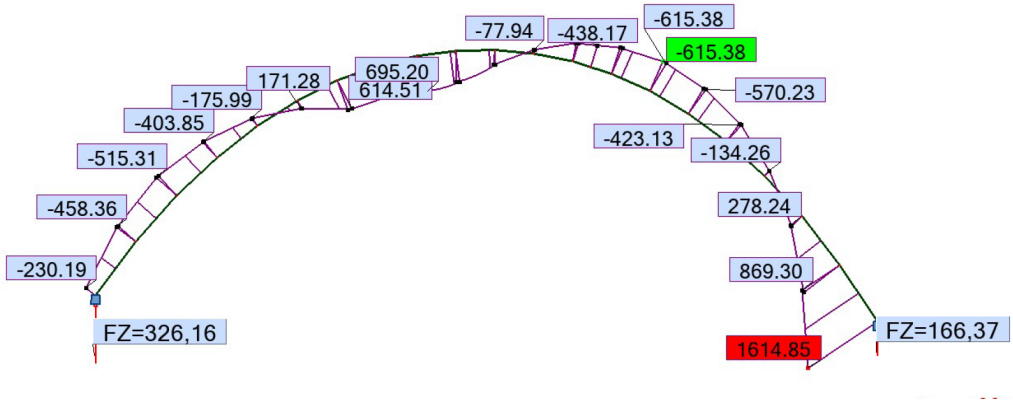

Figure C.13: Semitrailer truck moment diagram [kNm].

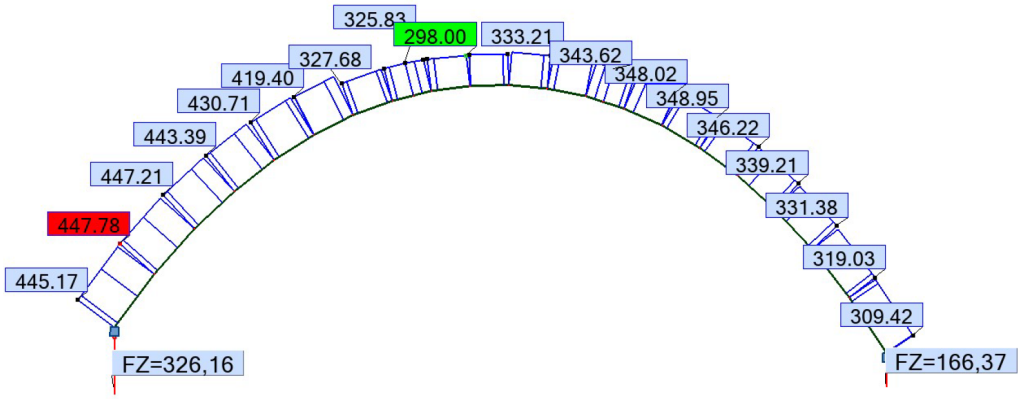

Figure C.14: Semitrailer truck normal force diagram [kN].

Load case 3a:

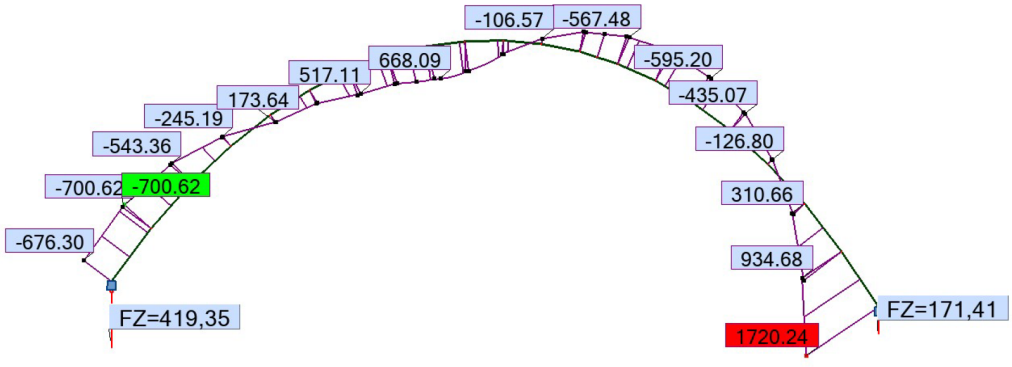

Figure C.15: B-train moment diagram [kNm].

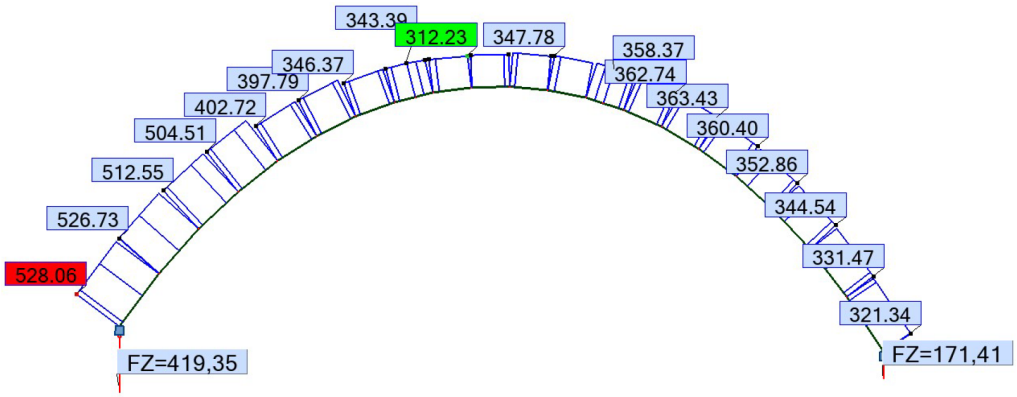

Figure C.16: B-train normal force diagram [kN].

Load case 3b:

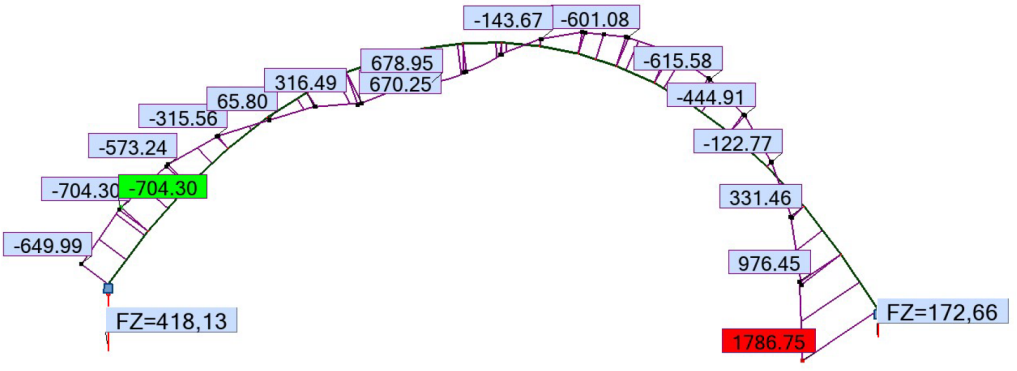

Figure C.17: B-train with different wheelbase moment diagram [kNm].

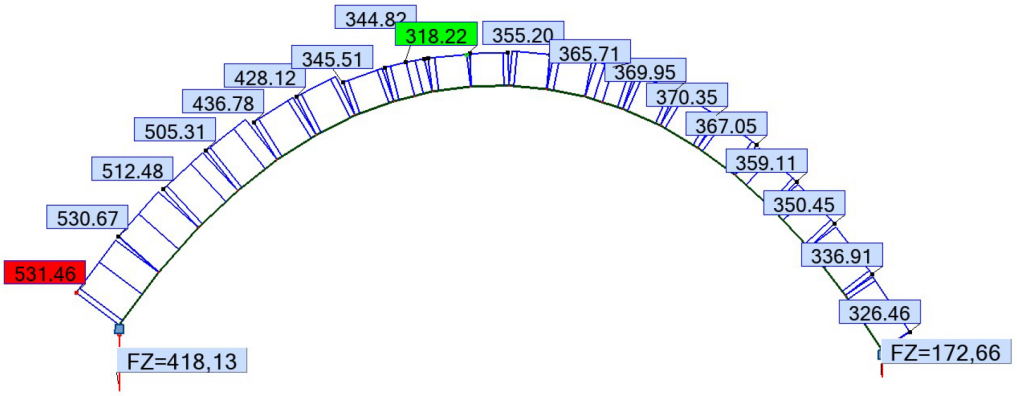

Figure C.18: B-train with different wheelbase normal force diagram [kN].

The Norwegian Public Road Administrations load model, Bk10/60 load (load case 4a):

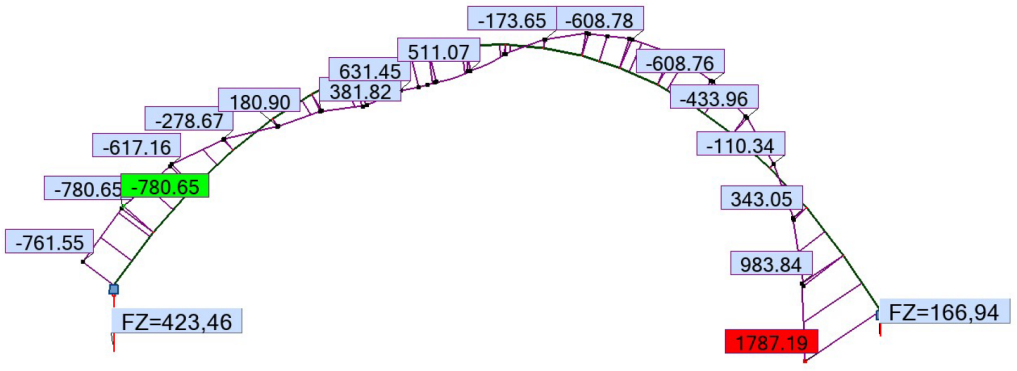

Figure C.19: The Norwegian Standard Bk10/60 moment diagram [kNm].

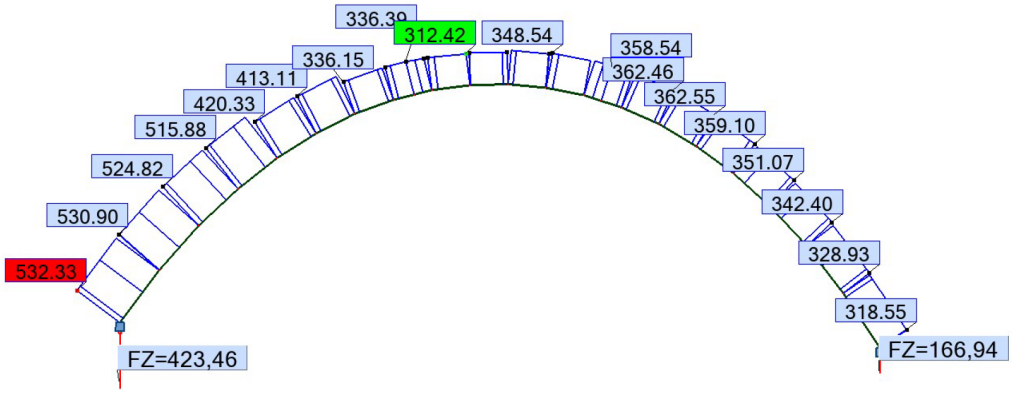

Figure C.20: The Norwegian Standard Bk10/60 normal force diagram [kN].

The Norwegian Public Road Administrations load model, Bk10/50 load, (load case 4b):

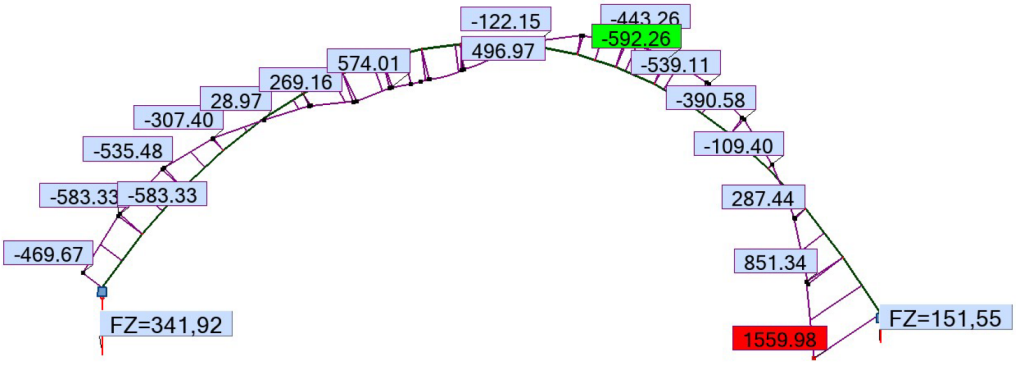

Figure C.21: The Norwegian Standard Bk10/50 moment diagram [kNm].

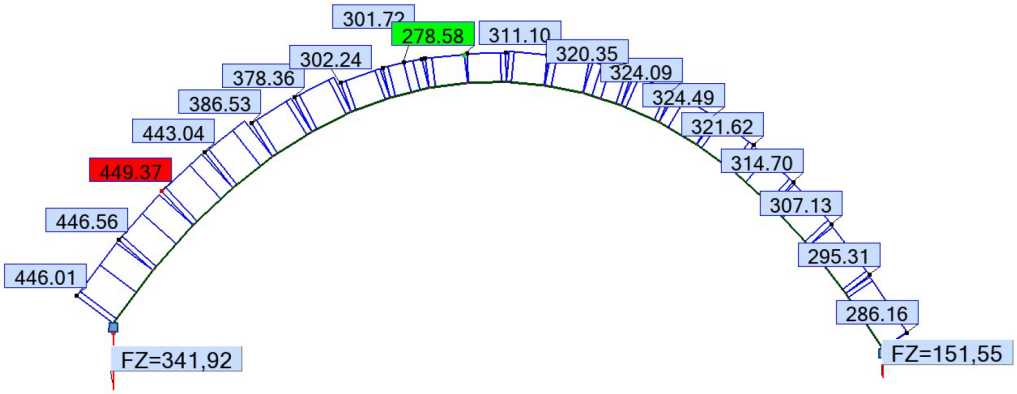

Figure C.22: The Norwegian Standard Bk10/50 normal force diagram [kN].

C.2.3 Bk12/100 special transport (load case 5)

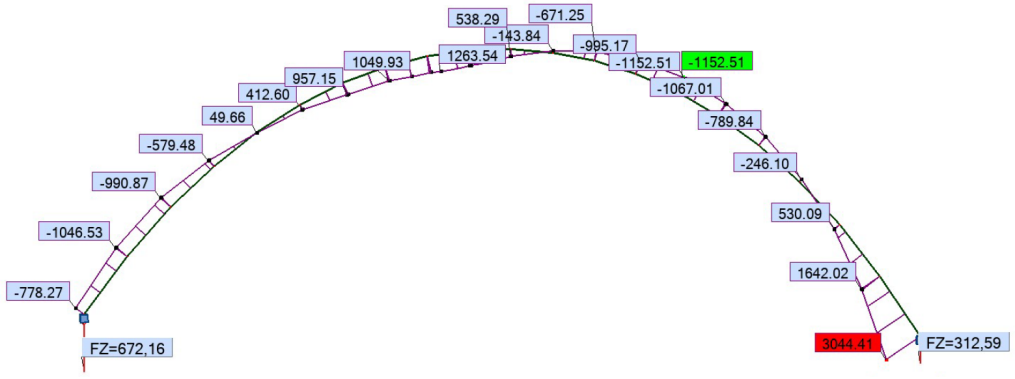

Figure C.23: Bk12/100 special transport moment diagram [kNm].

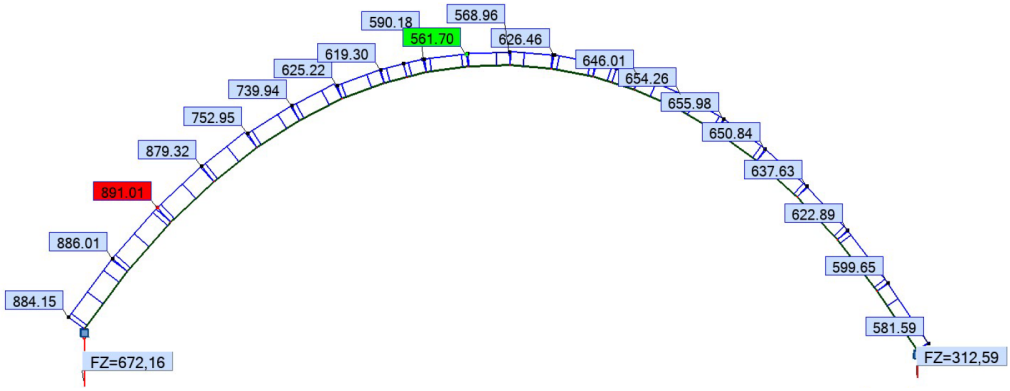

Figure C.24: Bk12/100 special transport normal force diagram [kN].

Appendix D

Cross-section B-B calculation method

MN-diagram derivation

The MN-diagram is derived by equation D.1 to D.9. Figure 7.26 is the basis for the derivation. The MN-diagram is derived by changing the strain state over the cross-section. x is chosen as the basic variable. x is the length from the top of the cross-section to the point where the stress is equal to zero.
Equation D.1 to D.5 considers the situation where x is less than the height.
When $x > h$:
Equation D.1 is the requirement for the concrete and the steel respectively. The average concrete strain shall not be bigger than $\varepsilon_{c3} = 1.75 \cdot 10^{-}3$. The second equation states that the reinforcement strain must be be smaller than the yield limit.

$$\begin{aligned} \varepsilon_c(x) &= 0.00175 \cdot \frac{x}{x - \frac{h}{2}} \\ \varepsilon_s(x) &= -\frac{f_y}{E_s} \leq \varepsilon_c \cdot \frac{x - d_i}{x} \leq \frac{f_y}{E_s} \end{aligned} \tag{D.1}$$

$$
\begin{aligned}
N_{s,i} &= A_{s,i} \cdot E_s \cdot \varepsilon_{s,i} \\
M_{s,i} &= N_{s,i} \cdot a_i
\end{aligned}
\tag{D.2}
$$

Where, d_i is the distance between the top of the cross-section A-And the reinforcement. The subscript i refers to the the different rows of reinforcement. The moment arm is $a_i = d_i - \frac{h}{2}$.

The compression zone is idealized to be rectangular. The effective height of the compression zone is $0.8x$. It must be controlled that the compression zone is not bigger than the cross-section itself. That is done by equation D.3.
If $0.8x \geq h$:

$$
\begin{aligned}
N_c &= f_c \cdot b \cdot h \\
M_c &= 0
\end{aligned}
\tag{D.3}
$$

If $0.8x \leq h$:

$$
\begin{aligned}
N_c &= 0.8x \cdot f_c \cdot b \\
M_c &= N_c \cdot (0.5h - 0.4x)
\end{aligned}
\tag{D.4}
$$

The moment and normal force contribution from the concrete and each row of reinforcement are added together in equation D.5.

$$
\begin{aligned}
N_1(x) &= N_c + \sum_{i=1}^{n} N_{s,i} \\
M(x)_1 &= M_c + \sum_{i=1}^{n} M_{s,i}
\end{aligned}
\tag{D.5}
$$

Equation D.6 to D.9 considers the situation when x is smaller than the height of the cross-section.
When $x < h$:

$$\begin{aligned} \varepsilon_c &= 3.5 \cdot 10^{-3} \\ \varepsilon_{s,i} &= -\frac{f_y}{E_s} \leq \varepsilon_c - \frac{\varepsilon_c}{x} \cdot d_i \leq \frac{f_y}{E_s} \end{aligned} \tag{D.6}$$

$$\begin{aligned} N_{s,i} &= A_{s,i} \cdot E_s \cdot \varepsilon_{s,i} \\ M_{s,i} &= N_{s,i} \cdot a_i \end{aligned} \tag{D.7}$$

Where, $a_i = d_i - \frac{h}{2}$

$$\begin{aligned} N_c &= f_c \cdot b \cdot 0.8x \\ M_c &= N_c \cdot (0.5h - 0.4x) \end{aligned} \tag{D.8}$$

$$\begin{aligned} N_2(x) &= N_c + \sum_{i=1}^{n} N_{s,i} \\ M_2(x) &= M_c + \sum_{i=1}^{n} M_{s,i} \end{aligned} \tag{D.9}$$

The moment and normal force contribution from the concrete and each row of reinforcement are added together in equation D.9. The contribution from the two above described situations is put together to one normal force vector and one moment vector in equation D.10.

$$N = [N_1, N_2]$$
$$M = [M_1, M_2] \tag{D.10}$$

$\mathbf{L_R}$ derivation

The variable x is discretized into eighth points. M and N in equation D.11 defines the corresponding points in the MN-diagram. A straight line is drawn between the points.

$$N = [n_1, n_2, ..., n_i]$$
$$M = [m_1, m_2, ..., m_i] \tag{D.11}$$

The slope of the line between the points is calculated by equation D.12.

$$s_i = \frac{\Delta N}{\Delta M} = \frac{n_{i+1} - n_i}{m_{i+1} - m_i} \tag{D.12}$$

A linear function is defined for all the lines in the MN-diagram. A function is also defined for the line that goes trough origin and the generated load data point.The slope of the line that goes trough origin to the generated normal force (n_0) and moment (m_0) load data is $\frac{n_0}{m_0}$. Equation D.14 calculates the intersection point between MN-diagram line and the load data line. This equation must be solved for all the lines. i refers to the line number.

$$\mathbf{Ax} = \mathbf{b}$$
$$\mathbf{x} = \mathbf{A}^{-1}\mathbf{b} \tag{D.13}$$

$$\begin{bmatrix} n_{int,i} \\ m_{int,i} \end{bmatrix} = \begin{bmatrix} 1 & -s_i \\ 1 & -\frac{n0_i}{m0_i} \end{bmatrix}^{-1} \begin{bmatrix} -a_i m_i + n_i \\ 0 \end{bmatrix} \tag{D.14}$$

In addition, it must be required that the both $n_{int,i}$ and $m_{int,i}$ have a positive value.

$$\begin{aligned} n_{int,i} > 0 \\ m_{int,i} > 0 \end{aligned} \tag{D.15}$$

The length between origin and the intersection point is calculated by equation D.16.

$$l_{int,i} = \sqrt{(n_{int,i})^2 + (m_{int,i})^2} \tag{D.16}$$

The length to each of the intersection points is put in a vector. The shortest of the lines defines L_R.

$$L_{int} = [l_{int,1}, l_{int,2}, ..., l_{int,i}] \tag{D.17}$$

$$L_R = \min(L_{int}) \tag{D.18}$$

Bibliography

[1] A.C. Cornell. A probability based structural code. *ACI Journal No.12, Proceedings V 66*, 1969.

[2] Norwegian Public Roads Administration. Documents and drawings. Documents and drawing given by Norwegian Public Roads Administration, 1940-1942.

[3] Anders Straume and Dag Bertelsen. Rapport Nr. 358 - Dokumentasjon av beregningsmoduler i EFFEKT 6.6. https://www.vegvesen.no/fag/publikasjoner/publikasjoner/statens+vegvesens+rapporter, 2015.

[4] Bent Grelk, Rambøll. Prøvingsrapport, Stavåbrua. , 2006.

[5] Dr. Johannes Berger. *VU Brückenbau; Einwirkungen auf Brücken*. Universität Innsbruck, 2018.

[6] Bo Sten, Rambøll. 16-0316 Stavåbrua spesialinspeksjon og klassifisering av bruer. , 2007.

[7] Bo Sten, Rambøll. 16-0316 Stavåbrua spesialinspeksjon. , 2017.

[8] Bo Sten, Rambøll. 16-0316 Stavå bru - Prøveresultater og registreinger. , 2018.

[9] Edited by D.Diamantidis. *Probabilistic assessment of Existing Structures*. A publication of Joint Committee on Structural Safety (JCSS), 2001.

[10] Byggeindustrie. FCC Construcción og Rambøll videre for byggingen av E6 Ulsberg - Vindåsliene. https://www.bygg.no/article/1410301, 2019.

[11] European community for standardization. *NS-EN 1991-2:2003 + NA:2010*. Norsk Standard, 2003.

[12] European community for standardization. *NS-EN 13791:2007*. Norsk Standard, 2007.

[13] European community for standardization. *NS-EN 1992-1-:2004 + NA:2008*. Norsk Standard, 2008.

[14] European community for standardization. *NS-EN 1990:2002/A1:2005/AC*. Norsk Standard, 2010.

[15] Det kongelige finansdepartement. Rundskriv R-109/14. https://www.regjeringen.no/globalassets/upload/fin/vedlegg/okstyring /rundskriv/faste/r _09_014.pdf, 2014.

[16] E. Basler. Untersuchungen über den Sicherheitsbegriff von Bauwerken. *Schweizer Archiv für angewandte Wissenschaft und Technik, 27 (1961) 4.*, 1961.

[17] Michael Faber, Dimitri Val, and Mark Stewart. Proof load testing for bridge assessment and upgrading. *Engineering Structures*, 22:1677–1689, 12 2000.

[18] G. Grandori. Paradigms and falsification in erthquake engineering. *Meccanica,*, 26:17–21, 1991.

[19] EIKLID GE, GERSTLE KH, and TULIN LG. Strain-hardening effects in reinforced concrete. *Magazine of Concrete Research*, 21(69):211–220, 1969.

[20] T. Vrouwenvelder J. Schneider. *Introduction to safety and reliability of structures*. International association for bridge and structural engineering, 3. edition edition, 2017.

[21] Jean-Armand Calgaro. Traffic Loads Traffic Loads on Road on Road Bridges Bridges and Footbridges. *Eurocodes Background and applications*, Brussels, 18-20 February 2008 – Dissemination of information workshop, 2008.

[22] Jean-Pierre Jacobs. Commentary Eurocode 2. European Concrete Platform ASBL, 2008.

[23] JSCC, Michael Faber, Ton Vrouwenvelder. Probabilistic Model Code. 2000.

[24] Prof.Dr.-Ing. Jochen Köhler. *Zuverlässigkeit von Gebäuden und systematische Schadenserfassung*. 2008. Holzbautag Biel.

[25] Per Kr. Larsen. *Konstruksjonsteknikk - Laster og bæresystemer, 2. utgave*. Fagbokforlaget, 2014.

[26] Hannes Ludescher. Berücksichtigung von dynamischen verkehrslasten beim tragsicherheitsnachweis von strassenbrücken. 2003.

[27] Ludescher, Hannes and Brühwiler, Eugen. Dynamic Amplification of Traffic Loads on Road Bridges. *Structural Engineering International*, 19:190–197, 05 2009.

[28] Michael P. Enright and Dan M. Frangopol. Service-Life Prediction of Deteriorating Concrete Bridges. *Journal of Structural Engineering*, Volume 124 Issue 3 - March 1998:309–317, 03 1998.

[29] Milan Holický, Alois Materna, Gerhard Sedlacek, Angel Arteaga, Luca Sanpaolesi, Ton Vrouwenvelder, Igor Kovse, Haig Gelvanessian. Handbook 2 Reliability backgrounds. *Book by Leonardo da Vinci Pilot Project CZ/02/B/F/PP-134007*, 2005.

[30] Milan Holický, Alois Materna, Gerhard Sedlacek, Angel Arteaga, Luca Sanpaolesi, Ton Vrouwenvelder, Igor Kovse, Haig Gelvanessian. Handbook 4 Design of bridges. *Book by Leonardo da Vinci Pilot Project CZ/02/B/F/PP-134007*, 2005.

[31] Nikolai Ryvoll. Meetings with Knut Ove Dahle, Igor Praskac and Arild Christiansen. Representatives from the Norwegian Public Road Administration.

[32] Nikolai Ryvoll. Sensitivity analysis of the reliability-based reassessment of the Stavå bridge structural integrity.

[33] Nikolai Ryvoll. Talk with Bjarne Rvoll on his experience working as an engineer on the Njunis tunnel project.

[34] Nikolai Ryvoll. Talk with friends and family, 31.12.

[35] Nikolai Ryvoll. Talk with truck drivers on the ferry between Lødingen and Bognes, 07.01.

[36] Nikolai Ryvoll. Talk with Anders Straume 04.10, 2019.

[37] Norges Lastebileier-forbund. Bruk av modulvogntog på E6 femdoblet siden 2016. https://lastebil.no/Aktuelt/Nyhetsarkiv/2019/Bruk-av-modulvogntog-paa-E6-femdoblet-siden-2016, 2019.

[38] Alan O'Connor and Eva Eichinger. Site-specific traffic load modelling for bridge assessment. *Bridge Engineering*, 160(4):185–194, 2007.

[39] H.J. Otway, M.E. Battat, R.K. Lohrding, R.D. Turner, and R.L. Cubitt. A risk analysis of the omega west reactor.

[40] André T. Beck Robert E. Melchers. *Structural Reliability Analysis and Prediction*. 3. edition edition, 2017.

[41] Samferdselsdepartementet. Forskrift om bruk av kjøretøy. https://lovdata.no/dokument/SF/forskrift/1990-01-25-92, 2013.

[42] et al. S.Jacobsen. *Compendium - Concrete Technology*. NTNU, 2016.

[43] Norsk Standard. NS 227; regler for utførelser av arbeider i armert betong. https://www.nb.no/items/514232b51e1cdd09a0465166961538e0?page=8searchText=ekstraordin%C3%A6re, 1939.

[44] Statistisk Sentralbyrå. Byggekostnadsindeks for veganlegg. https://www.ssb.no/bkianl, 2019.

[45] Statistisk Sentralbyrå. Kørelengder. https://www.ssb.no/transport-og-reiseliv/statistikker/klreg, 2019.

[46] Statistisk Sentralbyrå. Trafikkulykker med personskade. https://www.ssb.no/transport-og-reiseliv/statistikker/vtu/aar, 2019.

[47] A/S Strømbull. *Strømbulls Stålbok*. Emil Moestue A/S, 1941, https://www.nb.no/items/1a04189e64b32ef4432817658f2a8ca7?page=75searchText=.

[48] Sturla Rambjør og Heine Røstum, Aas Jakobsen. *Stavåbrua – Kritisk snitt og lastplassering* . Aas Jakobsen, 2019.

[49] Svein Ivar Sørensen. *Betongkonstrukjoner; beregninger og dimensjonering etter Eurocode 2*. Fagbokforlaget, 2014.

[50] The International Organization for Standardization. *ISO2394:2015 - General principles on reliability for structures*. 2015.

[51] The Norwegian Public Roads Administration. Håndbok V441 - Inspeksjonshåndbok for bruer, 2000.

[52] The Norwegian Public Roads Administration. Håndbok 239 - Bruklassifisering; Lastforskrifter 1929-1973 og brunormaler 1912-1958 , 2003.

[53] The Norwegian Public Roads Administration. Håndbok R412 Bruklassifisering, 2003.

[54] The Norwegian Public Roads Administration. Håndbok V460 - Beredskapsbroer. https://www.vegvesen.no/fag/publikasjoner/handboker, 2014.

[55] The Norwegian Public Roads Administration. Håndbok V712 - Konsekvensanalyser. https://www.vegvesen.no/fag/publikasjoner/handboker, 2018.

[56] The Norwegian Public Roads Administration. Vedlegg til håndbok R412 Bruklassifisering - Endringer og tilføyelser, 2018.

[57] The Norwegian Public Roads Administration. 13,5 tonn overlast resulterte i kjøreforbud og et vektgebyr på 65 000 kroner. https://www.vegvesen.no/om+statens+vegvesen/presse/nyheter/nasjonalt/13-5-tonn-overlast-resulterte-i-kjoreforbud-og-et-vektgebyr-pa-65-000-kroner, 2019.

[58] The Norwegian Public Roads Administration. Gebyr ved overlast. https://www.vegvesen.no/kjoretoy/yrkestransport/veglister-og-dispensasjoner/mobilkran, 2019.

[59] The Norwegian Public Roads Administration. Vegkart. https://www.vegvesen.no/nvdb/vegkart/v2/, 2019.

[60] The Norwegian Public Roads Administration. Vehicle lenght data. https://www.vegvesen.no/trafikkdata/start/eksport, 2019.

[61] TV 2. Tatt med 22 tonn overvekt – fikk sekssifret beløp i bot. https://www.tv2.no/a/9556793/, 2017.

[62] Statens Vegvesen. Trafikkdata berkåk.

[63] Vejdirektoratet. *Pålidelighedsbaseret klassifisering af eksisterende broers bæreevne*. Vejdirektoratet, 2004.

[64] Volvo. Volvo specifications sheet . http://segotn12827.rds.volvo.com/STPIFiles/Volvo/ModelRange/fh64t6ha_gbr_eng.pdf, 2019.

[65] Volvo. Volvo specifications sheet . http://segotn12827.rds.volvo.com/STPIFiles/Volvo/ModelRange/fh84pr6ha_gbr_eng.pdf, 2019.

Nikolai Øwre Ryvoll

Probability-based assessment of the Stavå bridge

NTNU
Norwegian University of
Science and Technology